

INVESTIGATION OF THE SUBSTRATE SPECIFICITY  
OF RECOMBINANT TRYPANOSOMA CRUZI TRANS-  
SIALIDASE

Jennifer Amanda Harrison

A Thesis Submitted for the Degree of PhD  
at the  
University of St Andrews



1999

Full metadata for this item is available in  
St Andrews Research Repository  
at:

<http://research-repository.st-andrews.ac.uk/>

Please use this identifier to cite or link to this item:

<http://hdl.handle.net/10023/14907>

This item is protected by original copyright



**INVESTIGATION OF THE SUBSTRATE SPECIFICITY  
OF RECOMBINANT *TRYPANOSOMA CRUZI* TRANS-  
SIALIDASE**

**JENNIFER A. HARRISON**

A thesis submitted for the degree of Doctor of Philosophy

University of St Andrews

December 1998



ProQuest Number: 10167293

All rights reserved

INFORMATION TO ALL USERS

The quality of this reproduction is dependent upon the quality of the copy submitted.

In the unlikely event that the author did not send a complete manuscript and there are missing pages, these will be noted. Also, if material had to be removed, a note will indicate the deletion.



ProQuest 10167293

Published by ProQuest LLC (2017). Copyright of the Dissertation is held by the Author.

All rights reserved.

This work is protected against unauthorized copying under Title 17, United States Code  
Microform Edition © ProQuest LLC.

ProQuest LLC.  
789 East Eisenhower Parkway  
P.O. Box 1346  
Ann Arbor, MI 48106 – 1346

Tr  
D 326



## **Abstract**

The protozoan blood-borne parasite *Trypanosoma cruzi* is the causative agent of Chagas' disease, an enervating and often fatal illness prevalent in South and Central America for which there is no effective treatment. *T. cruzi* has a cell-surface *trans*-sialidase which transfers sialic acid from mammalian oligosaccharides to the parasite. This action allows adhesion to and invasion of mammalian cells, subsequently allowing parasitic replication. This protein therefore is exploitable and represents a potential target for the development of chemotherapeutic agents. This thesis describes the purification of recombinant *trans*-sialidase and the development of a rapid, reliable spectrophotometric coupled assay to measure *trans*-sialidase activity. It also details the use of three mutually exclusive synthetic oligosaccharide libraries to map substrate recognition for the enzyme. Synthetic fragments of the natural branched oligosaccharide substrates have also been sialylated on a preparative scale, demonstrating the use of *trans*-sialidase in synthetic oligosaccharide chemistry.

I, Jennifer Amanda Harrison, hereby certify that this thesis, which is approximately 32,000 words in length, has been written by me, that it is the record of work carried out by me and that it has not been submitted in any previous application for a higher degree.

Date *15<sup>th</sup> December 1998* Signature of candidate *[Signature]*

I was admitted as a research student in October 1995 and as a candidate for the degree of Doctorate of Philosophy in December 1998; the higher study for which this is a record was carried out in the University of St Andrews between 1995 and 1998.

Date *15<sup>th</sup> December 1998* Signature of candidate

I hereby certify that the candidate has fulfilled the conditions of the Resolution and Regulations appropriate for the degree of Doctorate of Philosophy in the University of St Andrews and that the candidate is qualified to submit this thesis in application for that degree.

Date *15<sup>th</sup> December 1998* Signature of supervisor

Unrestricted

In submitting this thesis to the University of St Andrews I understand that I am giving permission for it to be made available for use in accordance with the regulations of the University Library for the time being in force, subject to any copyright vested in the work not being affected thereby. I also understand that the title and abstract will be published, and that a copy of the work may be made and supplied to any bona fide library or research worker.

Date *15<sup>th</sup> December 1998* Signature of candidate

## **Acknowledgements**

Thanks to all of the following people:

Mum and Dad for all of their love, help, support, commitment and encouragement.

Steve and Turbo for their love and help too.

Paul, for help, support and being my best friend in the early years.

---

### University and the Lab

Dr Rob Field for help and support during my Ph.D.

Dr Ravi Kartha for taking the pain out of organic synthesis. Bruce, for being my buddy, listening to my incessant moaning, providing me with lots of the “yellow stuff” and for designing and helping to create the infamous penguin suits. T. Climber for taking over my desk/bench and regularly showering my hair with muffins. Malcolm for showing me parts of T. Climber that I will never forget (even after the counselling!). Claire (and Quinton) for the chickpea curry recipe. Hiroki for the famous expression “Jenni....golf!” Randy and Practical for making my last few months a bit “large”. Chez, you will get over the car, but only after flowers every day for a year and plenty of candlelit dinners. Thanks also to all the rest of the group (far to many to mention!) for all the outings, curries, pub crawls, cakes.....etc!

---

Dave, thanks for the bed and breakfast and that celebrated works “Ooo ahh....”

And leaving the last word for Darren, for your love, help, support and organic tutorials. I couldn't have done it without you, babe.

To Mum and Dad who have showed me  
immense courage in the face of uncertainty and  
who have taught me never to give up.

<b>Contents</b>	<b>Page</b>
1. Introduction	1
Aims and Objectives	27
2. Assay development	28
3. <i>trans</i> -Sialidase synthetic substrate recognition	44
4. <i>trans</i> -Sialidase substrates based on natural surface oligosaccharides	62
5. <i>trans</i> -Sialidase substrate recognition of modified Gal $\beta$ -S-X analogues	91
6. Experimental	100
7. Conclusions	135
Appendix	140
References	148

<b>Section</b>	<b>Page</b>
<b>1. Introduction</b>	<b>1</b>
1.1 Chagas' Disease	2
1.1.2 Blood studies	3
1.1.3 The Disease and its effects	4
1.1.4 Host resistance to <i>trans</i> -sialidase	5
1.1.5 Possible Treatments	5
1.2 <i>Trypanosoma cruzi</i>	6
1.2.2 <i>T. cruzi</i> transmission vector	7
1.2.3 The life forms of <i>T. cruzi</i>	8
1.2.4 <i>T. cruzi</i> life cycle	9
1.3 The inflammation and Immune responses	10
1.3.2 Cell invasion	11
1.4 <i>trans</i> -Sialidase reactions	13
1.4.2 Parasitic attachment of <i>trans</i> -sialidase	13
1.4.3 <i>trans</i> -Sialidase primary structure	14
1.4.4 Comparison of the mechanism of <i>trans</i> -sialidase with other neuraminidases	15
1.4.5 Viral neuraminidases	17
1.4.5.2 Influenza A virus neuraminidase	17
1.4.6 Bacterial neuraminidases	18
1.4.6.2 <i>Salmonella Typhimurium</i> LH2neuraminidase	18
1.4.6.3 <i>Vibrio cholera</i> neuraminidase	19
1.4.6.4 <i>Micromonospora viridifaciens</i> neuraminidase	19
1.4.6.5 <i>Macrobodella decora</i> sialidase	21
1.4.7 Sequence alignments of <i>Trypanosoma cruzi trans</i> -sialidase with related sialidases/neuraminidases	21
1.5 Cloning and expression of <i>trans</i> -sialidase	22
1.5.2 Kinetic profile of <i>trans</i> -sialidase	23
1.5.3 Prospective mechanism for <i>trans</i> -sialidase	24
<b>Aims and objectives</b>	<b>27</b>
<b>2. Assay development</b>	<b>28</b>
2.1 Assay development	29
2.1.2 Neuraminidase assays – Spectrophotometric	29
2.2 Transferase assays – Radiochemical	31
2.3 Comparison of <i>trans</i> -sialidase transferase and hydrolase activities	32
2.4 Coupled assay for <i>trans</i> -sialidase using lactose as an acceptor	33
2.5 Comparison of <i>C. perfringens</i> neuraminidase activity with and without an acceptor	35

<b>Section</b>	<b>Page</b>
2.6 Coupled assay for <i>trans</i> -sialidase using Gal $\beta$ (1,3)GlcNAc $\beta$ -O-Octyl as an acceptor (Mark II)	35
2.7 Spectrophotometric coupled assay (mark II) using variable concentrations of donor substrate	38
2.8 Inhibitor study carried out with <i>trans</i> -sialidase and <i>C. perfringens</i> neuraminidase	41
2.9 Summary	42
<b>3. <i>trans</i>-Sialidase synthetic substrate recognition</b>	<b>44</b>
3.1.1 Development of glycosyl transferase inhibitors	45
3.1.2 Systematically modified Gal $\beta$ -O-Octyl library	45
3.1.3 Radiochemical assay of Gal $\beta$ -O-Octyl analogues	48
3.1.4 Potential sialylation of Gal $\beta$ -O-Octyl analogues (monitored by T.L.C.)	50
3.1.5 Conclusions	53
3.2 Modified Gal $\beta$ (1,4)GlcNAc $\beta$ -Octyl analogues	55
3.2.2 Substituted Gal $\beta$ (1,4)GlcNAc $\beta$ -Octyl radiochemical assay	56
3.2.3 Sialylation of compounds 5(i,ii,iii,iv)-10(i,ii,iii,iv) using Neu5Ac-O-PNP	59
3.2.4 Conclusions	60
<b>4. <i>trans</i>-Sialidase substrates based on natural surface oligosaccharides</b>	<b>62</b>
4.1 <i>Trypanosoma cruzi</i> G-strain (Epimastigotes)	63
4.1.2 Characterisation of the oligosaccharides accepting sialic acid	63
4.1.3 <i>Trypanosoma cruzi</i> Y-strain	65
4.2 Radiochemical assay of all the Gal $\beta$ (1,X)gal derivatives	68
4.3 Multi-sialylation of oligosaccharide containing resin	69
4.4 <i>trans</i> -Sialidase catalysed sialylation of di and trisaccharide acceptor substrates	70
4.4.1 Incubation of Gal $\beta$ (1,2)Gal-O-Me (14), Glc $\beta$ (1,2)Gal $\beta$ -O-Me (15) and Gal $\beta$ (1,3)Gal $\beta$ -OMe (16)	71
4.4.2 Incubation of Gal $\beta$ (1,6)Gal $\beta$ -O-CH <sub>2</sub> CH <sub>2</sub> SiMe <sub>3</sub> (18) Glc $\beta$ (1,6)Gal $\beta$ -O-Octyl (19) and Gal $\beta$ (1,6)Gal $\beta$ -O-Me (20)	72
4.4.3 Incubation of Gal $\beta$ (1,4)[Gal $\beta$ (1,6)Glc] $\beta$ -O-Octyl and Glc $\beta$ (1,6)Gal $\beta$ -O-Octyl	74
4.5 Sialylation of Gal $\beta$ (1,6)Gal $\beta$ -O-CH <sub>2</sub> CH <sub>2</sub> SiMe <sub>3</sub> (19)	76
4.5.2 Preparative scale synthesis of Neu $\alpha$ (2,3)Gal $\beta$ (1,6)Gal $\beta$ -O-CH <sub>2</sub> CH <sub>2</sub> SiMe <sub>3</sub> (19)	76
4.5.3 Characterisation of Neu5Ac $\alpha$ (2,3)Gal $\beta$ (1,6)Gal $\beta$ -O-CH <sub>2</sub> CH <sub>2</sub> Si(CH <sub>3</sub> ) <sub>3</sub> – (25) Electrospray Mass Spectrometry	78
4.5.4 Enzymatic digestion of Neu5Ac $\alpha$ (2,3)Gal $\beta$ (1,6)Gal $\beta$ -O-CH <sub>2</sub> CH <sub>2</sub> SiMe <sub>3</sub> (25)	78
4.5.5 Systematic degradation of Neu5Ac $\alpha$ (2,3)Gal $\beta$ (1,6)Gal $\beta$ -O-CH <sub>2</sub> CH <sub>2</sub> SiMe <sub>3</sub> (25)	80
4.6 Sialylation of Glc $\beta$ (1,6)Gal $\beta$ -Octyl (20)	81

<b>Section</b>	<b>Page</b>
4.6.2 Preparative scale synthesis of Neu $\alpha$ (2,3)Glc $\beta$ (1,6)Gal $\beta$ -O-Octyl (20)	81
4.6.3 Analysis of Neu5Ac $\alpha$ (2,3)[Glc $\beta$ (1,6)]Gal $\beta$ -O-Octyl – (26) Electrospray Mass Spectrometry	82
4.6.4 Systematic enzymatic digestion Neu5Ac $\alpha$ (2,3)[Glc $\beta$ (1,6)]Gal $\beta$ -O-Octyl (26)	83
4.6.5 Treatment of Neu5Ac $\alpha$ (2,3)[Glc $\beta$ (1,6)]Gal $\beta$ -O-Octyl (26) with <i>C. perfringens</i> neuraminidase and $\beta$ -glucosidase	85
4.6.6 Digestion of Neu5Ac $\alpha$ (2,3)[Glc $\beta$ (1,6)]Gal $\beta$ -O-Octyl (26) by other $\beta$ -glucosidases	86
4.7 Sialylation of Gal $\beta$ (1,4)[ $\beta$ Gal(1,6)]Glc $\beta$ -O-Octyl (21)	86
4.7.2 Preparative scale synthesis of Gal $\beta$ (1,4)[ $\beta$ Gal(1,6)]Glc $\beta$ -O-Octyl (21)	86
4.7.3 Analysis of Neu5Ac $\alpha$ (2,3)Gal $\beta$ (1,4)[ $\beta$ Gal(1,6)]Glc $\beta$ -O-Octyl – Electrospray Mass Spectrometry	89
4.8 Conclusions	90
<b>5. <i>trans</i>-Sialidase substrate recognition of modified Gal<math>\beta</math>-S-X analogues</b>	<b>91</b>
5.1 Substituted Gal $\beta$ -S-X analogues	92
5.2 Gal $\beta$ -S-X analogues radiochemical assay	94
5.3 Serial dilution of J6 and Gal $\beta$ (1,4)[ $\beta$ Gal(1,6)]Glc $\beta$ -O-Octyl (21)	97
5.4 Conclusions	98
<b>6. Experimental</b>	<b>100</b>
6.1 Assay development	104
6.1.2 Spectrophotometric assay of <i>trans</i> -sialidase and <i>C. perfringens</i> neuraminidase	104
6.1.3 Comparison of <i>trans</i> -sialidase transferase and hydrolase activities	105
6.1.3.2 Coupled assay for <i>trans</i> -sialidase using lactose as an acceptor (mark I)	105
6.1.4 Comparison of <i>C. perfringens</i> neuraminidase activity with and without acceptor	106
6.1.5 Coupled assay for <i>trans</i> -sialidase using Gal $\beta$ (1,3)GlcNAc $\beta$ -O-Octyl as an acceptor (mark II)	107
6.1.6 Spectrophotometric coupled assay using a variable concentration of donor substrate (Neu $\alpha$ (2,3)Gal $\beta$ -O-PNP) (mark II)	108
6.1.6.2 $K_m$ and $V_{max}$ for <i>trans</i> -sialidase	108
6.1.7 Incubation of <i>trans</i> -sialidase and <i>C. perfringens</i> neuraminidase with 2,3-dehydro-2-deoxy-Neu5Ac	109
6.2 Substituted Gal $\beta$ -O-Octyl analogues	111
6.2.2 Radiochemical assay of Gal $\beta$ -O-Octyl analogues	111
6.2.3 Synthetically substituted Gal $\beta$ -O-Octyl radiochemical incubations	111
6.3 Gal $\beta$ -O-Octyl analogue incubations using Neu5Ac-O-PNP	114
6.3.2 Gal $\beta$ (1,4)GlcNAc $\beta$ -Octyl analogues	115
6.3.3 Gal $\beta$ (1,4)GlcNAc $\beta$ -Octyl analogues radiochemical assay	115



<b>Section</b>	<b>Page</b>
6.3.4 Substituted Gal $\beta$ (1,4)GlcNAc $\beta$ -Octyl analogues incubations using Neu5Ac-O-PNP as a substrate (observed by T.L.C.)	116
6.4 Radiochemical assay of all the Gal $\beta$ (1,X)Gal analogues, [compounds (14)-(21)]	118
6.4.2 Incubation of Gal $\beta$ (1,X)Gal analogues	121
6.4.3 Incubation of Gal $\beta$ (1,2)Gal-O-Me, Glc $\beta$ (1,2)Gal $\beta$ -O-Me and Gal $\beta$ (1,3)Gal $\beta$ -O-Me	121
6.4.4 Incubation of Gal $\beta$ (1,6)Gal $\beta$ -O-CH <sub>2</sub> CH <sub>2</sub> Si(CH <sub>3</sub> ) <sub>3</sub> , Glc $\beta$ (1,6)Gal $\beta$ -O-Octyl and Gal $\beta$ (1,6)Gal $\beta$ -O-Me	121
6.4.5 Incubation of Gal $\beta$ (1,4)[Gal $\beta$ (1,6)Glc] $\beta$ -O-Octyl and Glc $\beta$ (1,6)Gal $\beta$ -O-Octyl	122
6.4.6 3 mg Preparative Scale Synthesis of Neu5Ac $\alpha$ (2,3)Gal $\beta$ (1,6)Gal $\beta$ -O-CH <sub>2</sub> CH <sub>2</sub> Si(CH <sub>3</sub> ) <sub>3</sub>	122
6.4.7 Purification of Neu5Ac $\alpha$ (2,3)Gal $\beta$ (1,6)Gal $\beta$ -O-CH <sub>2</sub> CH <sub>2</sub> Si(CH <sub>3</sub> ) <sub>3</sub>	122
6.4.8 Characterisation of Neu5Ac $\alpha$ (2,3)Gal $\beta$ (1,6)Gal $\beta$ -O-CH <sub>2</sub> CH <sub>2</sub> Si(CH <sub>3</sub> ) <sub>3</sub> – Electrospray Mass Spectrometry	122
6.4.9 Enzymatic digestion of Neu5Ac $\alpha$ (2,3)Gal $\beta$ (1,6)Gal $\beta$ -O-CH <sub>2</sub> CH <sub>2</sub> Si(CH <sub>3</sub> ) <sub>3</sub>	122
6.4.10 3 mg Preparative Scale Synthesis of Neu5Ac $\alpha$ (2,3)[Glc $\beta$ (1,6)]Gal $\beta$ -O-Octyl	123
6.4.11 Purification of Neu5Ac $\alpha$ (2,3)[Glc $\beta$ (1,6)]Gal $\beta$ -O-Octyl	124
6.4.12 Analysis of Neu5Ac $\alpha$ (2,3)[Glc $\beta$ (1,6)]Gal $\beta$ -O-Octyl – Electrospray Mass Spectrometry	124
6.4.13 Analysis of Neu5Ac $\alpha$ (2,3)[Glc $\beta$ (1,6)]Gal $\beta$ -O-Octyl – NMR	124
6.1.14 Systematic enzymatic digestion Neu5Ac $\alpha$ (2,3)[Glc $\beta$ (1,6)]Gal $\beta$ -O-Octyl	124
6.1.15 3 mg Preparative Scale Synthesis of Neu5Ac $\alpha$ (2,3)Gal $\beta$ (1,4)[ $\beta$ Gal(1,6)]Glc $\beta$ -O-Octyl	125
6.4.16 Incubation of Gal $\beta$ (1,4)[ $\beta$ Gal(1,6)]Glc $\beta$ -O-Octyl	126
6.4.17 Purification of Neu5Ac $\alpha$ (2,3)Gal $\beta$ (1,4)[ $\beta$ Gal(1,6)]Glc $\beta$ -O-Octyl	126
6.4.18 Analysis of Neu5Ac $\alpha$ (2,3)Gal $\beta$ (1,4)[ $\beta$ Gal(1,6)]Glc $\beta$ -O-Octyl – Electrospray Mass Spectrometry	126
6.5 Gal $\beta$ -S-X analogue radiochemical assay	127
6.6 Best substrates from Gal $\beta$ -S-X analogue radioactive screen	133
6.7 Serial dilution of Neu5Ac $\alpha$ (2,3)Gal $\beta$ (1,4)[ $\beta$ Gal(1,6)]Glc $\beta$ -O-Octyl (21) radioactive screen	133
6.8 Serial dilution of J6 (of Gal $\beta$ -S-X analogues) radioactive screen	134
<b>7. Conclusions</b>	<b>135</b>
7.1 <i>trans</i> -Sialidase isolation and purification	136
7.2 <i>trans</i> -Sialidase assay development	136
7.3 Radioactive screening of <i>trans</i> -sialidase potential substrate	136
7.4 Screening of Gal $\beta$ -O-Octyl and Gal $\beta$ (1,4)GlcNAc $\beta$ -O-Octyl	136
7.5 Chemo-enzymatic synthesis	138

<b>Section</b>	<b>Page</b>
7.6 Further work	139
<b>Appendix</b>	<b>140</b>
A1 <i>trans</i> -Sialidase purification	141
A1.2 Protein purification protocol - small culture preparation	142
A1.3 Cell Lysis	142
A1.4 Ni <sup>2+</sup> -NTA column purification	143
A1.4.2 Ni <sup>2+</sup> NTA column purification (HPLC)	143
A1.5 Anion Exchange Chromatography	143
A2 Kinetic properties of many enzymes	144
A2.2 Significance of <i>K</i> <sub>m</sub> and <i>V</i> <sub>max</sub> values	147

<b>List of Figures</b>		<b>Page</b>
Figure 1	Incidence of Chagas' disease in South and Central America	2
Figure 2	Structure of benznidazole and nifurtimox	5
Figure 3	Photograph of <i>Trypanosoma cruzi</i>	6
Figure 4	Photograph of the reduviid beetle ( <i>Triatoma infestans</i> ) A and faeces (amanstigote) B	7
Figure 5	2-D diagrammatic representation of the reduvid beetle	8
Figure 6	The three life forms of <i>T. cruzi</i> : (a) amanstigote (b) epimastigote and (c) trypomastigote	9
Figure 7	The life cycle of <i>T. cruzi</i>	10
Figure 8	Structure of sialic acid	11
Figure 9	The four steps of entry into mammalian cells by Trypomastigote <i>Trypanosoma cruzi</i>	12
Figure 10	Transfer of sialic acid by <i>trans</i> -sialidase	13
Figure 11	Schematic of trypomastigote and epimastigote <i>trans</i> -sialidase	14
Figure 12	Dendrogram of sialidase primary structures similarities based on identical amino acid residues	15
Figure 13	Dendrogram comparing all known neuraminidases	16
Figure 14	3-D ribbon drawing of the crystal structure of <i>Micromonospora viridifaciens</i> neuraminidase	20
Figure 15	Structure of 2,7-anhydrosialic acid	21
Figure 16	Diagram of pH and temperature dependence of the transferase activity of <i>trans</i> -sialidase	23
Figure 17A	An electrostatic or covalent interaction followed by hydrolysis of sugar-enzyme complex via H <sub>2</sub> O	25
Figure 17B	A short-lived $\alpha$ -lactone intermediate	26
Figure 18	Structure of <i>para</i> -Nitrophenol (PNP) and 4-methylumbelliferone (4-MU)	29
Figure 19	<i>trans</i> -sialidase in the presence and absence of a potential acceptor substrate, lactose	30
Figure 20	<i>C. perfringens</i> neuraminidase in the presence and absence of a potential acceptor substrate, lactose	31
Figure 21	Incorporation of [ <sup>14</sup> C] lactose	32
Figure 22	Coupled assay for <i>trans</i> -sialidase (mark I)	33
Figure 23	Comparison of <i>trans</i> -sialidase transferase and hydrolase activities with Neu5Ac-O-PNP and Neu5Ac $\alpha$ (2,3)-Gal- $\beta$ -O-PNP substrates	34
Figure 24	Comparison of <i>C. perfringens</i> neuraminidase with and without acceptor	35
Figure 25	Results of the coupled assay for <i>trans</i> -sialidase (Mark II)	36

<b>List of Figures cont.</b>	<b>Page</b>	
Figure 26	Coupled assay using Gal $\beta$ (1,3)GlcNAc $\beta$ -O-Octyl as an acceptor (mark II)	37
Figure 27	<i>trans</i> -sialidase: variable concentrations of Neu5Ac $\alpha$ (2,3)-Gal $\beta$ -O-PNP donor with and without acceptor (Mark II assay)	38
Figure 28A	Plot of 1/S vs 1/v for <i>trans</i> -sialidase, the transferase	39
Figure 28B	Plot of 1/S vs 1/v for <i>trans</i> -sialidase, the hydrolase	40
Figure 29A	2,3-dehydro-2-deoxy-Neu5Ac	41
Figure 29B	Inhibitor study carried out with <i>C. perfringens</i> neuraminidase and <i>trans</i> -sialidase	42
Figure 30	Synthetically substituted Gal $\beta$ -O-Octyl library	44
Figure 31	Biosynthesis of blood group antigens A and B by $\alpha$ (1,3)GalNAcT and $\alpha$ (1,3)GalT	46
Figure 32	Graph of radiochemical assay of Gal $\beta$ -Octyl analogues	49
Figure 33A	<i>trans</i> -sialidase substrate specificity with compounds 1(i,ii,iii,iv) and 3(i,ii,iii,iv)	50
Figure 33B	Compounds 4(i,ii,iii,iv)	51
Figure 33C	Sialylation of Gal $\beta$ -Octyl substrates 3(i,ii,iii,iv)	52
Figure 34	Approximate figures for the sialylation of Gal $\beta$ -O-Octyl analogues (observed by eye)	53
Figure 35	$\alpha$ (1,3)Galactosyltransferase catalysed synthesis of Gal $\beta$ (1,3)Gal $\beta$ (1,4) $\beta$ GlcNAc-OR	55
Figure 36	24 Gal $\beta$ (1,4)GlcNAc $\beta$ -Octyl analogues	55
Figure 37	$\alpha$ (1,3)GalT catalysed glycosylation relative rate	56
Figure 38	The four graphs of radiochemical assay of compounds 5(i,ii,iii,iv)-10(i,ii,iii,iv)	57
Figure 39A	Sialylation products of compounds 8(i,ii,iii,iv), 9(i,ii,iii,iv) and 10(i,ii,iii,iv)	58
Figure 39B	Compounds 11(i,ii,iii,iv)	59
Figure 40	Approximate figures of turnover for <i>trans</i> -sialidase product formation from Gal $\beta$ (1,4)GlcNAc $\beta$ -O-Octyl analogues	60
Figure 41	Diagrammatic representation of key positions required for sialylation by <i>trans</i> -sialidase	61
Figure 42	<i>O</i> -glycosidically linked GlcNAc-bound oligosaccharides isolated from 38/43 kDa glycoproteins from epimastigote <i>T. Cruzi</i> (G-strain)	64
Figure 43	The structures of the <i>O</i> -linked oligosaccharides found in <i>Trypanosoma cruzi</i> Y-strain	66
Figure 44	A variety of potential disaccharides and trisaccharides substrates for <i>T. cruzi trans</i> -sialidase	67

<b>List of Figures cont.</b>		<b>Page</b>
Figure 45	% E/Total (DPM) of all Gal $\beta$ (1,X)Gal	61
Figure 46	<i>p</i> -amino-benzyl-1-thio- $\beta$ -S-galacto-pyranoside (serial dilution)	69
Figure 47	Concentration of <i>p</i> -amino-benzyl-1-thio- $\beta$ -S-galacto-pyranoside versus % inhibition	70
Figure 48	Sialylation of Gal $\beta$ (1,2)Gal $\beta$ -O-Me, Glc $\beta$ (1,2)Gal $\beta$ -O-Me and Gal $\beta$ (1,3)Gal $\beta$ -O-Me	71
Figure 49	Sialylation of Gal $\beta$ (1,6)Gal $\beta$ -O-CH <sub>2</sub> CH <sub>2</sub> Si(CH <sub>3</sub> ) <sub>3</sub> , Glc $\beta$ (1,6)Gal $\beta$ -O-Octyl and Gal $\beta$ (1,6)Gal $\beta$ -O-Me	73
Figure 50	Sialylation of Gal $\beta$ (1,4)[Gal $\beta$ (1,6)Glc] $\beta$ -O-Octyl and Glc $\beta$ (1,6)Gal $\beta$ -O-Octyl	75
Figure 51	<i>trans</i> -sialidase sialylation of Gal $\beta$ (1,6)Gal $\beta$ -O-CH <sub>2</sub> CH <sub>2</sub> SiMe <sub>3</sub>	77
Figure 52	Mass Spectrum of Neu5Ac $\alpha$ (2,3)Gal $\beta$ (1,6)Gal $\beta$ -O-CH <sub>2</sub> CH <sub>2</sub> Si(CH <sub>3</sub> ) <sub>3</sub>	78
Figure 53	Systematic enzymatic digestion Neu5Ac $\alpha$ (2,3)Gal $\beta$ (1,6)Gal $\beta$ -O-CH <sub>2</sub> CH <sub>2</sub> SiMe <sub>3</sub> (25)	79
Figure 54	Diagram of systematic enzyme digestion Neu5Ac $\alpha$ (2,3)Gal $\beta$ (1,6)Gal $\beta$ -O-CH <sub>2</sub> CH <sub>2</sub> SiMe <sub>3</sub> (25)	80
Figure 55	Sialylation of Glc $\beta$ (1,6)Gal $\beta$ -Octyl (20)	82
Figure 56	Mass spectrum of Neu5Ac $\alpha$ (2,3)[Glc $\beta$ (1,6)]Gal $\beta$ -O-Octyl (26)	83
Figure 57	Systematic enzymatic digestion Neu5Ac $\alpha$ (2,3)[Glc $\beta$ (1,6)]Gal $\beta$ -O-Octyl (26)	84
Figure 58	Digestion of Neu5Ac $\alpha$ (2,3)[Glc $\beta$ (1,6)]Gal $\beta$ -O-Octyl (26) by <i>C. perfringens</i> neuraminidase and $\beta$ -glucosidase	85
Figure 59	Di-sialylation of Gal $\beta$ (1,4)[ $\beta$ Gal(1,6)]GlcNAc $\beta$ -O-Octyl (21)	87
Figure 60	Sialylation of Gal $\beta$ (1,4)[ $\beta$ Gal(1,6)]GlcNAc $\beta$ -O-Octyl (21)	88
Figure 61	Mass Spectrum of Neu5Ac $\alpha$ (2,3)Gal $\beta$ (1,4)[ $\beta$ Gal(1,6)]GlcNAc $\beta$ -O-Octyl	89
Figure 62	General scheme for the formation of the library of thio-galactosides	92
Figure 63	Reaction of Gal $\beta$ -S-X analogues	93
Figure 64	The complete substituted Gal $\beta$ -S-X oligosaccharide library	94
Figure 65	Graph of all the best <i>trans</i> -sialidase substrates	96
Figure 66	The best substrate of the substituted Gal $\beta$ -S-X oligosaccharide library J6	97
Figure 67	Graph of J6 and Gal $\beta$ (1,4)[ $\beta$ Gal(1,6)]GlcNAc $\beta$ -O-Octyl % turnover comparison	98
Figure 68	Graph of total radioactive counts (DPM) of each substituted Gal $\beta$ -O-Octyl	114

<b>List of Figures cont.</b>		<b>Page</b>
Figure 69	Graph of total counts of Gal $\beta$ (1,4)GlcNAc $\beta$ -Octyl analogues radioactive assay	118
Figure 70	Total radioactive counts of Galb-S-X analogue library	132
Figure 71	Modifications to saccharides which influence <i>trans</i> -sialidase sialyl transfer	137
Figure 72	<i>trans</i> -sialidase binding site showing the possible orientation of the substrate Gal $\beta$ (1,6)X	138
Figure 72B	Neu5Ac- $\alpha$ (2,3)-S-Gal	139
Figure 73	SDS-Gel of purified <i>trans</i> -sialidase	141
Figure 74	Reaction velocity as a function of substrate concentration	144
Figure 75	Lineweaver-Burke plot	146

<b>List of Tables</b>		<b>Page</b>
Table 1	Definition of Figure 7	10
Table 2	Sequence alignments of <i>Trypanosoma cruzi</i> <i>trans</i> -sialidase with related sialidases/neuraminidases	22
Table 3	Relative acceptor activity (%) of diasaccharide analogues using GalT A and B	47
Table 4	<i>trans</i> -sialidase and <i>C. perfringens</i> neuraminidase assay components	104
Table 5	Comparison of <i>trans</i> -sialidase and <i>C. perfringens</i> neuraminidase reaction rates	105
Table 6	Comparison of <i>trans</i> -sialidase transferase and hydrolase assay components	106
Table 7	Comparison of <i>trans</i> -sialidase transferase and hydrolase activities	106
Table 8	Comparison of <i>C. perfringens</i> neuraminidase with and without acceptor	106
Table 9	Coupled assay for <i>trans</i> -sialidase assay (mark II) components	107
Table 10	Results of coupled assay for <i>trans</i> -sialidase (mark II)	108
Table 11	<i>trans</i> -sialidase: variable concentrations of donor substrate with and without acceptor (mark II)	108
Table 12	1/[S] and 1/v values for <i>trans</i> -sialidase, the transferase	109
Table 13	1/[S] and 1/v values for <i>trans</i> -sialidase, the hydrolase	109
Table 14	Assay components of spectrophotometric inhibitor study on <i>trans</i> -sialidase and <i>C. perfringens</i> neuraminidase	110
Table 15	Results of the spectrophotometric inhibitor study on <i>trans</i> -sialidase and <i>C. perfringens</i> neuraminidase	110
Table 16	Substituted Gal $\beta$ -Octyl analogues radiochemical assay	113
Table 17	Substituted Gal $\beta$ -Octyl analogues radioactive screen	113
Table 18	Assay components of substituted Gal $\beta$ -O-Octyl analogue incubations, monitored by T.L.C	113
Table 19	Amine substituted Gal $\beta$ (1,4)GlcNAc $\beta$ -O-Octyl analogues radioactive screen	114
Table 20	Acid substituted Gal $\beta$ (1,4)GlcNAc $\beta$ -O-Octyl analogues radioactive screen	116
Table 21	Amide substituted Gal $\beta$ (1,4)GlcNAc $\beta$ -O-Octyl analogues radioactive screen	117
Table 22	Guanidino substituted Gal $\beta$ (1,4)GlcNAc $\beta$ -O-Octyl analogues radioactive screen	117
Table 23	Average % E/Total (DPM) of all Gal $\beta$ (1,X)Gal	119

<b>List of Tables cont.</b>		<b>Page</b>
Table 24	Total counts of Gal $\beta$ (1,X)Gal [compounds (14)-(21)] radioactive screen	119
Table 25	Total counts of Gal $\beta$ (1,X)Gal [compounds (14)-(21)] radioactive screen	120
Table 26	Serial dilution of <i>p</i> -amino-benzyl-1-Thio- $\beta$ -S-galacto-pyranoside	120
Table 27	Relative inhibition of <i>p</i> -amino-benzyl-1-thio- $\beta$ -S-galacto-pyranoside	121
Table 28	Radioactive Screen A1-A10	127
Table 29	Radioactive Screen B1-B10	127
Table 30	Radioactive Screen C1-C10	128
Table 31	Radioactive Screen D1-D10	128
Table 32	Radioactive Screen E1-E10	129
Table 33	Radioactive Screen F1-F10	129
Table 34	Radioactive Screen G1-G10	130
Table 35	Radioactive Screen H1-H10	130
Table 36	Radioactive Screen I1-I10	131
Table 37	Radioactive Screen J1-J10	131
Table 38	Best substrates from Gal $\beta$ (1,X)Gal analogue radioactive screen	133
Table 39	Serial dilution of Neu5Ac $\alpha$ (2,3)Gal $\beta$ (1,4)[ $\beta$ Gal(1,6)]GlcNAc $\beta$ -Octyl radioactive screen	133
Table 40	Serial dilution of J6 (Gal $\beta$ -S-X analogue) radioactive screen	134
Table 41	Average protein purification table	142



### Abbreviations Used in the Text (suggested by IUPAC and IUBMB)

*	[ <sup>14</sup> C] radio-label
Δ	Change
Da/e	Mass/charge ratio
E/Total	Eluent/Total (Radiochemical assay)
Ac	Acetyl
AABBS	American Association of Blood Bank Standards
Amanstigote	Life form of <i>Trypanosoma cruzi</i> (Non infectious)
ARC	American Red Cross
Asp box	(Ser/Thr-X-Asp-[X]-Gly-X-Thr-Trp/Phe)
Bn	Benzyl
BSA	Bovine serum albumin
Chagoma	Biological swelling as a result of <i>T. cruzi</i>
Da	Daltons
Disacch	Disaccharide
DPM	Disintegrations per minute
<i>E. coli</i>	<i>Escherichia coli</i>
EIA	Enzyme Immuno Assay
Enz	Enzyme
Epimastigote	Life form of <i>Trypanosoma cruzi</i> (Infects insects)
FDA	Food and Drug Administration
FAB	Fast atom bombardment
Fuc	Fucose
G.C.	Gas chromatography
Gal- <i>f</i>	Galacto- <i>furanose</i>
Gal- <i>p</i>	Galacto- <i>pyranose</i>
Gal	Galactose
GalNAc	<i>N</i> -Acetylgalactosamine
Glc	Glucose
GlcNAc	<i>N</i> -Acetylglucosamine
GPI	glycosyl-phosphatidylinositol
GR	Glutathione Reductase
GSH	Reduced Glutathione

HA	Hemagglutinin
HEPES	(N-[2-Hydroxyethyl]piperazine-N'-[2-ethenesulfonic acid])
HIV	Human immuno virus
HPLC	High performance liquid chromatography
IC <sub>50</sub>	50 % inhibition concentration
IgG	Immunoglobulin G
IgM	Immunoglobulin M
IFN- $\gamma$	Interferon gamma
IIF	Immunofluorescence Assay
Lac	Gal $\beta$ (1,4)Glc
LacNAc	<i>N</i> -Acetyllactosamine (Gal $\beta$ (1,4)GlcNAc)
Macrophage	A large phagocytic white blood cell
Man	Mannose
MS	Mass spectrometry
Monosacch	Monosaccharide
Mucin	Endothelial (Cell-lining) Cells
Murine	Mouse/Mice
NAc	<i>N</i> -Acetyl
Neu5Ac	<i>N</i> -acetylneuraminic acid
Neu5Ac2en	2,3-dehydro- <i>N</i> -acetylneuraminic acid
Neu5NH <sub>2</sub>	Neuraminic acid
NMR	Nuclear magnetic resonance
OD	Optical density
Oct	Octyl
PAGE	Poly acrylamide gel electrophoresis
<i>p</i> NP	<i>p</i> -nitrophenyl
RIPA	Radioimmunoprecipitation Assay
Rf	Ratio of product height/solvent front (T.L.C. reference)
RNA	Ribonucleic acid
SDS	Sodium dodecyl sulfate
T.L.C.	Thin layer chromatography
TR	Trypanothione Reductase
Trypomastigote	Life form of <i>Trypanosoma cruzi</i> (Infects humans)

TS	Transition state
T[SH] <sub>2</sub>	Trypanothione
WHO	World Health Organization
Xyl	Xylose
Neuraminidase = Sialidase	

# Chapter 1

## Introduction

## 1.1 Chagas' Disease

The parasite *Trypanosoma cruzi* is the causative agent of Chagas' disease, a debilitating condition discovered in 1909 in Brazil by Carlos Chagas. This disease is already endemic in Latin America, affecting approximately 8 % of the population of South and Central America as indicated in **Figure 1** (Colli 1993, Muller and Baker 1990). This number is only an estimation since difficult geography and inadequate reporting may underestimate the numbers exposed.

**Figure 1 Incidence of Chagas' disease in South and Central America (Highlighted in black) Muller and Baker 1990**



The migration of population from Latin America to the United States to escape poor housing and living conditions has highlighted this disease (Kirchhoff *et al* 1997). Blood studies carried out in the southern most States of North America (i.e. California and Florida) assessed the potential risk of the spread of disease.

### 1.1.2 Blood studies

Population migration is often a problem for both health organisations and governments trying to prevent spread of disease (*Kirchhoff et al 1997*). The Food and Drug Administration (FDA), American Association of Blood Banks Standards (AABBS) and the American Red Cross (ARC) carried out their own investigations, from June 1993-1995, screening blood from blood donors in the US for anti *T. cruzi* antibodies. The tests showed that 3-4 % of the blood donors that had lived in an endemic area, in poor housing, or had received a blood transfusion in that country had specific antibodies to *T. cruzi* (*i.e.* that they had been in contact with the disease) (*Kirchhoff et al 1997*). However, no one born in the US had antibodies to *T. cruzi*. This indicates that frequent travellers to a Chagas' disease endemic country are at little risk provided they do not live there or receive a blood transfusion there (*Kirchhoff et al 1997*). All blood transfusion samples are now routinely screened with the (commercially available) immunoassays used in these studies. In the USA, FDA research indicates that there has been only one reported case of blood with possible *T. cruzi* antibodies present being transfused (discovered retrospectively but with no sign of infection). Similarly, ARC studies uncovered 11 possible recipients of contaminated blood but with no trace of disease (*Kirchhoff et al 1997*).

A similar voluntary study was carried out on a group of one hundred Latin American immigrants (60 men 40 women) living in Berlin, Germany, between May and August 1995 (*Frank et al 1997*). This study assessed the conceivable risk of infection of *T. cruzi* in congenital transmission and blood transfusion, previously cautioned by the World Health Organisation (WHO). An indirect immunofluorescence assay (IIF) using antigenic immobilised trypomastigotes (parasites) was used to test all subjects. A control group of non-Latin American Germans was also tested. The positive IIF samples were subsequently assessed by ELISA using crude Peruvian *T. cruzi* strain. Only five of the 100 samples tested positive to both tests (*Frank et al 1997*). To exclude any potentiality of cross-reactivity, the group was also tested with *Leishmania infantum* antigens. All samples, which gave positive tests with *Leishmania infantum*, were excluded from the study. Five subjects tested positive to IIF/ELISA but only two (one male, one female) were

negative to the *Leishmania* assay also. These two individuals were from Urban South America, although it is believed that Chagas' disease is more prevalent in rural areas (Frank *et al* 1997). Hence, the relative existence of *T. cruzi* in this sample of South American immigrants is 2 %. The estimation of the risk of blood infection from *T. cruzi* by the WHO is 4 to 5 % (Frank *et al* 1997). Blood transfusion in Brazil is believed to be responsible for 20 % of the 100,000 new cases of *T. cruzi* each year, with a 13-25 % risk of infection with each unit of blood transfused (Frank *et al* 1997). It is thought that the number of immigrants from South and Central America now living in Europe is approximately 300,000 hence, the WHO estimates that there are 15,000 *T. cruzi* carriers in Europe (Frank *et al* 1997).

### 1.1.3 The Disease and its effects

Chagas' disease has two forms: chronic and acute (Muller and Baker 1990). The acute form lasts for only a few months, with *T. cruzi* replicating very quickly in the host causing death. In the chronic form, the patient may not develop any symptoms for many years (approximately eight). After infecting the host, the parasite remains dormant (Muller and Baker 1990). The initial incubation time for the disease can be up to a few weeks with only one in four patients developing the disease (Kirchhoff *et al* 1997). Hence, life expectancy and symptoms of sufferers are very varied (Muller and Baker 1990, Smyth 1994): only immuno-compromised patients (*i.e.* HIV patients) exhibit all symptoms early on in the sickness (Kirchhoff *et al* 1997).

On contracting the disease, the parasite re-sites in the blood stream where it removes sialic acid from soluble and human cell surface glycoconjugates. Neurones are particularly vulnerable (Muller and Baker 1990). Pseudo cysts released by the parasite are mainly concentrated in the gastrointestinal tract, oesophagus, colon or the heart. The resultant enlargement of tissue, causing considerable distress and discomfort is known as a Chagoma (Smyth 1990 and Muller and Baker 1990).

Swelling of the colon can lead to rupture of the stomach, whereas oesophageal swelling causes starvation. However, the most common fatal condition is pseudo cyst aggregation in the heart and denervation, causing permanent cardiac damage and heart failure. "Swollen eyes" are also a classic symptom of an infected patient (Smyth 1990).

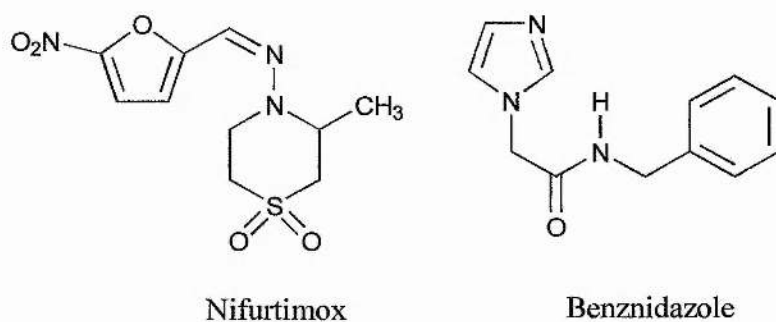
### 1.1.4 Host resistance to *trans*-sialidase

The macrophage is the principal resistance mechanism shown in both *in vitro* and *in vivo* experimental studies to the *T. cruzi* pathogen (Gazzinelli *et al* 1997). The IFN- $\gamma$  macrophage is produced in the respiratory tract in response to the pathogen, which in turn liberates reactive oxygen species to destroy the parasite (Gazzinelli *et al* 1997). The microbiocidal activity against *T. cruzi* displayed by murine macrophages is largely because of oxygen-independent nitric oxide synthesis. This hypothesis has been tested with nitric oxide synthesis inducing compounds and with murine macrophages which show increased anti-parasitic activity (Gazzinelli *et al* 1997).

### 1.1.5 Possible treatments

Currently there is no known cure or effective treatment for Chagas' disease. The nitrogen heterocycles nifurtimox and benznidazole are commonly used, but have little effect and only early on in the sickness. Both are toxic to the patients (Muller and Baker 1990). The structure of these drugs is shown below in **Figure 2**.

**Figure 2** Structure of nifurtimox and benznidazole



Trypanosomes, like mammals, use reduced glutathione (GSH) to prevent possible damage by free radicals (Cassels *et al* 1995). However they lack the essential enzyme glutathione reductase (GR), and consequently use a non-enzymatic process involving trypanothione (T[SH]<sub>2</sub>) to produce GSH (Cassels *et al* 1995). Trypanothione reductase (TR) maintains the correct level of GSH required. TR and GR are completely distinct, are non-interchangeable and can therefore be exploited as potential drug targets. Interestingly, nifurtimox, used as a trypanothione reductase

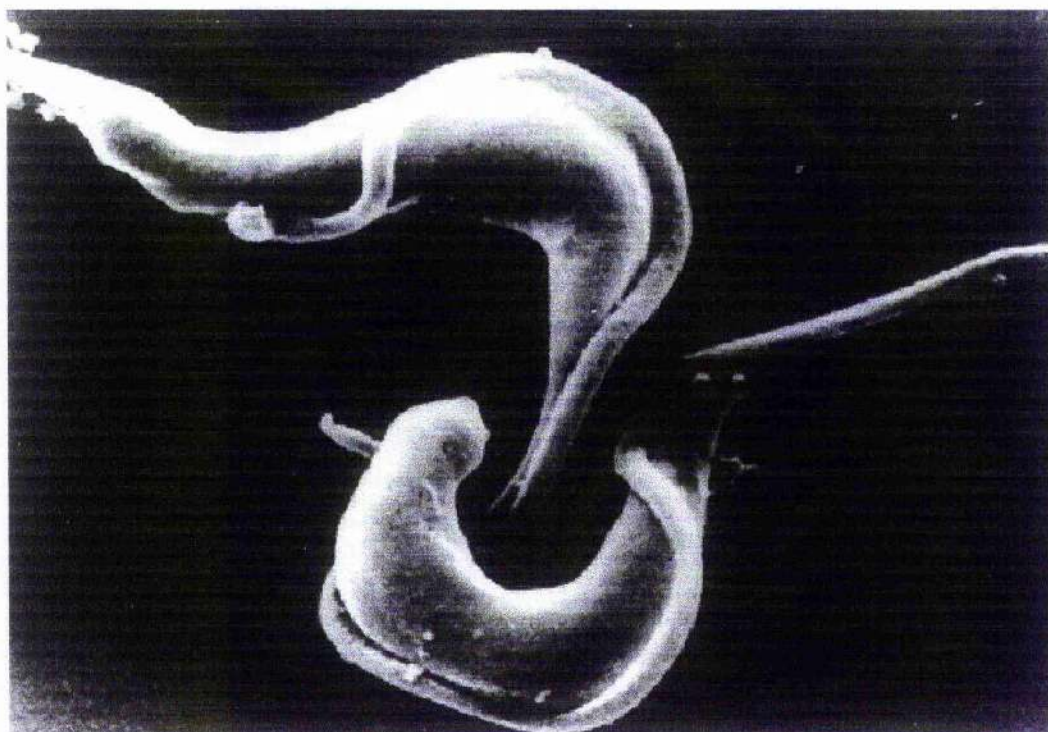


inhibitor, is a better inhibitor of GR than TR, which explains some of the highly toxic effects exhibited by patients (Cassels *et al* 1995). The ability to inhibit one enzyme selectively is an essential commodity of any possible compound used as a drug. Many such compounds have been identified but other criteria such as poor solubility or low potency have limited their uses.

### 1.2 *Trypanosoma cruzi*

*Trypanosoma cruzi* is an elongated protozoon of between 15-25  $\mu\text{m}$  in length, with a curved flagella, shown in **Figure 3**. It does not have a surface coat and cannot undergo any antigen variation, in contrast to its African counterpart *T. brucei* (Ferguson *et al* 1994). To avoid detection by the hosts immune system the parasite quickly moves out of the bloodstream into cells (Smyth 1994).

**Figure 3** Photograph of *Trypanosoma cruzi* (1000 x magnification)

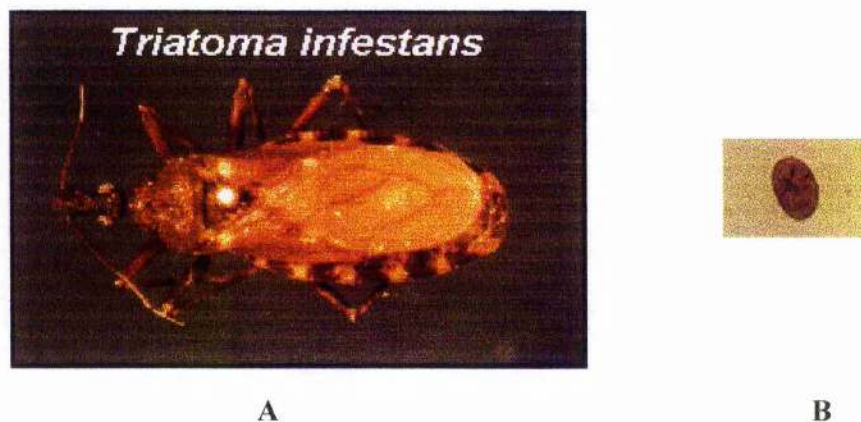


### 1.2.2 *T. cruzi* transmission vector

The *T. cruzi* transmission vector is the brightly coloured reduvid beetle, shown below in **Figure 4A**. In this vector, the parasite is restricted to the gut. The beetle uses a proboscis located anterior to puncture the hosts' skin to gain access to the blood stream (Colli 1993). After ingestion of a blood meal, the beetle immediately defecates on the surface of the hosts' skin. The beetle puncturing the hosts' skin causes an irritation and the inevitable scratching. The parasite then gains entry to the bloodstream via the faeces (or in some cases via mucus membranes). A photograph of the faeces is shown below in **Figure 4B**.

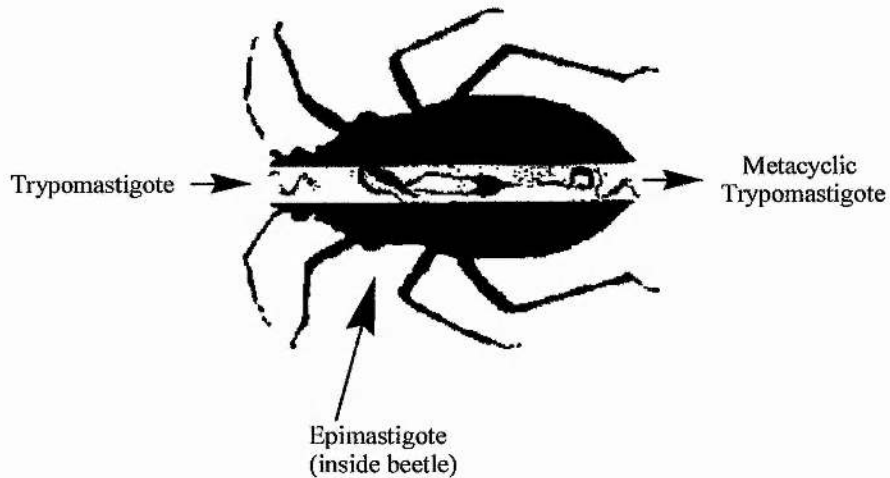
**Figure 4** Photograph of the reduvid beetle (*Triatoma infestans*) A and faeces (amastigote) B

[http://vflylab.angis.org.au/edesktop/WWW\\_Projects/Animals\\_Plants/TrypanosomaCruzi\\_thuynh/Start.html](http://vflylab.angis.org.au/edesktop/WWW_Projects/Animals_Plants/TrypanosomaCruzi_thuynh/Start.html)



The life forms of the parasite in the invertebrate host are different to the mammalian host. **Figure 5** shows a 2-D representation of the parasitic life forms proboscis to the exterior the reduvid beetle. The beetle ingests the parasite as trypomastigote, which metamorphoses to the epimastigote to allow replication. It will then manipulate itself into the metacyclic trypomastigote form before excretion (defecation).

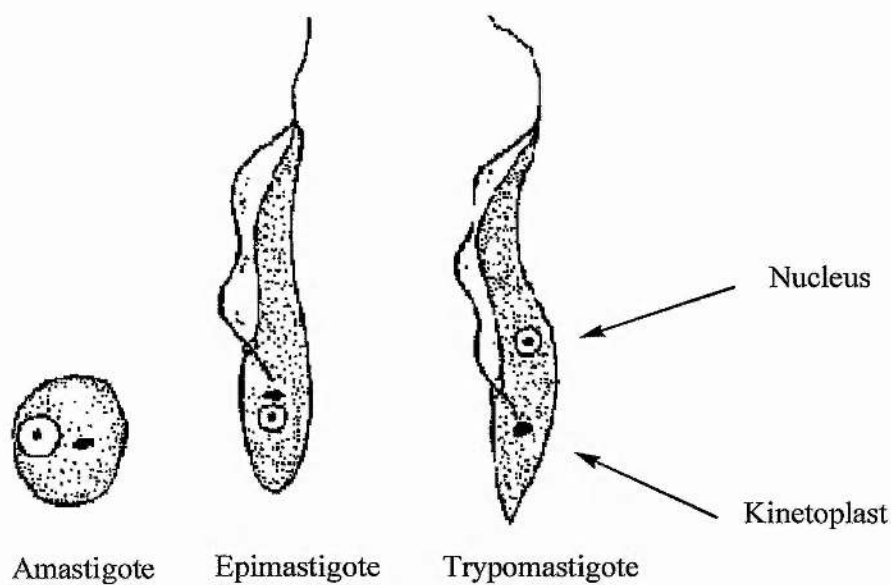
**Figure 5** 2-D diagrammatic representation of the reduvid beetle *Colli* 1993



### 1.2.3 The Life forms of *T. cruzi*

The parasite has three life forms, amastigote, epimastigote and trypomastigote (*Smyth* 1994). The highly infectious trypomastigote form circulates in the bloodstream and invades cells to escape from the hosts' immune system. In order to replicate, the parasite must manipulate itself into the amastigote form (*Schenkman* and *Brines* 1994). It has to revert into the trypomastigote form to escape into the blood stream of the host to recirculate. This stage of the parasite life cycle has an important role in the enzyme activity: in the trypomastigote form, *trans*-sialidase potential is greatest, whereas the amastigote life form shows no such enzymatic activity (*Schenkman* and *Brines* 1994). A digramatic representation of the three parasitic forms is illustrated in **Figure 6**.

**Figure 6** The three life forms of *T. cruzi* : (a) amastigote (b) epimastigote and (c) trypomastigote *Smyth 1994*



#### 1.2.4 *T. cruzi* life cycle

The complete life cycle of *T. cruzi* showing the manipulation of life forms within both the mammalian and insect vectors is shown below in **Figure 7**.

**Figure 7** The life cycle of *T. cruzi* (adapted from Smyth 1994)

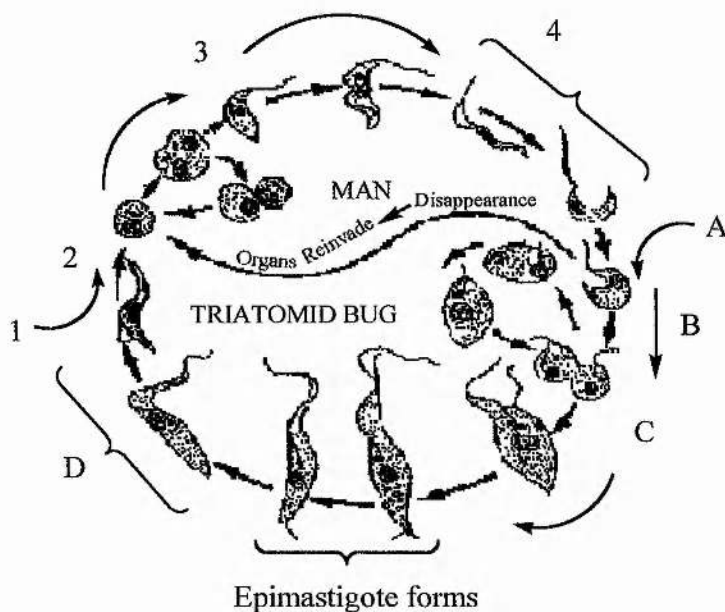


**Table 1** Definition of Figure 7

Man	Insect
1. Bite	A. Bite
2. Initial infection by faeces	B. Infected blood taken up by bug
3. Amastigote forms multiply in heart or reticulo-endothelial	C. Multiplication in mid-gut spreading to hind-gut
4. Transformation of trypanosomes – appear in peripheral blood	D. Transformation to metacyclic form in rectum

### 1.3 The Inflammation and Immune Responses

After the onset of the acute phase of Chagas' disease, usually 30-90 days, there is a massive accelerated immune response by the human host. The mechanism for this activation is as yet unknown (Gazzinelli *et al* 1997). On the surface of both amastigote and trypomastigote parasite form of the parasite are abundant Glycophosphoinositol-linked (GPI) mucins (*O*-linked glycoproteins). Mucins are generally structurally important to endothelial cells for protection and lubrication. *T. cruzi* GPI mucins stimulate inflammatory macrophages to produce cytokines. It is believed that it is the GPI anchored structures, that stimulate this response (Gazzinelli *et al* 1997). Metacyclic trypomastigotes and epimastigotes also have GPI mucins but

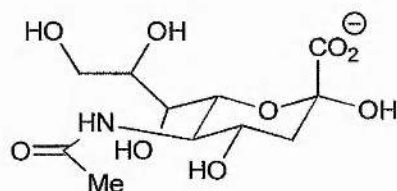


these GPI anchors are not able stimulate a response. A possible explanation for this is that the amastigote and trypomastigote GPI anchors are structurally distinct, hence producing a different response (*Gazzinelli et al 1997*). Most patients produce a significant immune response (predominately IgG and IgM isotopes) to trypomastigote GPI mucins, most of the antibodies bled at this stage recognise Gal $\alpha$ (1,3)Gal found in these mucins (*Gazzinelli et al 1997*).

### 1.3.2 Cell invasion

Sialic acid plays a major role in parasite cell invasion (*Smyth 1994*). The structure is shown below in **Figure 8**; sialic acid is transferred from the host to the parasite, sialylating the trypomastigote. The deprotonated carboxylic acid of the sialic acid gives the parasite a net surface negative charge assisting cell adhesion and hence cell invasion, **Figure 9** (*Schenkman and Vandekerckhove 1993*).

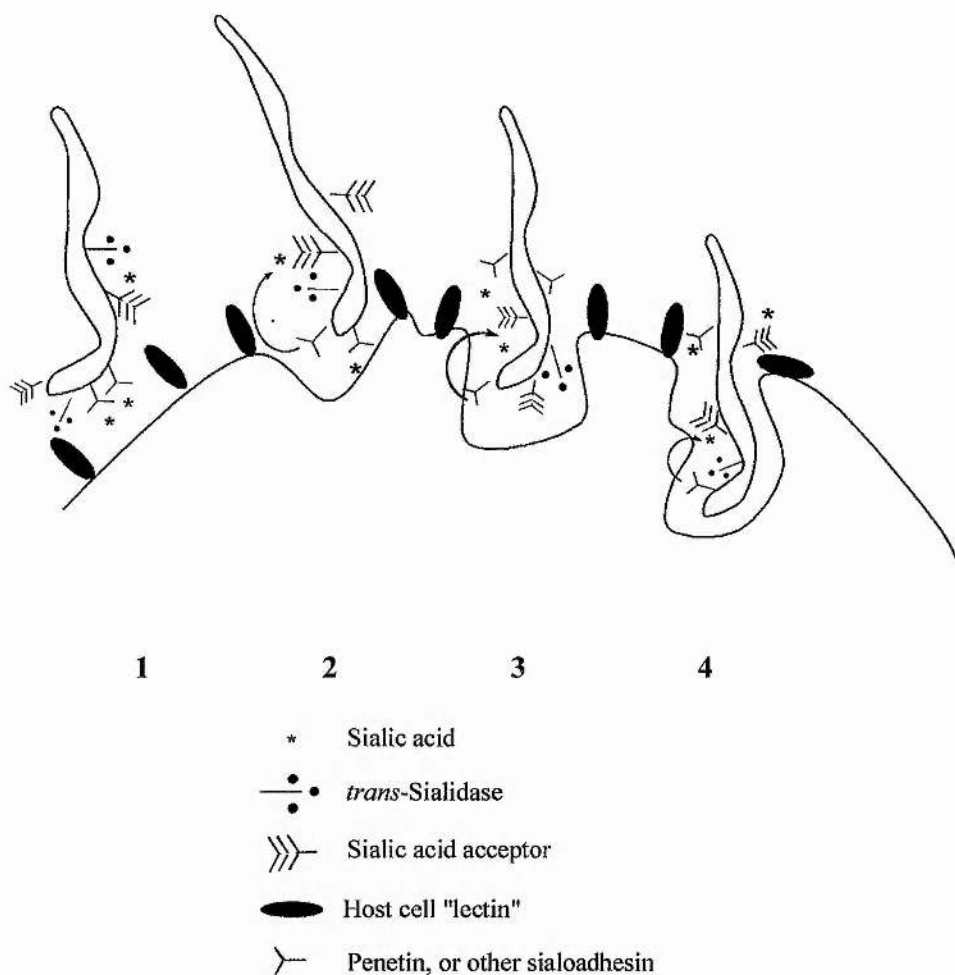
**Figure 8** Structure of sialic acid (Neu5Ac)



Sialic acid (Neu5Ac)

It is believed that trypomastigote *trans*-sialidase removes sialic acid from the cells of the host, transferring it onto itself, allowing the parasite to “stick” to the cell surface. The parasite is then engulfed into the cell by the process on endocytosis. These steps are illustrated below in **Figure 9**.

**Figure 9** The four steps of entry into mammalian cells by Trypomastigote *Trypanosoma cruzi* (adapted from *Schenkman* 1993)

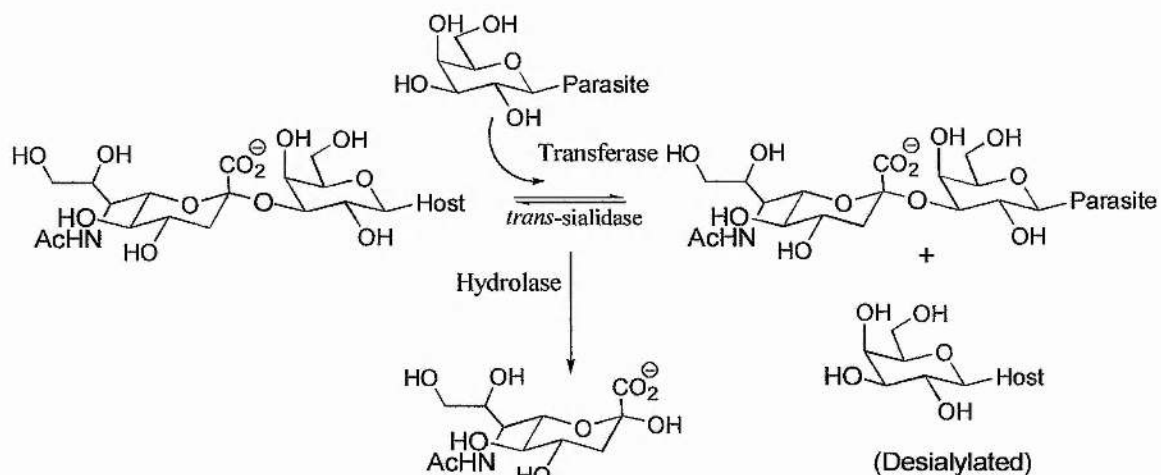


After invasion, the host produces an immune reaction, yielding a phagosome, which encapsulates the parasite (*Schenkman* and *Frevert* 1992). However, within a few minutes the parasite is free once more. It is believed that *trans*-sialidase enables the parasite to escape more easily by disrupting the membrane of the phagosome (*Schenkman* and *Vandekerckhove* 1993). These conclusions were based on studies carried out on blood cells with a high sialic acid content.

## 1.4 *trans*-Sialidase reactions

*trans*-sialidase has two activities: a hydrolase and a transferase activity (Scudder *et al* 1993). This enzyme is unique in that it preferentially catalyses the transfer reaction of sialic acid to mucin-like molecules forming an  $\alpha$ 2,3 bond with  $\beta$ -galactose acceptors on the surface of the parasite (Schenkman *et al* 1997). Although it is primarily a transferase, it does have some residual hydrolase activity, **Figure 10**. The transfer reaction is freely reversible.

**Figure 10** Transfer of sialic acid by *trans*-sialidase

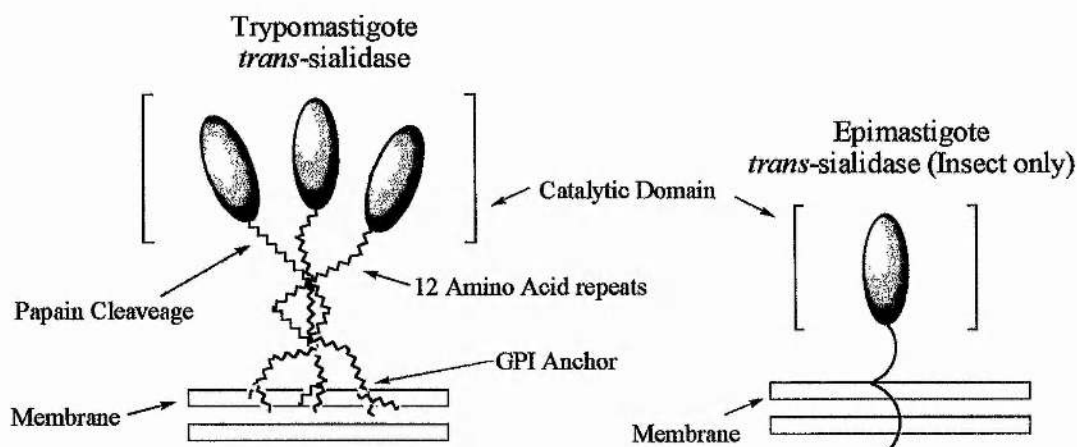


### 1.4.2 Parasitic attachment of *trans*-sialidase

*trans*-Sialidase is attached to the surface of the trypomastigote via a GPI anchor. However its attachment to the epimastigote is trans-membrane. A diagrammatic representation of these points is shown in **Figure 11**. This diagram also shows the catalytic domain of *trans*-sialidase.



**Figure 11** Schematic of trypomastigote and epimastigote *trans*-sialidase (adapted *Schenkman and Nussenzweig* 1992)



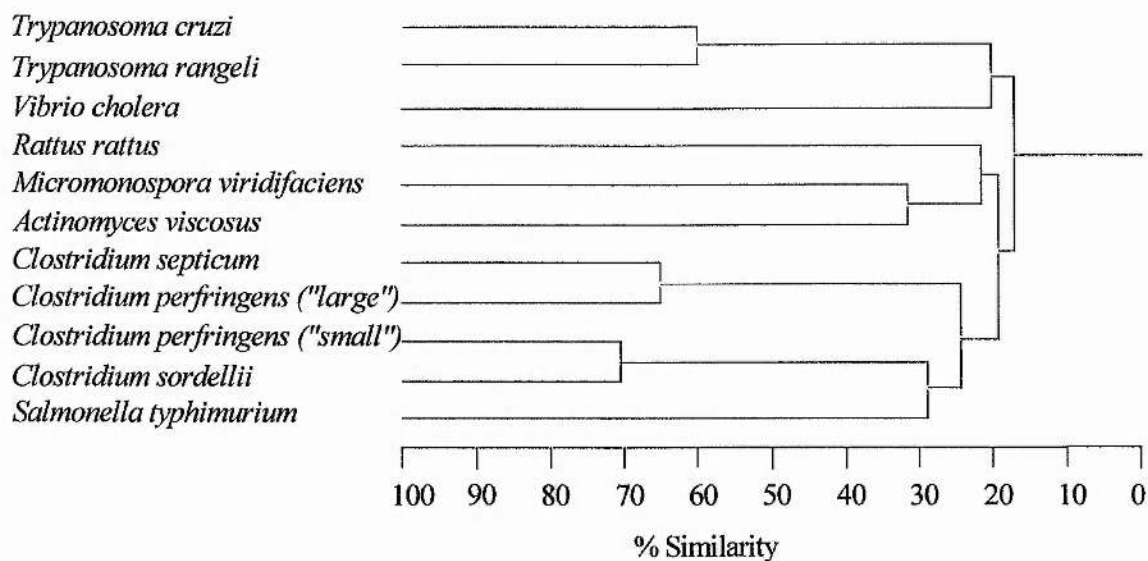
After selected proteolysis using papain at the site indicated, a 70 kDa unit is left in which full enzymatic activity is retained. The 15 kDa cleaved fragment contains 12 amino acid unit repeats located at the carboxyl terminal, which is attached to the parasite via a GPI anchor. This 15 kDa is not essential for enzymatic activity, stability or for correct folding of the protein during biosynthesis (*Schenkman and Chaves* 1994).

Significantly, other related sialidases and glycosidases catalyse both transfer and hydrolysis reactions but rates of the hydrolysis reactions are always much faster (typically greater than 100 times faster). The relationship between *trans*-sialidase and *C. perfringens* neuraminidase will be discussed further in Chapter 2.

### 1.4.3 *trans*-Sialidase primary structure

The primary sequence of the *T. cruzi* sialidase has 1162 amino acids arranged into four domains (*Takle and Cross* 1993). It also contains three elements conserved in most sialidases. **Figure 12** illustrates the percentage similarities of these and other related neuraminidases.

**Figure 12** Dendrogram of sialidase primary structures similarities based on identical amino acid residues (Biology of Sialic acids, *Rosenberg*).



#### 1.4.4 Comparison of the mechanism of *trans*-sialidase and with other neuraminidases

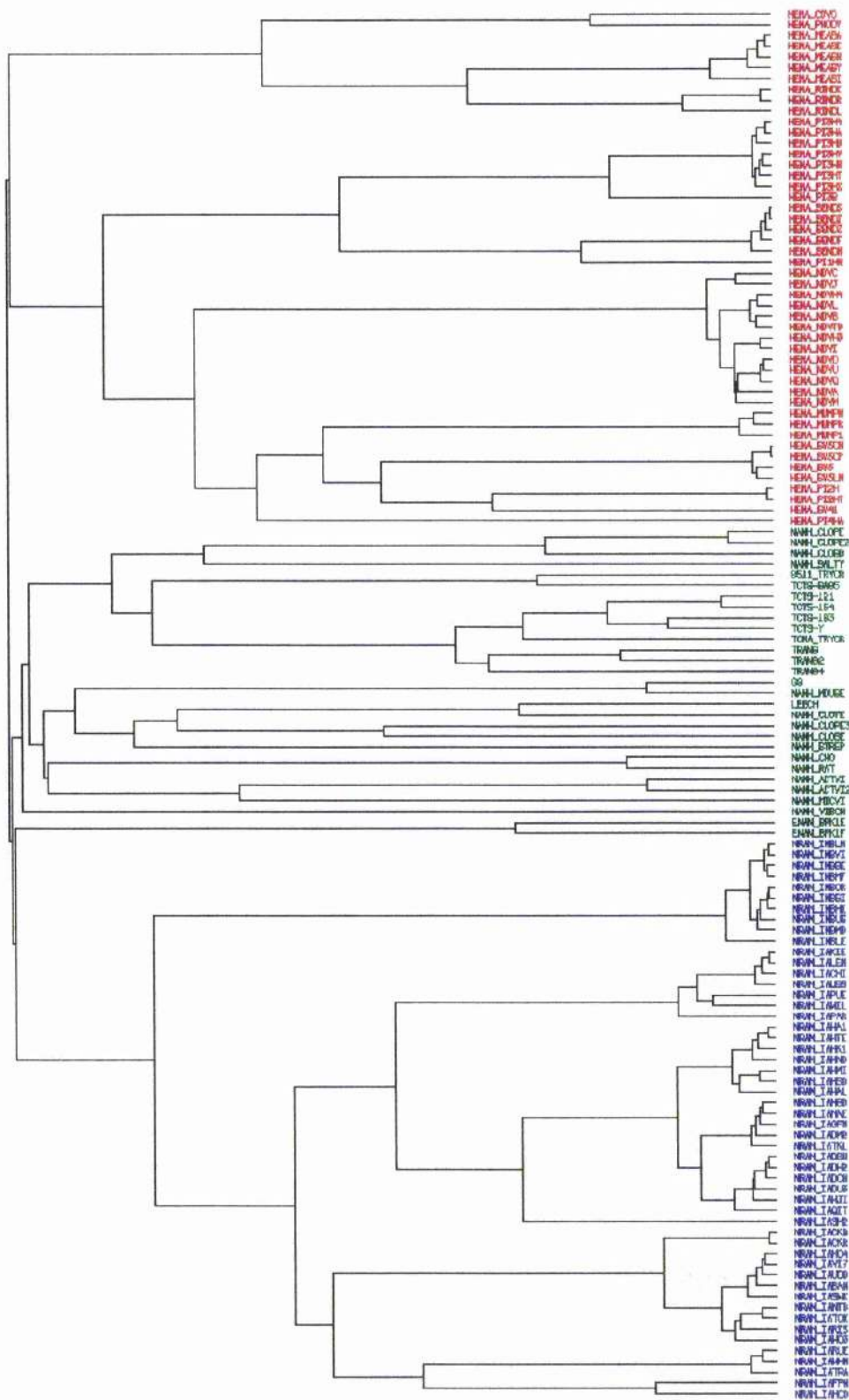
Sialidases are common place in many microbial pathogens, for example *Salmonella typhimurium* and *Vibrio cholera* amongst others. Sialidases have also been implicated in infections by Influenza A and B virus, and they have been therapeutic targets for many years. In Influenza A and B, the sialidase enzyme is responsible for the destruction of receptors, allowing the virus to spread and replicate (*Bamford 1995*). It is this recognition of sialic acid by the Influenza receptor that has provided the biggest target for rational drug design (*Bamford 1995*). Most of the essential information on enzyme substrate recognition has been elucidated from the x-ray crystal structure (*Taylor et al 1995*).

Sialidases have been isolated from various mammalian tissues as well as bacteria and viruses (*Taylor et al 1995*). The divergence of location and structure of sialidases/neuraminidases creates a large super-family (approximately 40 members) of related enzymes (*Taylor 1996*). The relationship between some of these neuraminidases is illustrated below in **Figure 13**.

An expansion of the legend of **Figure 13** is shown below.

Hemagglutinin- Neuraminidase viruses (HN shown in Red)	Non-viral sialidase (shown in green)	Influenza neuraminidases (shown in blue)	Influenza neuraminidase (split into 9 NA sub- types, blue)
HEMA_CDVO	NANH_CLOPE	NRAM_INBLN	NRAM_IALEN
HEMA_PHODV	NANH_CLOPE2	NRAM_INBVI	NRAM_IACHI
HEMA_MEASA	NANH_CLOSO	NRAM_INBBE	NRAM_IAUSS
HEMA_MEASE	NANH_SALTY	NRAM_INBMF	NRAM_IAPUE
HEMA_MEASH	8511_TRYCR	NRAM_INBOR	NRAM_IAWIL
HEMA_MEASY	TCTS_SA85	NRAM_INBSI	NRAM_IAPAR
HEMA_MEASI	TCTS_121	NRAM_INBHK	NRAM_IAHAI
HEMA_RINDK	TCTS_154	NRAM_INBUS	NRAM_IAHTE
HEMA_RINDR	TCTS_193	NRAM_INBMD	NRAM_IAHKI
HEMA_RINDL	TCTS_Y	NRAM_INBLE	NRAM_IAHNO
HEMA_PI3H4	TCNA_TRYCR	NRAM_IAKIE	NRAM_IAHMI
HEMA_PI3HA	TRANG		NRAM_IAHSO
HEMA_PI3HU	TRANG2		NRAM_IAHAL
HEMA_PI3HV	TRANG4		NRAM_IAHGD
HEMA_PI3HW	(Human and mouse MHC/lysosomal)		NRAM_IAMAE
HEMA_PI3HT	G9		NRAM_IAGFN
HEMA_PI3HX	NANH_MOUSE		NRAM_IADM2
HEMA_PI3B	LEECH		NRAM_IATKL
HEMA_SENDS5	NANH_CLOTE		NRAM_IADBU
HEMA_SENDJ	NANH_CLOPE3		NRAM_IADH2
HEMA_SENDZ	NANH_CLOSE		NRAM_IADCH
HEMA_SENDF	NANH_STREP		NRAM_IADU3
HEMA_SENDH	(Mammalian cytosolic)		NRAM_IAHJI
HEMA_PIIHW	NANH_CHO		NRAM_IAQIT
HEMA_NDVC	NANH_RAT		NRAM_IASH2
HEMA_NDVJ	(Bacterial)		NRAM_IACKQ
HEMA_NDVI	NANH_ACTVI		NRAM_IACKR
HEMA_NDVD	NANH_ACTVI2		NRAM_IAHO4
HEMA_NDVU	NANH_MICVI		NRAM_IAVI7
HEMA_NDVQ	NANH_VIBCH		NRAM_IAUDO
HEMA_NDVA	(Bacteriophage)		NRAM_IABAN
HEMA_NDVM	ENAN_BPK1E		NRAM_IASWK
HEMA_MUMPM	ENAN_BPK1F		NRAM_IANT6
HEMA_MUMPR			NRAM_IATOK
HEMA_MUMP1			NRAM_IARI5
HEMA_SV5CM			NRAM_IAHO3
HEMA_SV5CP			NRAM_IARUE
HEMA_SV5			NRAM_IAWHM
HEMA_SV5LN			NRAM_IATRA
HEMA_PI2H			NRAM_IAFPW
HEMA_PI2HT			NRAM_IAHCO
HEMA_SV41			
HEMA_PI4HA			

**Figure 13** Dendrogram comparing all known neuraminidases (This diagram is the property of Prof. G. L. Taylor, University of Bath, UK and is reproduced with his permission).



It is suggested that bacterial sialidases are a causative agent of microbial infections in animals, whereas mammalian neuraminidases largely catabolise sialoglycoconjugates (Taylor 1996). Sialidases can be important in the regulation of cell surface sialic acids, for example in the immune system, where the life time of certain circulating cells has to be regulated (Taylor 1996). It is the fine adjustment of sialidase versus sialic acid, which is paramount to maintaining this balance in biological systems. It is the exploitation of these terminal sialic acids by pathogens which causes disease.

There seems to be significant variation, however, in the mechanism of action of various neuraminidases. Two distinct families of sialidases are apparent: one has greater enzymatic activity when a divalent metal is bound in the co-ordination site; the other family show no significant increase in activity in the presence of metal ions (Taylor *et al* 1993). In some cases, electrostatic interactions between enzyme and sugar are important and in other cases hydrogen bonding at the anomeric centre is significant, since these charge interactions can assist with the stabilisation of the transition state and can control the overall stereochemistry of the reaction. Generally, one or more carboxylic acids in the binding site catalyse or stabilise the reaction.

#### **1.4.5 Viral Neuraminidases**

Viral neuraminidases are responsible for the promotion of infection in mammalian cells (Von Itstein *et al* 1993). Since self-agglutination of new viral particles may stop replication of the disease, viral neuraminidases remove the key sugar involved, namely sialic acid.

##### **1.4.5.2 Influenza A virus neuraminidase**

Influenza virus neuraminidase is tetrameric, 240 kDa in size, consisting of four identical monomer units, joined by eight disulphide bridges. Each monomer incorporates a protein fold known as a super-barrel or  $\beta$ -propeller (Taylor *et al* 1995). The pseudo-symmetrical arrangement of this structure comprises of four  $\beta$ -sheets antiparallel to each other, repeated six times (i.e. six propeller blades). This gives rise to a six fold rotation axis about its centre. All sub-types of Influenza A and B virus duplicate this motif, although the amino acid sequence (conservation identity of  $\leq 40\%$ ) would not suggest this (Taylor *et al* 1995). Influenza A is classed as an



RNA virus, having an RNA genome in a membrane envelope. The membrane itself (1000 Å in diameter) envelopes three proteins. The two most important proteins in the membrane are hemagglutinin (HA) and neuraminidase, both trans-membrane glycoproteins (*Portner et al 1995*). HA is responsible for cell invasion via receptor-mediated endocytosis, using sialic acid from the surface of vulnerable cells in the respiratory tract (*Portner et al 1995*). Before HA releases the viral RNA into the cytosol, neuraminidase must cleave the terminal sialic acid to prevent the virus being removed and destroyed by the host. The enzymatic activity of the virus improves significantly with the binding of  $\text{Ca}^{2+}$ , hydrolysis appearing to proceed with retention of configuration (*Von Itstein 1995*).

#### **1.4.6 Bacterial neuraminidases**

Bacterial sialidases have limited sequence homology, approximately 30 % to each other, although all contain conserved motifs: RIP/RLP (Arg-Ile/Leu-Pro) followed by an Asp box (Ser/Thr-X-Asp-[X]-Gly-X-Thr-Trp/Phe) where X represents any amino acid (*Taylor et al 1993*). The conservation between bacterial and viral sialidases is lower still at approximately 15 %. Many bacteria produce sialidases to remove sialic acid as an energy and carbon source. The bacterial cell is equipped with the necessary cell organelles to deliver and catabolise sialic acid (*Taylor et al 1996*). Bacterial sialidases vary in size between 40-120 kDa and are mostly monomeric units, either anchored to the cell surface, or are soluble when secreted (*Taylor et al 1996*).

##### **1.4.6.2 *Salmonella typhimurium* LT2 - neuraminidase**

*Salmonella typhimurium* neuraminidase is 42 kDa and has one of the simplest protein architectures, consisting of only one propeller fold characteristic of the neuraminidase super-family. The primary protein arrangement is four  $\beta$ -sheets organised antiparallel relative to each other, repeated six times, to form the propeller type arrangement (*Taylor et al 1995*). Between the  $\beta$ -sheets lie large regions of hydrophobic residues, aiding the stabilisation of this secondary element. This enzyme is a monomer of approximately 391 residues and it is believed that proton donation is required for leaving group departure (*Sinnott and Laver 1994*). It does not bind  $\text{Ca}^{2+}$  to enhance enzymatic activity and contains only one disulphide bridge (*Sinnott and*

Laver 1994).

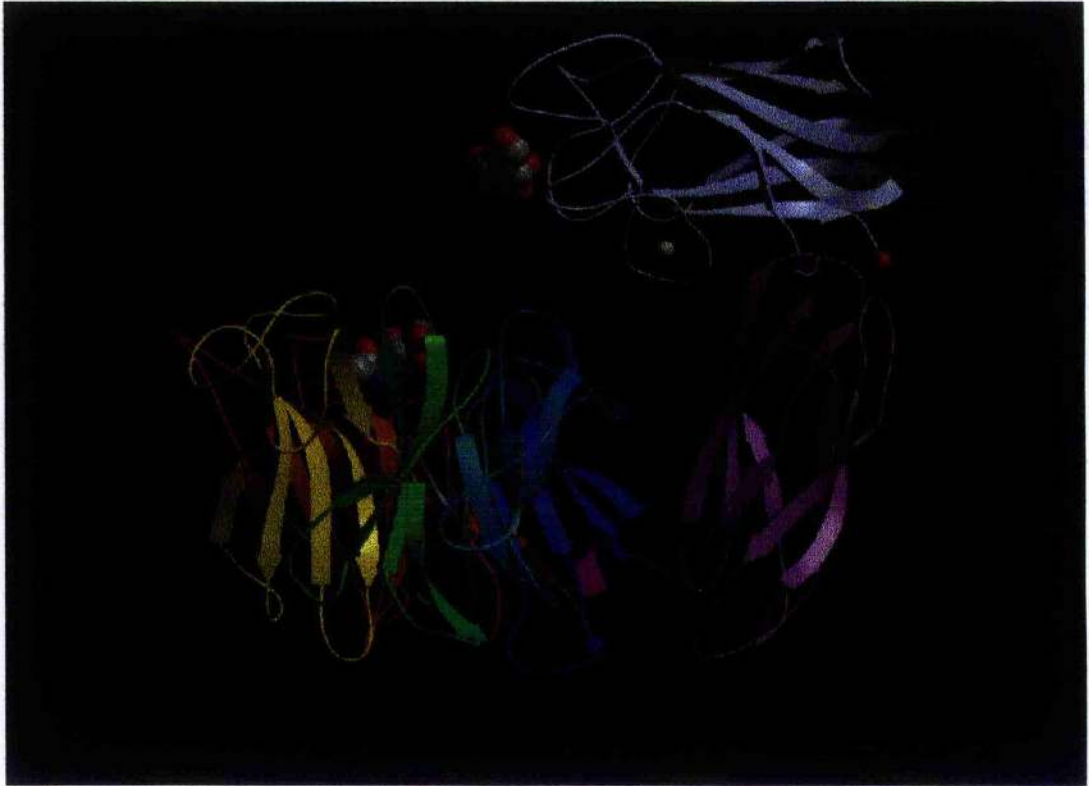
#### 1.4.6.3 *Vibrio cholera* neuraminidase

*Vibrio cholera* neuraminidase is a larger bacterial enzyme, 82 kDa, and has three protein regions: the typical neuraminidase fold, a  $\beta$ -propeller consisting of 54  $\beta$ -sheets with five segments containing  $\alpha$ -helices and two lectin-containing domains at either side flanking this fold (Taylor *et al* 1994). This lectin domain contains 200 residues, making up seven  $\beta$ -sheets and six antiparallel  $\beta$ -strands (Taylor *et al* 1994). The neuraminidase is part of pathogenic mucinase multi-enzyme complex. This complex includes a proteinase and an endo- $\beta$ -N-acetylhexosaminidase. Its role is to cleave terminal sialic acid from glycoconjugates to create GM<sub>1</sub> (the cholera toxin receptor) on the lining of the gastrointestinal tract (Taylor *et al* 1994). Cholera toxin can then attach itself to this binding site and invade cells. The lipid fluidity created by the neuraminidase assists this process. In this enzyme, the sugar adopts a chair conformation and the hydrolysis proceeds with retention of configuration (Von Itstein *et al* 1995), probably via a double-displacement mechanism (Sinnott and Guo 1993). *Vibrio cholera* neuraminidase requires Ca<sup>2+</sup> at the catalytic site to allow it to function correctly (Sinnott and Guo 1993).

#### 1.4.6.4 *Micromonospora viridifaciens* neuraminidase

A non-pathogenic *Actinomycete* soil bacteria contains a neuraminidase, *Micromonospora viridifaciens*. *M. viridifaciens* neuraminidase contains the typical super-barrel fold (41 kDa) found in the neuraminidase super-family. However, this enzyme has an additional lectin motif made up of antiparallel  $\beta$ -strands, forming an “arm” arrangement (~ 30 kDa). The 3-D crystal structure of *Micromonospora viridifaciens* neuraminidase is shown below in **Figure 14** (Taylor *et al* 1995, 1996).

**Figure 14** 3-D ribbon drawing of the crystal structure of *Micromonospora viridifaciens* neuraminidase (Taylor et al 1995)



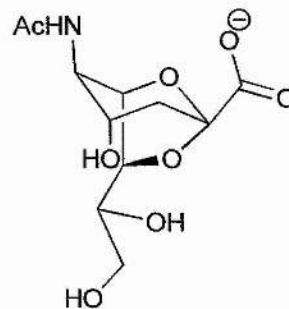
The catalytic domain of *T. cruzi trans*-sialidase has a molecular weight of 70 kDa encompassing a 40 kDa  $\beta$ -propeller fold and two lectin domains, comparable with *Micromonospora viridifaciens* neuraminidase. It is therefore acceptable to predict that the structure of *Micromonospora viridifaciens* neuraminidase, which has more than one binding site for galactose would be a feasible model for *T. cruzi trans*-sialidase. Hence it is reasonable to assume that there is more than one galactose binding site in *T. cruzi trans*-sialidase, possibly having a similar role to the Influenza virus trans-membrane glycoprotein, HA. *Micromonospora viridifaciens* neuraminidase has a similar sequence homology and activity to *Clostridium perfringens* neuraminidase (Schauer et al 1992). The *N*-terminal sequencing of *C. perfringens* neuraminidase is similar to that of *T. cruzi trans*-sialidase, as well as that of *Micromonospora viridifaciens* (Pereira 1995).



#### 1.4.6.5 *Macrobodella decora* sialidase

*Macrobodella decora* sialidase has a multi domain structure, with a similar topology to that *Vibrio cholera* neuraminidase, with a mass of ~ 80 kDa. Two lectin domains flank the catalytic domain of this sialidase (Luo1998). The catalytic domain is organised as  $\beta$ -propeller fold creating pseudo six-fold symmetry. Isolated North American (*Macrobodella decora*) leeches have produced some unusual enzymes. As well as possessing a typical sialidase, they also have an unusual sialidase, sialidase L, a 2,3-specific hydrolase that yields the (transient) 2,7-anhydro equivalent of the commonly produced sialic acid, shown in **Figure 15**, (Sinnott *et al* 1993, Li *et al* 1996). It appears to have a similar active site to Influenza virus and *Micromonospora viridifaciens* (Luo1998). The release of 2,7 anhydro-sialic acid, indicated that *Macrobodella decora* sialidase transfers sialic acid glycoconjugates instead of hydrolysing them, and requires the glyceryl side chain in an axial position during the transition state (Luo1998).

**Figure 15** Structure of 2,7-anhydrosialic acid



#### 1.4.7 Sequence alignments of *Trypanosoma cruzi* trans-sialidase with related sialidases/neuraminidases

The amino acid sequences of a variety of neuraminidases were analysed and then compared to the amino acid sequence of *Trypanosoma cruzi* trans-sialidase. The results are shown below in **Table 2**.

**Table 2** Amino acid sequence alignment of *Trypanosoma cruzi trans-sialidase* with related sialidases/neuraminidases

<i>Salmonella typhimurium</i> <u>Neuraminidase</u>	D <sup>62</sup> → 61	W <sup>121</sup> → 120	E <sup>231</sup> → 15	R <sup>292</sup> → 50	R <sup>246</sup> → 46	Y <sup>342</sup> → 19	E <sup>361</sup> → 294	R <sup>635</sup>
<i>Influenza A Virus</i> <u>neuraminidase</u>	D <sup>151</sup> → 27	W <sup>178</sup> → 99	E <sup>277</sup> → 32	R <sup>309</sup> → 62	R <sup>371</sup> → 35	Y <sup>406</sup> → 19	E <sup>425</sup> → 287	R <sup>712</sup>
<i>Trypanosoma cruzi</i> <u>trans-sialidase</u>	D <sup>19/27/28</sup> → 56/48/47	W <sup>75</sup> → 110	E <sup>185</sup> → 15	R <sup>200</sup> → 53	R <sup>253</sup> → 44	Y <sup>297</sup> → 20	E <sup>317</sup> → ?	
<i>Vibrio Cholera</i> <u>neuraminidase</u>	R <sup>37</sup> → 81	R <sup>118</sup> → 107	R <sup>224</sup> → 26	D <sup>250</sup> → 61	W <sup>31</sup> → 307	E <sup>619</sup> → 121	Y <sup>740</sup> → 16	E <sup>756</sup>
<i>Micromonospora</i> <i>Viridifaciens</i> <u>neuraminidase</u>	R <sup>151</sup> → 97	R <sup>248</sup> → 100	R <sup>348</sup> → 30	D <sup>378</sup> → 60	W <sup>61</sup> → ?			

We can see that *Trypanosoma cruzi trans-sialidase* has amino acid residues which are conserved in the catalytic area of *Salmonella typhimurium* and Influenza A virus neuraminidase. It is also possible to align the amino acid sequence of *Micromonospora viridifaciens* neuraminidase with *Vibrio cholera* neuraminidase. However there does not appear to be any conservation with *Trypanosoma cruzi trans-sialidase* (or *Salmonella typhimurium* and Influenza A virus neuraminidase). Any of the amino acids mentioned above may be important in the neuraminidase mechanism of action or provide the necessary residues for hydrogen bonding at the active site of the enzyme.

### 1.5 Cloning and expression of *trans-sialidase*

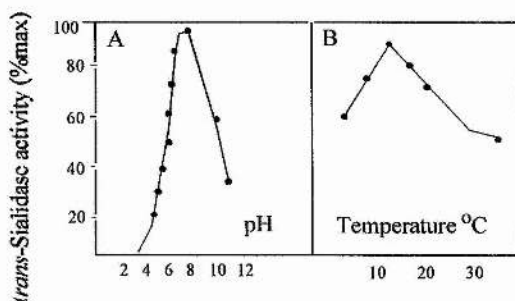
The genetic structure of *T. cruzi trans-sialidase* contains many features common to neuraminidases. Notably, it contains information about the make up of the enzymatic domain on the *N*-terminus and also the antigenic domain, the shed acute phase antigen

(SAPA) at the C-terminus (12 amino acid repeats in tandem) (Frasch *et al* 1995, Schenkman and Vandekerckhove 1993, Schenkman and Eichinger 1993). By a combination of site directed mutagenesis followed by enzyme activity studies, it was noted that only 2 of the 624 amino acids of the sequence are actually essential for full transferase activity (Frasch *et al* 1995). Mutation of Tyr<sup>342</sup> (in any way) caused the enzyme to lose all activity and Pro<sup>231</sup> mutation resulted in partial activity only. It is suspected that these residues are in the active site (Frasch *et al* 1995). When these residues and the surrounding area are compared to the active site of *Salmonella typhimurium* neuraminidase, fourteen of the twenty residues of the *Salmonella typhimurium* enzyme are either conserved, or in a comparable positions (including Tyr<sup>342</sup>) to *trans*-sialidase.

### 1.5.2 Kinetic profile of *trans*-sialidase

Studies carried out on recombinant *trans*-sialidase concur with those completed using wild-type protein, the temperature being critical to the behaviour of the enzyme. The hydrolysis rate of sialyl lactose by *trans*-sialidase steadily increases up to 35 °C (Schenkman *et al* 1997). However, the transferase reaction rate is maximum at a temperature of 13 °C (approximately). Also, most neuraminidases function best in an acidic medium (around pH5), hence the pH 8 optimum for *trans*-sialidase is unusual. The pH and temperature dependence of *T. cruzi trans*-sialidase is illustrated below in Figure 16.

**Figure 16** Diagram of pH and temperature dependence of the transferase activity of *trans*-sialidase Scudder *et al* 1993



### 1.5.3 Prospective mechanism for *trans*-sialidase

It is possible that *trans*-sialidase catalysed hydrolysis may proceed with retention of configuration, since all other neuraminidases investigated proceed with retention (Taylor *et al* 1993, 1994, 1995, Von Itzstein and Pegg 1992 and Von Itzstein and Wilson 1995).

**There are two main postulates:**

1. The enzyme has two binding sites one for the sialic acid (donating substrate) and one for the accepting substrate, allowing simultaneous binding. However, this is unlikely as there is little precedent for two binding sites in neuraminidases. However studies carried out to compare the hydrolysis and transfer reactions using 4-methylumbelliferyl-*N*-acetyl-neuraminic acid (Schenkman *et al* 1997), indicate that the transfer reaction does not increase (at any temperature) with an increase in lactose, indicating that the rate limiting step is the release of the aglycon (Schenkman *et al* 1997). There may also be two binding sites for *trans*-sialidase, i.e. a donor and an acceptor binding site.
2. The enzyme may have only one binding site, the donor and acceptor having to enter and leave from the same site to maintain the retention of configuration. This would require a relatively long-lived reaction intermediate i.e. a glycosyl oxocarbenium ion, a sialyl-enzyme (covalent) complex or an  $\alpha$ -lactone intermediate, **Figures 17A and B** (Von Itzstein *et al* 1995, Sinnott *et al* 1992, Sinnott and Guo 1993).

**Figure 17A An electrostatic or covalent interaction followed by hydrolysis of sugar-enzyme complex via H<sub>2</sub>O**

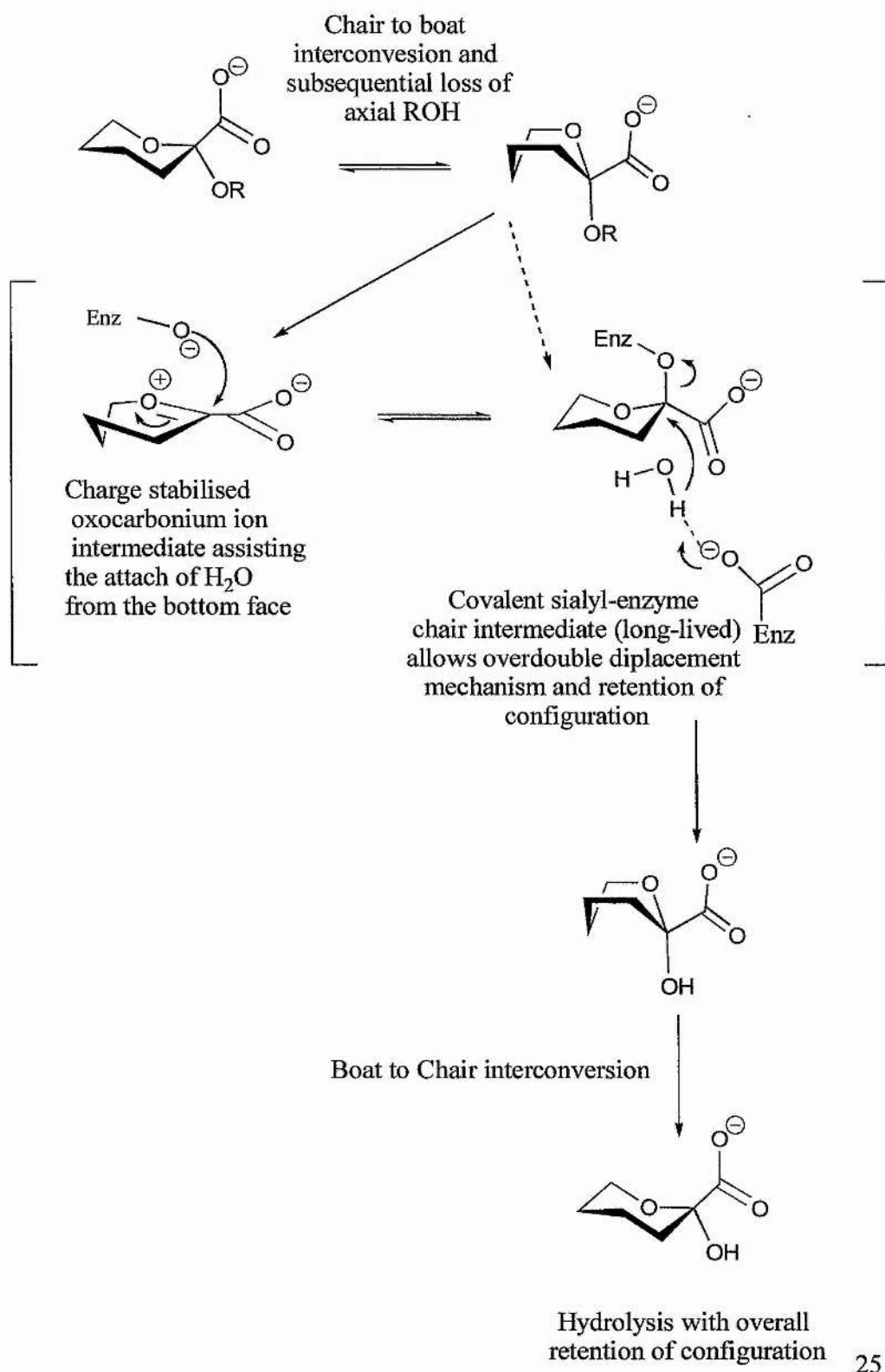
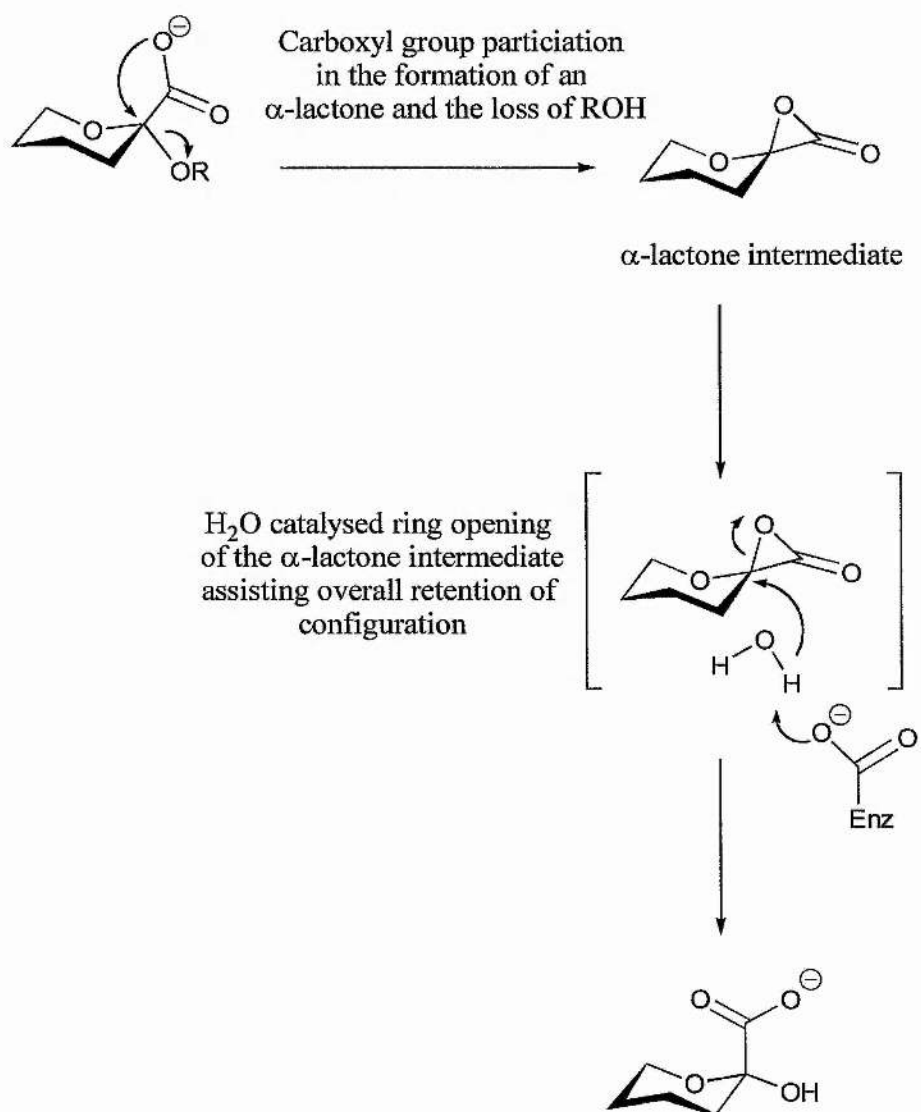


**Figure 17B** A short-lived  $\alpha$ -lactone intermediate



## **Aims and objectives**

To isolate *T. cruzi trans*-sialidase and purify recombinant using standard protein purification techniques to the level of a single band on SDS-PAGE (silver stained).

To develop a sensitive, rapid spectrophotometric assay for *trans*-sialidase

To assess the acceptor specificity of *T. cruzi trans*-sialidase using:

- Systematically modified acceptors (synthetic compound libraries)
- Fragments of the naturally occurring mucin glycans

# Chapter 2

## Assay development



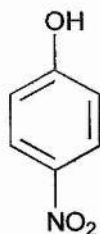
## 2.1 Assay development

Purification of an enzyme from a crude *E. coli* extract requires a method (i.e. an assay) of establishing whether or not the enzyme is present and the quantity of activity. The assay should be relatively simple, preferably giving an instantaneous read-out to identify active fractions at a glance. It was necessary to develop such a method to assist the elucidation of an enzyme profile for *trans*-sialidase.

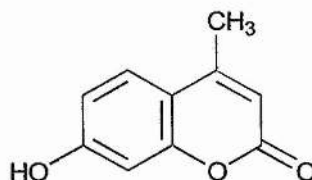
### 2.1.2 Neuraminidase assays - Spectrophotometric

Neuraminidase (hydrolase) assays are well documented in the literature (Sinnott and Guo 1993 and Sinnott *et al* 1993). These assays monitor the hydrolysis rates of neuraminidases, generally using Neu5Ac-O-PNP as a substrate, the enzyme cleaving the bond between the sugar and *p*-nitrophenol. The *p*-nitrophenol liberated is monitored at 400 nm. This process can be adapted to use methyl umbelliferyl glycosides as alternative substrates, the fluorescence of the product being monitored at 365 nm (Schauer *et al* 1997), **Figure 18**.

**Figure 18** Structure of *para*-nitrophenol (PNP) and 4-methylumbelliferone (4-MU)



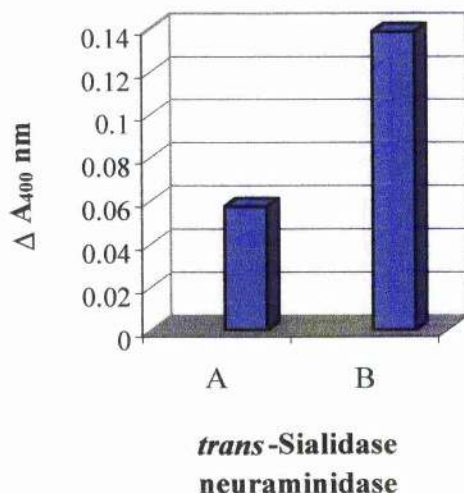
*para*-Nitrophenol (PNP)



4-Methylumbelliferone (4-MU)

A study was carried out on *trans*-sialidase and *C. perfringens* neuraminidase (loosely based on the spectrophotometric assay designed by Scudder *et al* 1993). *trans*-Sialidase and *Clostridium perfringens* neuraminidase were both assayed with the substrate Neu5Ac-O-PNP. The use of *C. perfringens* neuraminidase in an assay has been outlined by Quash *et al* 1992 and Schauer *et al* 1991. Shown below in **Figure 19** is a plot of the *trans*-sialidase assay (Neu5Ac-O-PNP donor substrate) in the presence and absence of a potential acceptor substrate, lactose.

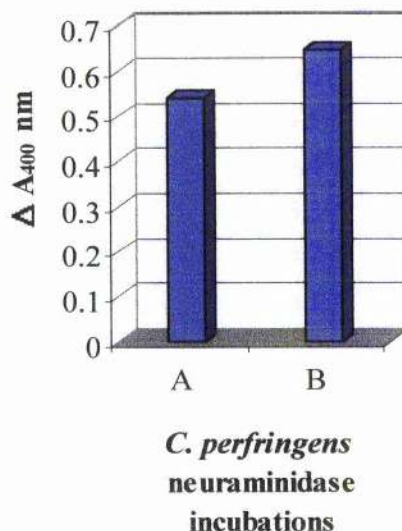
**Figure 19** *trans*-Sialidase in the presence and absence of a potential acceptor substrate, lactose (30 min incubation)



Legend	Incubations
A	<i>trans</i> -sialidase without lactose (Neu5Ac-O-PNP donor)
B	<i>trans</i> -sialidase with lactose (Neu5Ac-O-PNP donor)

This graph indicates that the transferase rate of *trans*-sialidase is significantly greater than that of the hydrolase. A similar experiment was carried out using *C. perfringens* neuraminidase in the presence and absence of lactose. The result is shown in **Figure 20**.

**Figure 20** *C. perfringens* neuraminidase in the presence and absence of a potential acceptor substrate, lactose (30 min incubation)



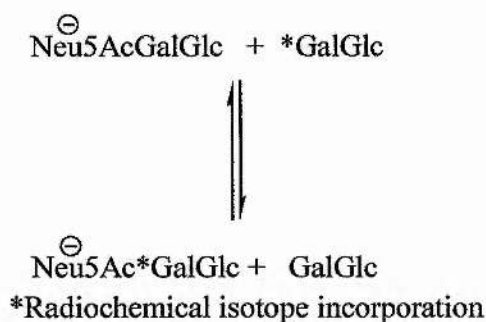
Legend	Incubations
A	<i>C. perfringens</i> neuraminidase without lactose (Neu5Ac-O-PNP donor)
B	<i>C. perfringens</i> neuraminidase with lactose (Neu5Ac-O-PNP donor)

**Figure 20** indicates that *C. perfringens* neuraminidase is a good hydrolase of Neu5Ac-O-PNP, the presence of lactose having an insignificant effect on the release of PNP. By comparison, *trans*-sialidase is a poor hydrolase of Neu5Ac-O-PNP, although still having significant hydrolase activity. This study suggests that Neu5Ac-O-PNP is a reliable substrate to measure hydrolase activity of *C. perfringens* neuraminidase, but is an unsuitable substrate to measure *trans*-sialidase transferase and hydrolase reactions.

## 2.2 Transferase assays – Radiochemical

Radiochemical assays for *trans*-sialidase monitor the incorporation of a radiochemical precursor, in this example [ $^{14}\text{C}$ ] lactose (Pereira *et al* 1995, Vetere *et al* 1996). This incorporation process, shown below in **Figure 21**, results in the formation of anionic radiolabelled Neu5Ac\*GalGlc which can be separated from uncharged material by anion exchange chromatography.

**Figure 21** Incorporation of [<sup>14</sup>C] lactose

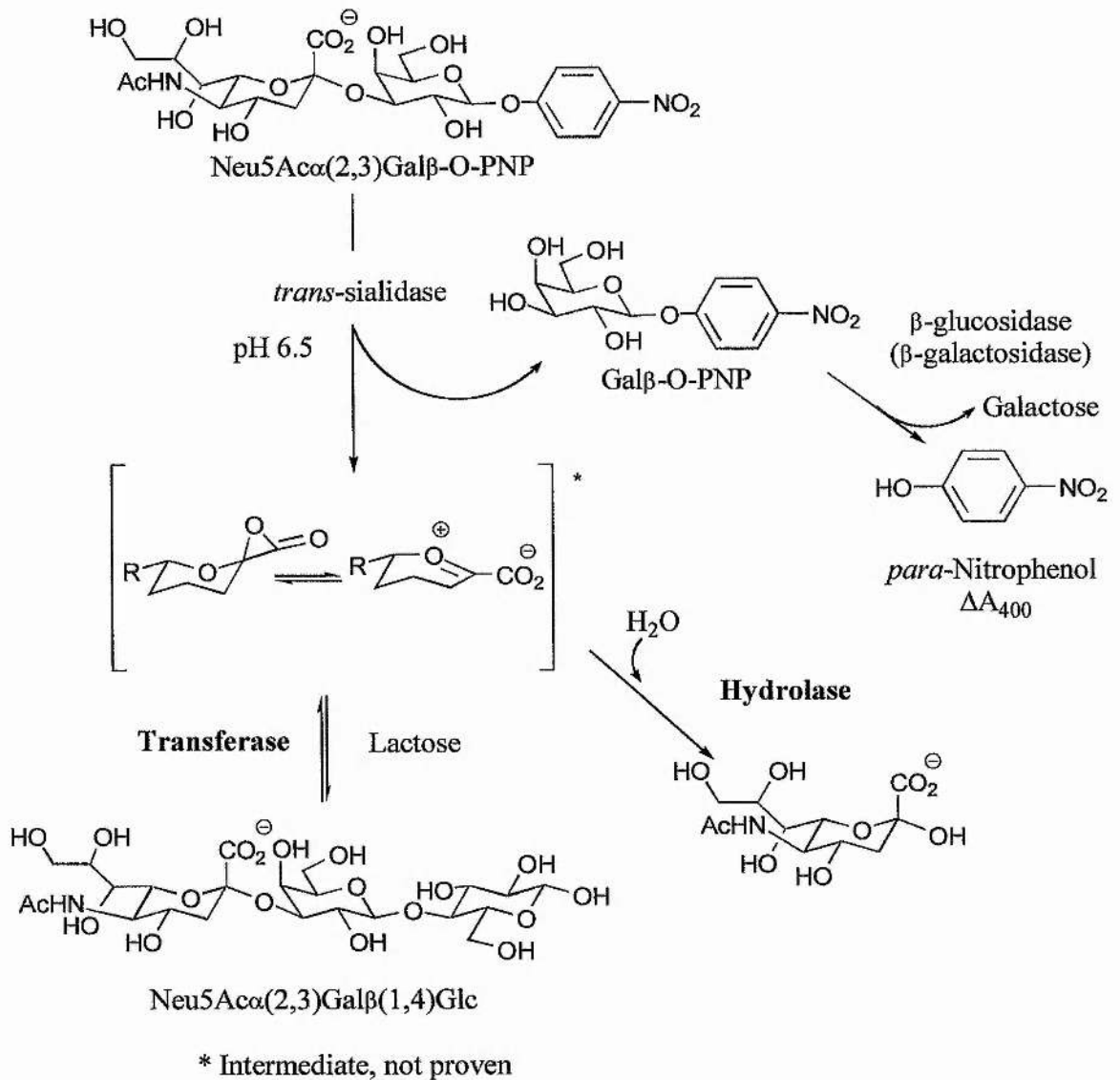


*trans*-Sialidase reversibly transfers sialic acid from sialyl lactose on to [<sup>14</sup>C] lactose. Sialyl-transferase activity can be monitored by this assay but it is not a convenient assay to rapidly screen column fractions. It is also undesirable since the assay uses radiochemicals making it a potential biological hazard, and involves a chromatographic procedure for separation on QAE-Sephadex media. This process can be arduous due to the nature of the media and separation under gravity.

### 2.3 Comparison of *trans*-sialidase transferase and hydrolase activities

Since *trans*-sialidase is both a hydrolase and a transferase, an assay to measure both of these rates of reaction would best serve the rapid screening of protein purification column fractions. Hence a spectrophotometric coupled assay (mark I) was designed for *trans*-sialidase. This assay was designed to work as follows: Neu5Ac $\alpha$ (2,3)Gal $\beta$ -O-PNP acts as a donor substrate for *trans*-sialidase and lactose as an acceptor. (From previous experiments it has been established that Neu5Ac-Gal-PNP is a better substrate for *trans*-sialidase than Neu5Ac-O-PNP).  $\beta$ -Glucosidase (crude, almonds) containing some  $\beta$ -galactosidase activity was used to hydrolyse the resulting Gal $\beta$ -O-PNP bond and release PNP which was monitored at 400 nm. The coupled assay (mark I) is shown below in **Figure 22**.

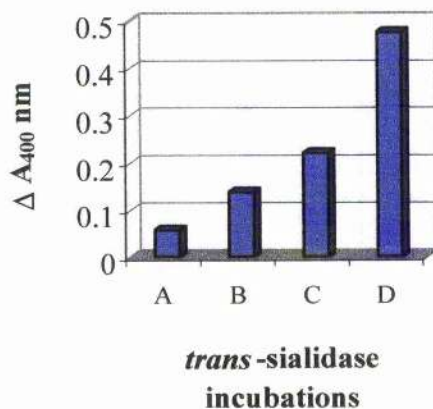
**Figure 22** Coupled assay for *trans*-sialidase (mark I)



This assay proved successful initially as it was a quick and sensitive technique for detecting the presence of *trans*-sialidase. Shown below in **Figure 23** is a plot comparing the coupled assay (measuring both hydrolase and transferase activities) as well as data from the previous spectrophotometric assay (using Neu5Ac-PNP as a substrate). This representation clearly indicates the preference of a disaccharide substrate over a monosaccharide donor for *trans*-sialidase.



**Figure 23** Comparison of *trans*-sialidase transferase and hydrolase activities with Neu5Ac-O-PNP and Neu5Ac $\alpha$ (2,3)-Gal $\beta$ -O-PNP substrates

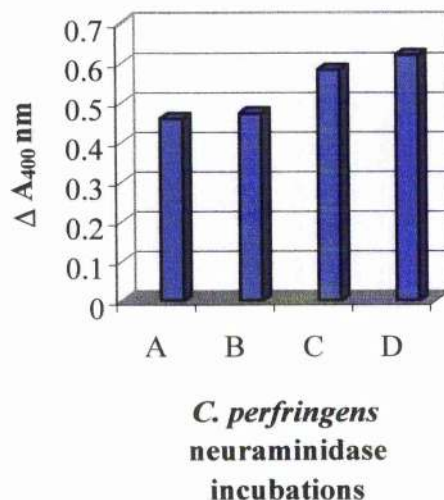


Legend	Incubations
A	Neu5Ac-O-PNP, <i>trans</i> -sialidase without lactose
B	Neu5Ac-O-PNP, <i>trans</i> -sialidase with lactose
C	Neu5Ac $\alpha$ (2,3)-Gal $\beta$ -O-PNP, <i>trans</i> -sialidase without lactose
D	Neu5Ac $\alpha$ (2,3)-Gal $\beta$ -O-PNP, <i>trans</i> -sialidase with lactose

### 2.5 Comparison of *C. perfringens* neuraminidase activity with and without an acceptor

The coupled assay (mark I) (using the disaccharide donor substrate, Neu5Ac $\alpha$ (2,3)-Gal $\beta$ -O-PNP) was set up replacing *trans*-sialidase with *C. perfringens* neuraminidase. It has already been established for *trans*-sialidase that Neu5Ac $\alpha$ (2,3)-Gal $\beta$ -O-PNP is a more reliable substrate. It was expected that the presence of lactose would be insignificant to *C. perfringens* neuraminidase. **Figure 24** shows the results of this study (combined with previous findings using Neu5Ac-O-PNP as a donor).

**Figure 24 Comparison of *C. perfringens* neuraminidase with and without acceptor**



Legend	Incubations
A	Neu5Ac $\alpha$ (2,3)-Gal $\beta$ -O-PNP, <i>C. perfringens</i> without lactose
B	Neu5Ac $\alpha$ (2,3)-Gal $\beta$ -O-PNP, <i>C. perfringens</i> with lactose
C	Neu5Ac-O-PNP, <i>C. perfringens</i> without lactose
D	Neu5Ac-O-PNP, <i>C. perfringens</i> with lactose

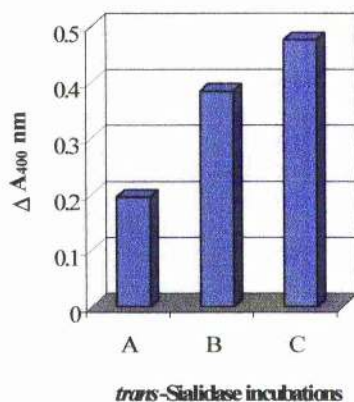
As suspected the presence of lactose had no significant effect. The absorption change using the Neu5Ac $\alpha$ (2,3)-Gal $\beta$ -O-PNP donor is slightly lower than using Neu5Ac-O-PNP. This is probably as a result of a lower free PNP background and is insignificant.

## 2.6 Coupled assay for *trans*-sialidase using Gal $\beta$ (1,3)GlcNAc $\beta$ -O-Octyl as an acceptor (mark II)

The first coupled assay for *trans*-sialidase was successful in the initial stages, however latterly it became problematic since lactose was being degraded by the  $\beta$ -galactosidase activity which was present in this "one-pot" assay. Also the acidic pH resulted in the donor sugar being subject to spontaneous hydrolysis and hence releasing PNP. In order to combat this problem the pH was increased. As a result of the rise in pH, another  $\beta$ -galactosidase had to be selected, since the pH for maximum enzymatic activity is 6.0 for the  $\beta$ -glucosidase (crude, almonds).  $\beta$ -Galactosidase from *E. coli* with a maximum activity at pH 7.3 was selected. Since this pH is just above neutral it helps to prevent spontaneous hydrolysis of the donor substrate.

However, this brought a further complication in that lactose, the acceptor sugar, was now subject to hydrolysis by the  $\beta$ -galactosidase, since lactose is the natural substrate for the *E. coli* enzyme. Glucose release, cleaved by  $\beta$ -galactosidase from a variety of potential substrates based on the general structure  $\text{Gal}\beta(1,\text{X})\text{GlcNAc}$  was assessed with a commercially available (*Sigma Chemicals Ltd*) glucose testing kit and by T.L.C. It was found that lactose would prove unsuccessful as an acceptor and hence another Gal-X had to be selected which would not be subject to the same level of hydrolysis.  $\text{Gal}\beta(1,3)\text{GlcNAc}\beta\text{-O-Octyl}$  was selected as an alternative and tested with  $\beta$ -galactosidase and the glucose testing kit. It was found to be stable to hydrolysis by the  $\beta$ -galactosidase and hence it was decided to proceed with this sugar as the new acceptor substrate. The results of the coupled assay (mark II) are shown below in **Figure 25**. The assay was carried out for 30 minutes.

**Figure 25** Results of the coupled assay for *trans*-sialidase (mark II) (30 Min incubations)

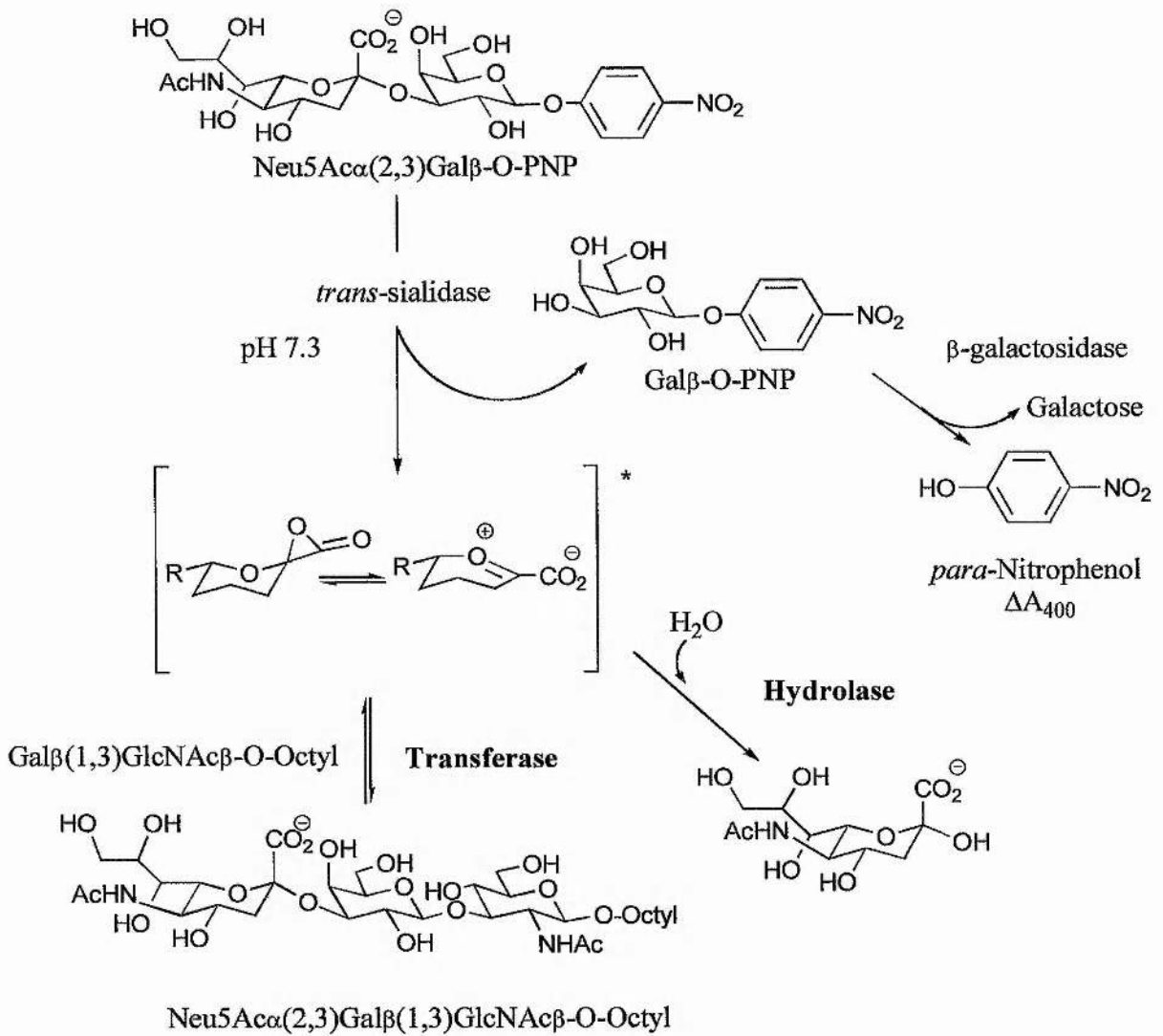


Legend	Incubations
A	Water (10 $\mu$ l)
B	Lactose (5 mM, 10 $\mu$ l)
C	$\text{Gal}\beta(1,3)\text{GlcNAc}\beta\text{-O-Octyl}$ (5 mM, 10 $\mu$ l)

This graph clearly indicates that *trans*-sialidase reactions are significantly better with the substrate  $\text{Gal}\beta(1,3)\text{GlcNAc}\beta\text{-O-Octyl}$ . The coupled assay (mark II) is outlined below in **Figure 26**.



**Figure 26** Coupled assay using Gal $\beta$ (1,3)GlcNAc $\beta$ -O-Octyl as an acceptor (mark II)



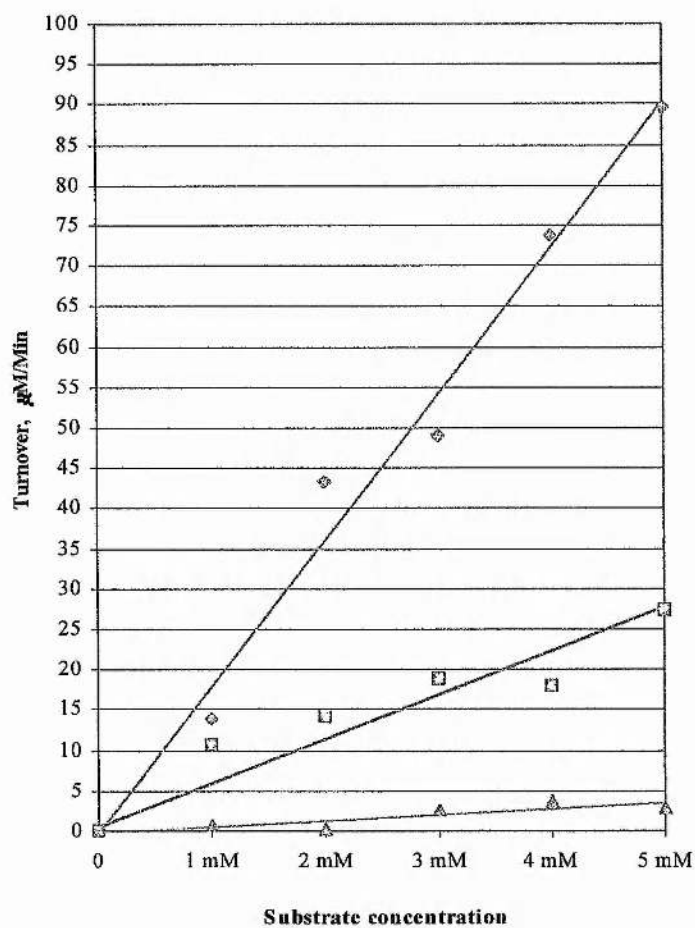
\* Intermediate, not proven

The second assay using Gal $\beta$ (1,3)GlcNAc $\beta$ -O-Octyl as a substrate has proved much more successful with the self-cleavage of the donor now negligible. Studies with this assay show that there is a reliable measurable hydrolase activity for *trans*-sialidase with a disaccharide donor substrate.

## 2.7 Spectrophotometric coupled assay (mark II) using variable concentrations of donor substrate

The transfer rate of *trans*-sialidase is five times faster than that of the hydrolysis rate, and the non-enzymatic rate is only one twelfth as fast as the transfer, this is shown below in Figure 27.

**Figure 27** *trans*-sialidase: variable concentrations of Neu5Ac $\alpha$ (2,3)-Gal $\beta$ -O-PNP donor substrate with and without acceptor (mark II assay)



Legend	Incubations
Background (Green triangle)	Non-enzymatic rate
No acceptor (Red square)	(-) Gal $\beta$ (1,3)GlcNAc $\beta$ -O-Octyl
Acceptor (Blue diamond)	(+) Gal $\beta$ (1,3)GlcNAc $\beta$ -O-Octyl (1mM)

Using the above data, we can construct double reciprocal plots according to Michaelis-Menten kinetic parameters. These are shown below in **Figure 28A** and **B**.

**Figure 28A** Plot of  $1/S$  vs  $1/v$  for *trans*-sialidase, the transferase

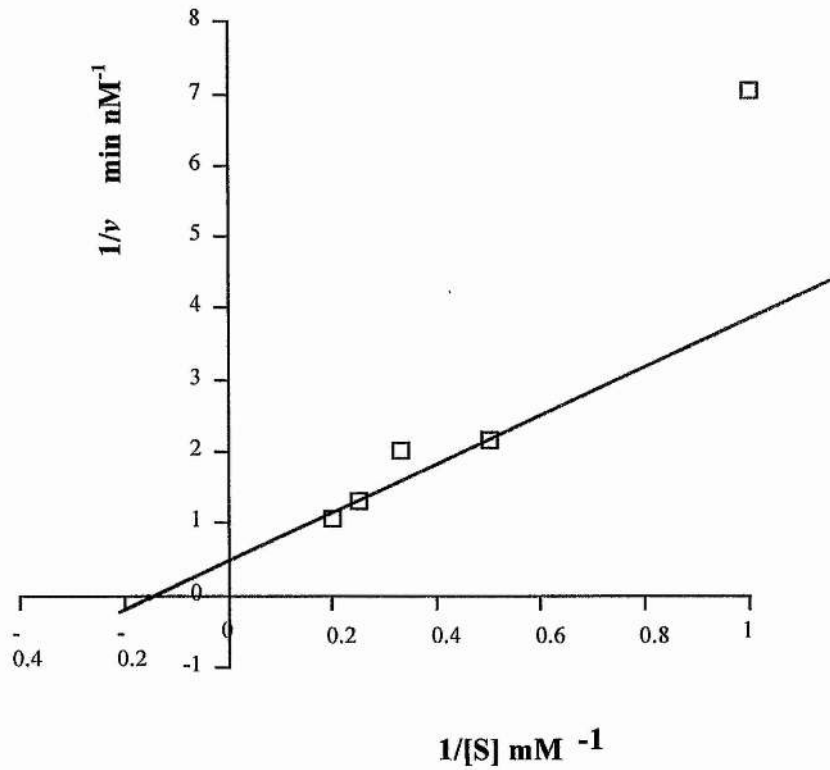
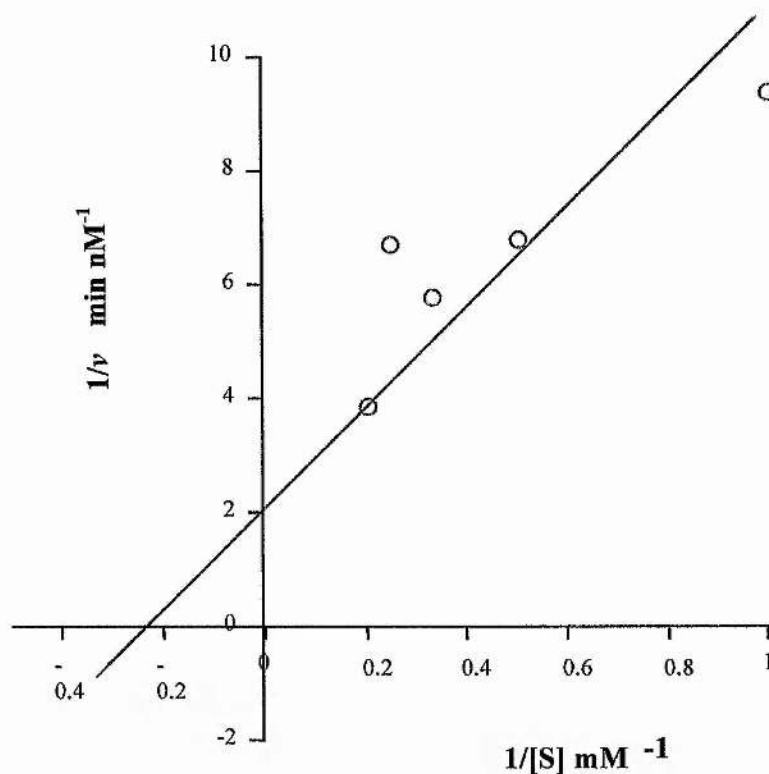


**Figure 28B** Plot of  $1/S$  vs  $1/v$  for *trans*-sialidase, the hydrolase



The error on these graphs (**Figures 28A and B**) is of the magnitude of  $\pm 20\%$ . This data is therefore does not allow us to obtain accurate  $K_m$  or  $V_{max}$  values for *trans*-sialidase activities. The large error is due to the relative instability of the donor substrate. However the data acquired does allow us to make an estimation of  $K_m$  and  $V_{max}$  for *trans*-sialidase. The lines drawn in above are estimated by eye (and are not as a result of linear regression). The results were estimated as follows: *trans*-sialidase, the transferase has a  $K_m = 7 \text{ mM}$  and a  $V_{max} = 2 \text{ nM min}^{-1}$  whereas *trans*-sialidase the hydrolase has a  $K_m = 4 \text{ mM}$  and a  $V_{max} = 0.5 \text{ nM min}^{-1}$ . The data is sufficient for the general comment that the  $K_m$  value for *trans*-sialidase (hydrolase and transferase) is in the low mM range. This is a reasonable result and comparable with the hydrolysis of *p*-nitrophenol glycosides by other neuraminidases.

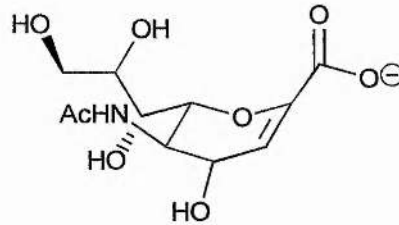
The  $K_m$  value for the hydrolysis of Neu5Ac-O-PNP for some of these enzymes is as follows, *Vibrio cholera* neuraminidase (pH 5.0, 37°C)  $K_m = 1.63 \text{ mM}$  (Sinnott and Guo 1993), *Influenza* virus neuraminidase (pH 6.0, 37°C)  $K_m = 1.17 \text{ mM}$  (Sinnott

and Guo 1993), *Salmonella Typhimurium* neuraminidase (pH 5.5, 37°C)  $K_m = 0.87$  mM (Sinnott *et al* 1994) and *Macrobodella decora* neuraminidase (pH 5.5, 37°C)  $K_m = 5.7$  mM (Sinnott *et al* 1993).

## 2.8 Inhibitor study carried out with *trans*-sialidase and *C. perfringens* neuraminidase

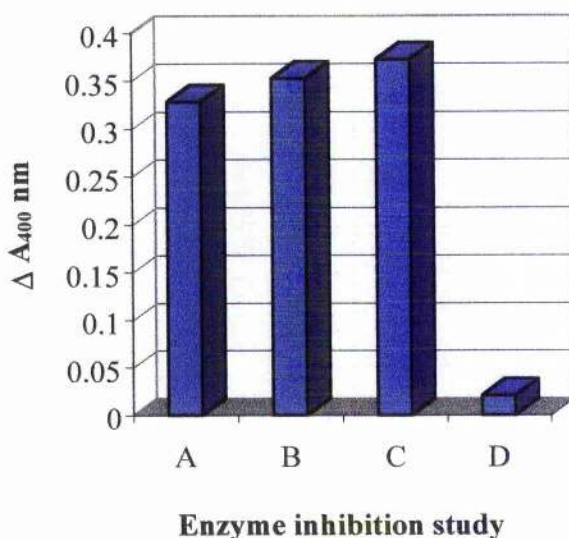
An inhibitor study was carried out on *trans*-sialidase and *C. perfringens* neuraminidase using the established neuraminidase inhibitor 2,3-dehydro-2-deoxy-Neu5Ac, shown below in **Figure 29A** (Von Itzstein and Pegg 1993, Von Itzstein *et al* 1993).

**Figure 29A** 2,3-dehydro-2-deoxy-Neu5Ac



*trans*-Sialidase and *C. perfringens* neuraminidase were incubated with 2,3-dehydro-2-deoxy-Neu5Ac, which acts as an inhibitor of *C. perfringens* neuraminidase, but not *trans*-sialidase. A comparison of relative hydrolase activity of *C. perfringens* neuraminidase and transferase activity of *trans*-sialidase with and without 2,3-dehydro-2-deoxy-Neu5Ac (inhibitor) present was calculated. The relative turnover rate calculated and the results are illustrated below in **Figure 29B**.

**Figure 29B Inhibitor study carried out with *C. perfringens* neuraminidase and *trans*-sialidase**



Legend	Incubations
A	<i>trans</i> -sialidase (-) Inhibitor (1 mM)
B	<i>trans</i> -sialidase (+) Inhibitor (1 mM)
C	<i>C. perfringens</i> (-) Inhibitor (1 mM)
D	<i>C. perfringens</i> (+) Inhibitor (1 mM)

*trans*-Sialidase activity with inhibitor present is > 90 %, whereas *C. perfringens* neuraminidase activity is < 5 % when there is inhibitor present. This result confirms that 2,3-dehydro-2-deoxy-Neu5Ac is an inhibitor of *C. perfringens* neuraminidase but not *trans*-sialidase.

## 2.9 Summary

It has been well documented that *trans*-sialidase is preferentially a sialyl-transferase, although it does possess some hydrolase activity (Scudder *et al* 1993). By assaying *trans*-sialidase with both Neu5Ac $\alpha$ (2,3)-Gal $\beta$ -O-PNP as well as the commonly used Neu5Ac-O-PNP (Sinnott and Guo 1993 and Sinnott *et al* 1993), it was established that *trans*-sialidase favours a Neu5Ac $\alpha$ (2,3)-Gal $\beta$ -O-PNP as a donor sugar. Hence a spectrophotometric coupled assay (mark I) using Neu5Ac $\alpha$ (2,3)-Gal $\beta$ -O-PNP as a donor substrate was developed for *trans*-sialidase. This also incorporated an acceptor substrate, lactose and  $\beta$ -glucosidase (with  $\beta$ -galactosidase activity). This

assay was a little unreliable due to the acid instability of the Neu $\alpha$ (2,3)Gal $\beta$ -O-PNP. This assay was modified slightly to give *trans*-sialidase spectrophotometric assay (mark II). In the *trans*-sialidase assay (mark II), lactose is replaced with Gal $\beta$ (1,3)GlcNAc $\beta$ -O-Octyl and the pH was increased from 6.5 to 7.3. This is now a reliable assay for the rapid assessment of *trans*-sialidase activity (i.e. in protein purification column fractions).

Using the coupled assay (mark II)  $K_m$  and  $V_{max}$  for *trans*-sialidase were measured with increasing concentrations of Neu5Ac $\alpha$ (2,3)-Gal $\beta$ -O-PNP substrate and a fixed amount of Gal $\beta$ (1,3)GlcNAc $\beta$ -O-Octyl or H<sub>2</sub>O. The results were estimated at:

*trans*-sialidase (transferase)  $K_m = 7 \text{ mM}$  and  $V_{max} = 2 \text{ nM min}^{-1}$

*trans*-sialidase (hydrolase) are  $K_m = 4 \text{ mM}$  and  $V_{max} = 0.5 \text{ nM min}^{-1}$

Using the coupled assay (mark II) it has also been shown that *C. perfringens* neuraminidase is inhibited at 1mM, by a known neuraminidase inhibitor 2,3-dehydro-2-deoxy-Neu5Ac (Von Itzstein and Pegg 1993, Von Itzstein et al 1993). *trans*-sialidase, however is not inhibited at 1mM.

# Chapter 3

## *trans*-Sialidase synthetic substrate recognition



### 3.1.1 Development of glycosyl transferase inhibitors

Carbohydrates have a role to play in many biological functions on the surface of cells, as well as being required for energy consumption and structural properties. Modern techniques have greatly assisted the location of carbohydrates within biological systems. Almost all surface proteins are glycoproteins (*Tolvanen et al* 1996) and the nine commonly used monosaccharides in their pyranose forms found in biological systems are (D-Glc, D-Gal, D-Man, D-Fuc, D-Xyl, D-GlcNAc, D-GalNAc, Neu5Ac) (*Hindsgaul et al* 1997).

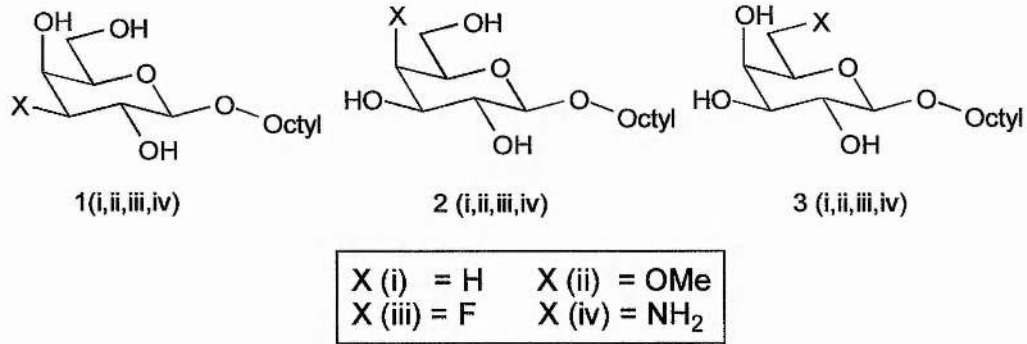
The biosynthesis of cell surface oligosaccharides is performed by glycosyl transferases. Hence glycosyl transferases are a potential target for therapeutics, since in theory they have the ability to cause structural modifications to cell-surface glycoconjugates. In order to do this successfully, it is necessary for the enzyme-substrate binding model to be established and a minimum requirement for acceptor substrate specificity to be identified. This should help to prevent affecting any other glycosylation processes. The mapping of the key interactions of an enzyme binding site is usually carried out by assaying the enzyme with a systematically modified series of substrate analogues to indicate the functional groups which are paramount in the glycosyl transferase substrate-interaction. There is an important interaction between the hydroxyl at the glycosylation position on the acceptor sugar (i.e. C<sub>3</sub> on galactose in *trans*-sialidase binding site) and the binding site in some glycosyl transferases (*Hindsgaul et al* 1997).

### 3.1.2 Systematically modified Gal $\beta$ -O-Octyl library

It has been well documented that *Trypanosoma cruzi trans*-sialidase will only transfer sialic acid onto the three position of a terminal galactose moiety when an acceptor sugar is available. In an attempt to fully characterise the enzyme and its recognition of galactose, an investigation was carried out using synthetically modified galactose. Galactose $\beta$ -O-Octyl was modified at the three, four and six hydroxyl positions by replacing the OH with either H, F, OMe or NH<sub>2</sub> to create a library of modified octyl-galactosides. The synthesis of these compounds was carried out by Todd Lowary, Alberta, Canada. These gal $\beta$ -O-Octyl analogues had been synthesised for a study investigating the active site of glycosyl transferases

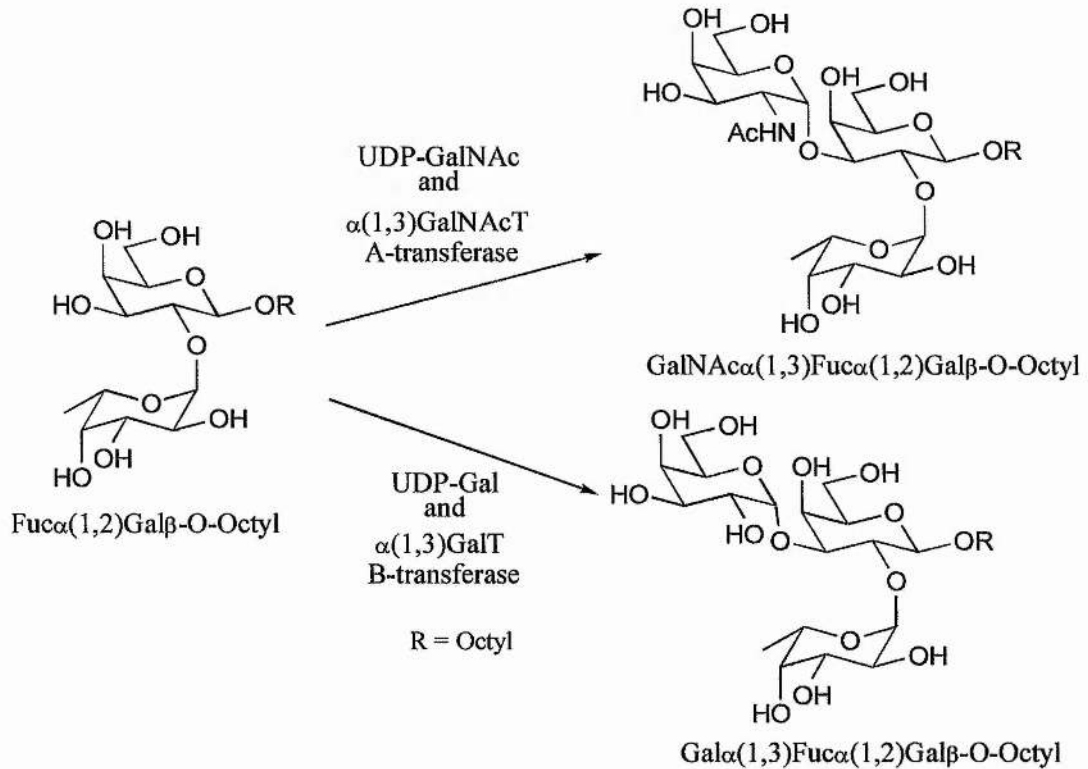
responsible for A and B blood group biosynthesis (*Hindsgaul et al 1993*). The modifications to Gal $\beta$ -O-Octyl are illustrated below in **Figure 30**.

**Figure 30** Synthetically substituted Gal $\beta$ -O-Octyl library (*Lowary et al 1993*)



The compounds listed above were one of the components which were coupled (to fucose) to give a library of potential inhibitors, based on the general structure Fuc $\alpha$ (1,2)Gal $\beta$ -O-Octyl, a known acceptor of glycosyl transferases (*Lowary et al 1994*). The glycosylation of this structure by  $\alpha$ (1,3)GalNAcT and  $\alpha$ (1,3)GalT to produce blood group A and B antigens (respectively) is shown below in **Figure 31**.

**Figure 31** Biosynthesis of blood group antigens A and B by  $\alpha$ (1,3)GalNAcT and  $\alpha$ (1,3)GalT *Lowary et al 1994*



Each of the Fuc $\alpha$ (1,3)Gal $\beta$ -O-Octyl analogues were assessed by a radiochemical assay measuring the rate of transfer [ $^3$ H]Gal or GalNAc, from the UDP-X parent. The results of the assay are shown below in **Table 3**.

**Table 3** Relative acceptor activity (%) of disaccharide analogues using GalT A and B *Lowary et al* 1993, 1994

Substrate analogues	*A transferase	*B transferase
Unmodified disaccharide	100	100
3- Deoxy	0	0
4- Deoxy	0.1	0.2
6- Deoxy	35	22
3- Methoxy	0.4	0
4- Methoxy	0.3	0
6- Methoxy	13.4	3.2
3- Fluoro	0.3	0.1
4- Fluoro	0	0
6- Fluoro	43	30
3- Amino	0.8	0.1
4- Amino	0	0.3
6- Amino	4.7	2.0
No enzyme	0	0

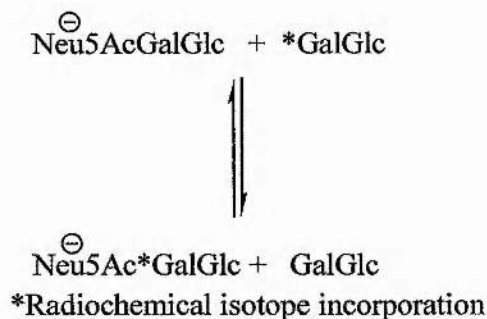
\*All substrates were used at concentrations of 2.5  $\mu$ M for A transferase and 1.0  $\mu$ M for B transferase.

In this example, Gal $\beta$ -O-Octyl substrate analogues are being tested as substrates of blood group A and B transferases.

### 3.1.3 Radiochemical assay of Gal $\beta$ -O-Octyl analogues (*Pereira et al 1995, Vetere et al 1996*)

The radiochemical assay employed monitors the incorporation of [ $^{14}\text{C}$ ] lactose and results in the formation of anionic radiolabelled Neu5Ac\*GalGlc. This incorporation process shown below in **Figure 21** (see Assay development, page 32).

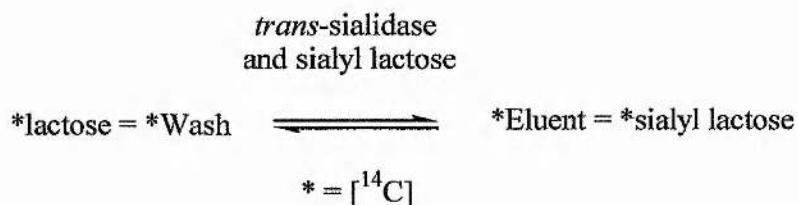
**Figure 21** Incorporation of [ $^{14}\text{C}$ ] lactose



In this assay (with no alternative substrate present), *trans*-sialidase will reversibly transfer sialic acid from sialyl lactose to [ $^{14}\text{C}$ ] lactose. The charged material can be separated from uncharged material by anion exchange chromatography as follows:

The assay mixture is loaded onto A25 resin (*Sigma Chemical Ltd*) and washed with water to remove all non-sialylated material (wash). The resin is then eluted with  $\text{NH}_4\text{OAc}$  (1 M) (eluent).

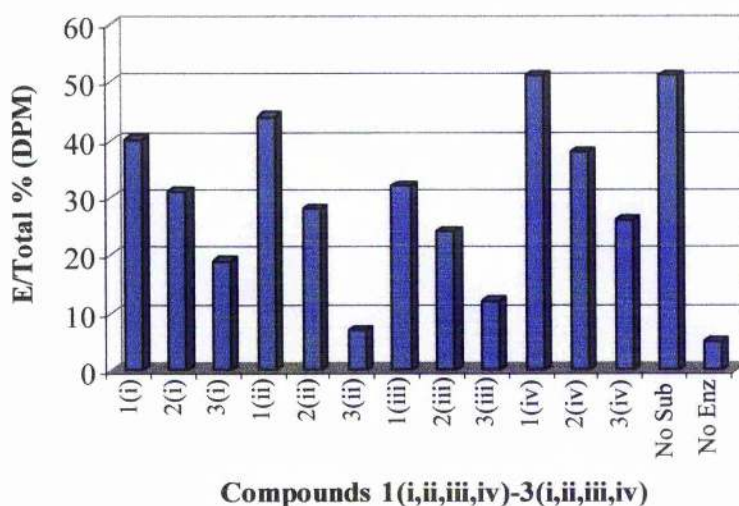
Since *trans*-sialidase is a reversible sialyl transferase (provided the substrate/acceptor concentrations are equal and an equilibrium is established) the total number of radioactive counts in wash and the eluent should be approximately equal, thus:



If a better *trans*-sialidase substrate is added to the assay to compete with [ $^{14}\text{C}$ ] lactose, this will result in the unsialylated [ $^{14}\text{C}$ ] lactose being washed off the resin with  $\text{H}_2\text{O}$ . Hence the radioactive counts in the eluent will be significantly smaller. In some cases the alternative substrate is unsuitable for *trans*-sialidase to sialylate, hence the radioactive result will mirror that of no substrate present. The graph below

is a plot of the number of counts in the eluent divided by the total number of counts in each assay. In this representation, the lower the value, the better the substrate is. The higher figures indicate that some of the compounds compete with lactose for *trans*-sialidase but are not sialylated. Since the hydroxyl group at position 3 is paramount for  $\alpha(2,3)$  sialyl coupling (Schenkman *et al* 1997), it was expected that any modifications to the 3-OH group would render the sugar a non-substrate. However, there was no information available regarding interactions of the hydroxyl groups at positions 4 and 6. Compounds 1(i,ii,iii,iv)-3(i,ii,iii,iv) were radiochemically assayed and the results plotted (see experimental page 111), **Figure 32**.

**Figure 32** Graph of radiochemical assay of Gal $\beta$ -Octyl analogues



**Legend of Figure 32**

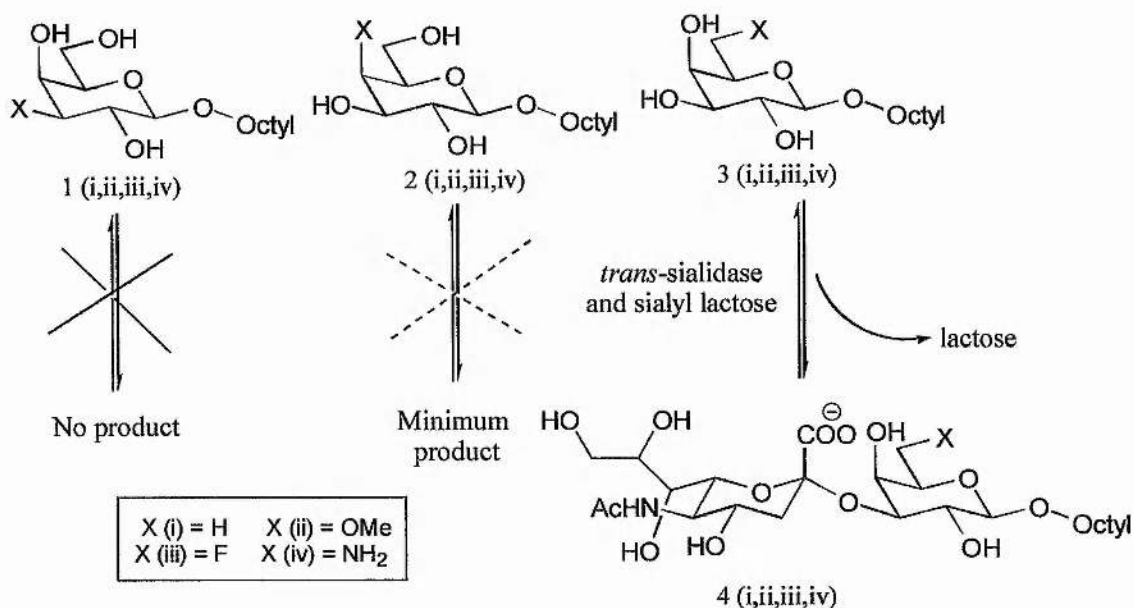
Legend	Compound	Legend	Compound	Legend	Compound
1(i)	3H-Gal $\beta$ -Octyl	3(ii)	6MeO-Gal $\beta$ -Octyl	2(iv)	4NH <sub>2</sub> -Gal $\beta$ -Octyl
2(i)	4H-Gal $\beta$ -Octyl	1(iii)	3F-Gal $\beta$ -Octyl	3(iv)	6NH <sub>2</sub> -Gal $\beta$ -Octyl
3(i)	6H-Gal $\beta$ -Octyl	2(ii)	4F-Gal $\beta$ -Octyl	No Sub	No substrate
1(ii)	3MeO-Gal $\beta$ -Octyl	3(iii)	6F-Gal $\beta$ -Octyl	No Enz	No Enzyme
2(ii)	4MeO-Gal $\beta$ -Octyl	1(iv)	3NH <sub>2</sub> -Gal $\beta$ -Octyl		

**Figure 32** indicates that indeed that *trans*-sialidase is not able to sialylate compounds 1(i,ii,iii,iv). However *trans*-sialidase is able to sialylate compounds 2(i,ii,iii,iv), but only minimally. Surprisingly though, *trans*-sialidase is able to



sialylate compounds 3(i,ii,iii,iv) easily. This plot gives an indication of *trans*-sialidase substrate specificity. This point is illustrated below in **Figure 33A**.

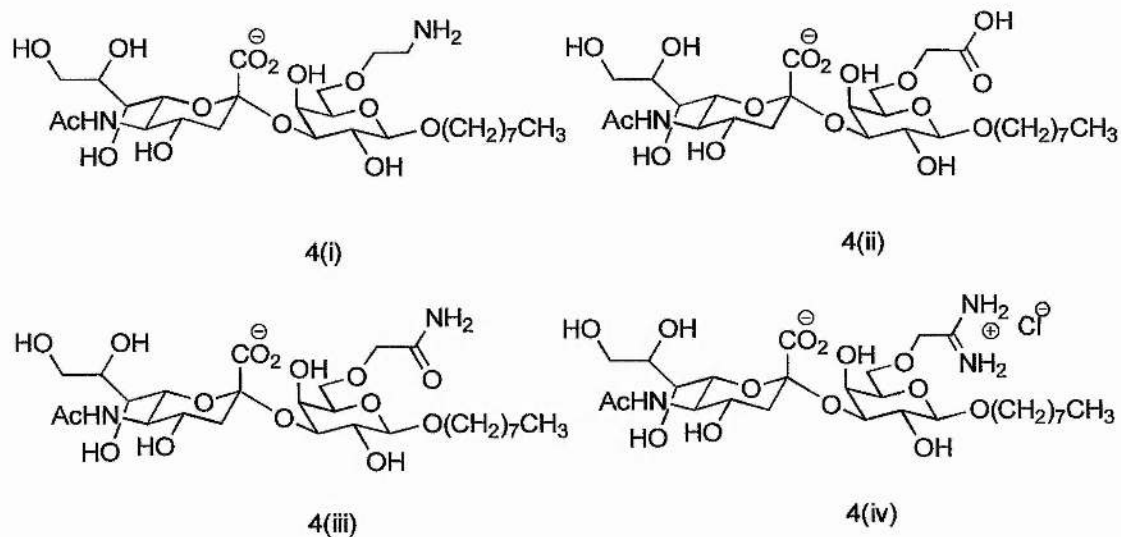
**Figure 33A** *trans*-sialidase substrate specificity with compounds 1(i,ii,iii,iv) – 3 (i,ii,iii,iv)



### 3.1.4 Potential sialylation of Gal $\beta$ -O-Octyl analogues 1(i-iv)-3(i-iv) (monitored by T.L.C.)

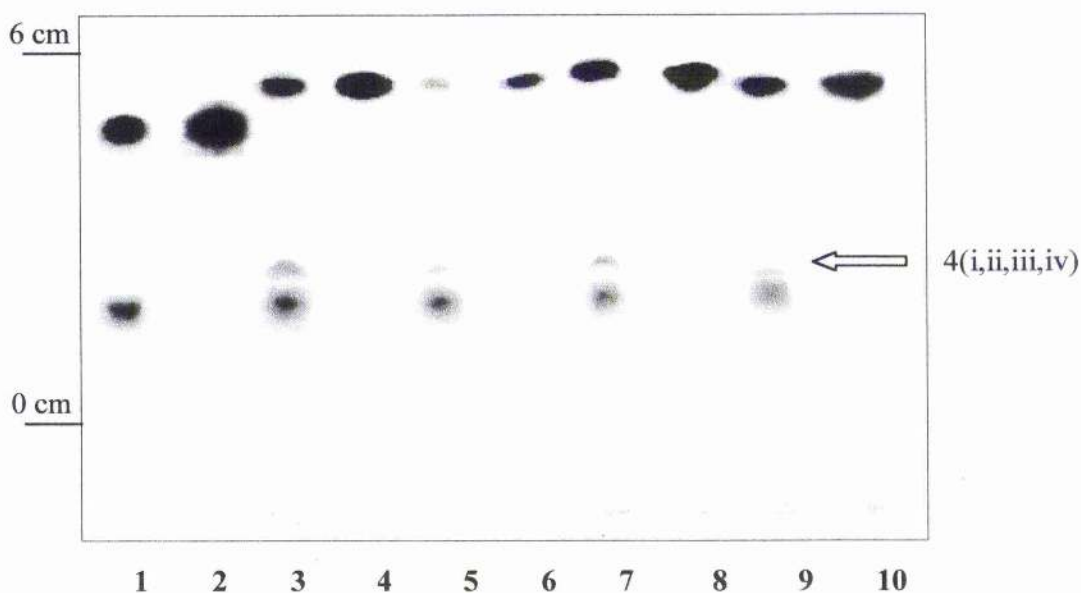
Compounds 1(i,ii,iii,iv) – 3(i,ii,iii,iv) (page 46) were incubated at 37°C with *trans*-sialidase (crude) and Neu5Ac-O-PNP. This was to assess the potential of compounds 1(i,ii,iii,iv) – 3(i,ii,iii,iv) as substrates of *trans*-sialidase (see page 114 for conditions). The results were monitored by T.L.C. As before, compounds 3(i,ii,iii,iv) were all sialylated by *trans*-sialidase. The products of these incubations gave compounds 4(i,ii,iii,iv), which are reiterated below in **Figure 33B**.

**Figure 33B** Compounds 4(i,ii,iii,iv)



The T.L.C. plate of substrates 3(i,ii,iii,iv) which gave sialylated products 4(i,ii,iii,iv) were photographed and are shown below in **Figure 33C**.

**Figure 33C Sialylation of Gal $\beta$ -O-Octyl substrates 3(i,ii,iii,iv)**



**Legend of Figure 33C** (Minor product Rf values are not indicated)

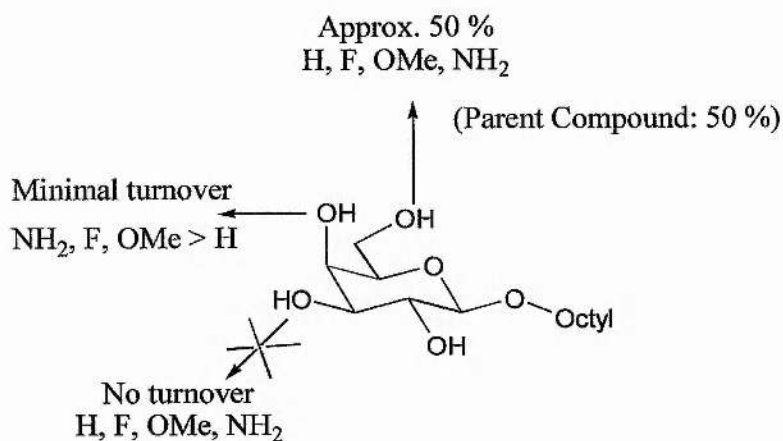
Lane 1 Gal $\beta$ -Octyl Incubation, Rf = 0.8	Lane 6 6H Gal $\beta$ -Octyl marker, Rf = 0.8
Lane 2 Gal $\beta$ -Octyl marker, Rf = 0.7	Lane 7 6OMe Gal $\beta$ -Octyl Incubation, Rf = 0.8, 0.5
Lane 3 6F Gal $\beta$ -Octyl Incubation, Rf = 0.8, 0.5	Lane 8 6OMe Gal $\beta$ -Octyl marker, Rf = 0.8
Lane 4 6F Gal $\beta$ -Octyl marker, Rf = 0.8	Lane 9 6NH <sub>2</sub> Gal $\beta$ -Octyl Incubation, Rf = 0.8, 0.5
Lane 5 6H Gal $\beta$ -Octyl Incubation, Rf = 0.8, 0.5	Lane 10 6NH <sub>2</sub> Gal $\beta$ -Octyl marker, Rf = 0.8

(In all cases, the marks at Rf = 0.4 and 0.1 are crude *trans*-sialidase)

This T.L.C. shows all of compounds 3(i,ii,iii,iv) have become sialylated producing a spot with an Rf = 0.5 (approx.). As suspected modification of the hydroxyl group at position three of Gal $\beta$ -O-Octyl, renders that attachment of sialic acid impossible and hence any modifications at that position render compounds 1(i,ii,iii,iv) competitive non-sialylable substrates. Modification at the hydroxyl groups at position four allows the attachment of sialic acid at position three, however the turnover is minimal compared to the unmodified turnover at 50 %. Surprisingly, modification at the six position of galactose made no significant difference to the turnover and sialylation occurs readily. All of the above figures are approximate and based on a turnover assessment made by eye. This conclusion is illustrated below in **Figure 34**.



**Figure 34** Approximate figures for the sialylation of Gal $\beta$ -O-Octyl analogues (observed by eye from T.L.C.)



### 3.1.5 Conclusions

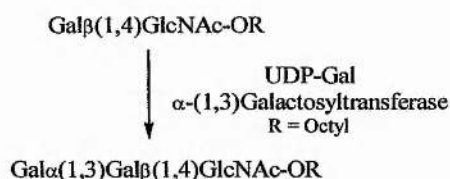
Compounds 1(i,ii,iii,iv) - 3(i,ii,iii,iv) (Lowary *et al* 1993) were assessed as potential *trans*-sialidase substrates. The study was two fold, incorporating both a radiochemical assay (Pereira *et al* 1995, Vetere *et al* 1996) and an incubation with Neu5Ac-O-PNP followed by an assessment of sialylated products by T.L.C. The results of the radiochemical study indicate that (as expected) modification of the hydroxyl group at position 3 of the galactose analogues renders the sugar non-sialylatable. Modification to the hydroxyl group at 4 of the galactose analogues does not prevent sialylation, but the turnover is minimal. This indicates that the hydroxyl groups at positions 3 and 4 of the galactose analogues are significant to enzyme turnover. Modification to the hydroxyl group of position 6, surprisingly does not affect sialylation of galactose by *trans*-sialidase. This suggests that hydroxyl group at position 6 plays little or no role in enzyme binding. The radiochemical observations agree with the observations and assessment made by T.L.C. Since the hydroxyl group at position 6 may be modified, i.e. compounds 3(i,ii,iii,iv) causing no significant loss of enzymatic turnover, it may be possible to exploit this property in synthetic oligosaccharide chemistry. For example, it may be possible to incorporate a solid phase linker (usually polymer beads) at the hydroxyl at position 6 to immobilise the galactose analogue. This method was pioneered in 1963 by Bruce Merrifield for solid phase synthesis of polypeptides (Whittaker *et al* 1996). The advantage of this approach is that the reactions will generally be driven to completion. Also the products can be isolated relatively easily by filtering off the

insoluble support and then cleaving off the linker (*Whittaker et al 1996*). There are other examples of exploitation of *trans*-sialidase in synthetic oligosaccharide chemistry, for example *Paulson and Ito (1993)* have exploited *trans*-sialidase to create synthetic building blocks to assist in the synthesis of the sialylated ganglioside, GM<sub>4</sub>.

### 3.2 Modified Gal $\beta$ (1,4)GlcNAc $\beta$ -O-Octyl library

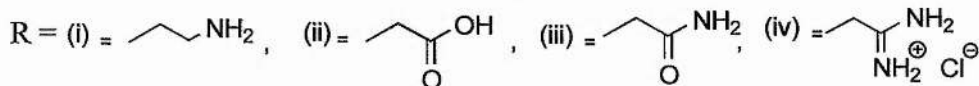
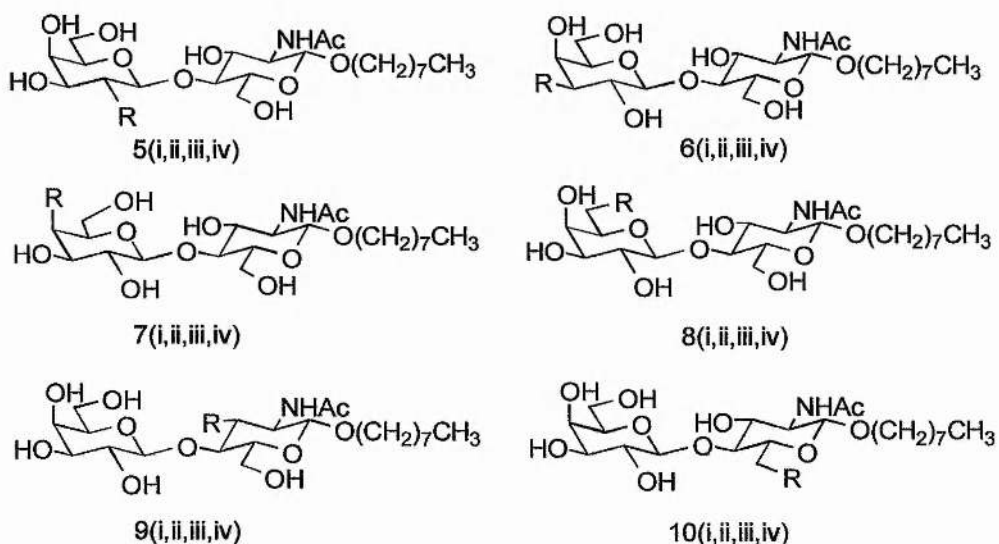
A similar study to 3.1, was carried out on a library of modified Gal $\beta$ (1,4)GlcNAc $\beta$ -O-Octyl sugars, obtained from Ole Hindsgaul's laboratory, Alberta, Canada. These Gal $\beta$ (1,4)GlcNAc $\beta$ -O-Octyl analogues were originally synthesised as potential inhibitors of  $\alpha$ -(1,3)galactosyltransferase. **Figure 35** shows glycosylation which is catalysed by  $\alpha$ -(1,3)galactosyltransferase (obtained from calf thymus).

**Figure 35**  $\alpha$ -(1,3)galactosyltransferase catalysed synthesis of Gal $\alpha$ (1,3)Gal $\beta$ (1,4) $\beta$ GlcNAc-OR (*Palcic et al 1998*)



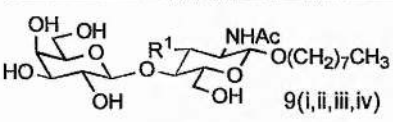
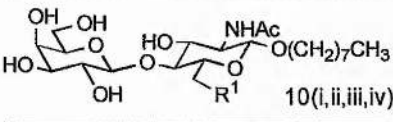
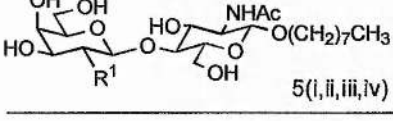
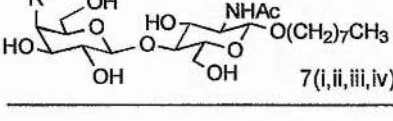
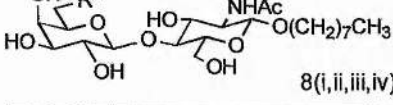
Gal $\beta$ (1,4)GlcNAc $\beta$ -O-Octyl analogues [compounds 5(i,ii,iii,iv)-10(i,ii,iii,iv)], **Figure 36**) were synthesised enzymatically. These analogues were modified at the two prime, three prime, four prime, six prime, three and six hydroxyl groups in turn with four substituents. In each case a hydroxyl group was replaced with either an acid, amine, amide or guanidino group. These modifications are illustrated below in **Figure 36**, compounds 5(i,ii,iii,iv)-10(i,ii,iii,iv).

**Figure 36** 24 Gal $\beta$ (1,4)GlcNAc $\beta$ -O-Octyl analogues (*Hindsgaul et al 1996*)



Compounds 5(i,ii,iii,iv)-10(i,ii,iii,iv) [except 8(i,ii,iii,iv)] were radiochemically assayed using a disaccharide analogue (10.8 nM), UDP-[6-<sup>3</sup>H]Gal (100,000 DPM), enzyme solution and assay buffers to make a final volume of 20  $\mu$ l. They were assayed at 37 °C for 30 mins. Shown below in **Figure 37** is a table illustrating the relative rate of glycosylation using  $\alpha$ -(1,3)GalT.

**Figure 37**  $\alpha$ -(1,3)GalT catalysed glycosylation relative rate (*Palcic et al* 1998)

Gal $\beta$ (1,4)GlcNAc $\beta$ -O-Octyl analogues	R <sup>1</sup>	Relative rate* (%)
 9(i, ii, iii, iv)	OCH <sub>2</sub> CH <sub>2</sub> NH <sub>2</sub> OCH <sub>2</sub> CO <sub>2</sub> H OCH <sub>2</sub> CONH <sub>2</sub> <sup>+</sup> Cl <sup>-</sup> NH <sub>2</sub> OCH <sub>2</sub> C=NH <sub>2</sub> <sup>+</sup> Cl <sup>-</sup> NH <sub>2</sub>	< 1 < 1 < 1 < 1
 10(i, ii, iii, iv)	OCH <sub>2</sub> CH <sub>2</sub> NH <sub>2</sub> OCH <sub>2</sub> CO <sub>2</sub> H OCH <sub>2</sub> CONH <sub>2</sub> <sup>+</sup> Cl <sup>-</sup> NH <sub>2</sub> OCH <sub>2</sub> C=NH <sub>2</sub> <sup>+</sup> Cl <sup>-</sup> NH <sub>2</sub>	11 54 56 10
 5(i, ii, iii, iv)	OCH <sub>2</sub> CH <sub>2</sub> NH <sub>2</sub> OCH <sub>2</sub> CO <sub>2</sub> H OCH <sub>2</sub> CONH <sub>2</sub> <sup>+</sup> Cl <sup>-</sup> NH <sub>2</sub> OCH <sub>2</sub> C=NH <sub>2</sub> <sup>+</sup> Cl <sup>-</sup> NH <sub>2</sub>	5 1 1 1
 7(i, ii, iii, iv)	OCH <sub>2</sub> CH <sub>2</sub> NH <sub>2</sub> OCH <sub>2</sub> CO <sub>2</sub> H OCH <sub>2</sub> CONH <sub>2</sub> <sup>+</sup> Cl <sup>-</sup> NH <sub>2</sub> OCH <sub>2</sub> C=NH <sub>2</sub> <sup>+</sup> Cl <sup>-</sup> NH <sub>2</sub>	1 < 1 < 1 < 1
 8(i, ii, iii, iv)	OCH <sub>2</sub> CH <sub>2</sub> NH <sub>2</sub> OCH <sub>2</sub> CO <sub>2</sub> H OCH <sub>2</sub> CONH <sub>2</sub> <sup>+</sup> Cl <sup>-</sup> NH <sub>2</sub> OCH <sub>2</sub> C=NH <sub>2</sub> <sup>+</sup> Cl <sup>-</sup> NH <sub>2</sub>	20 7 7 5

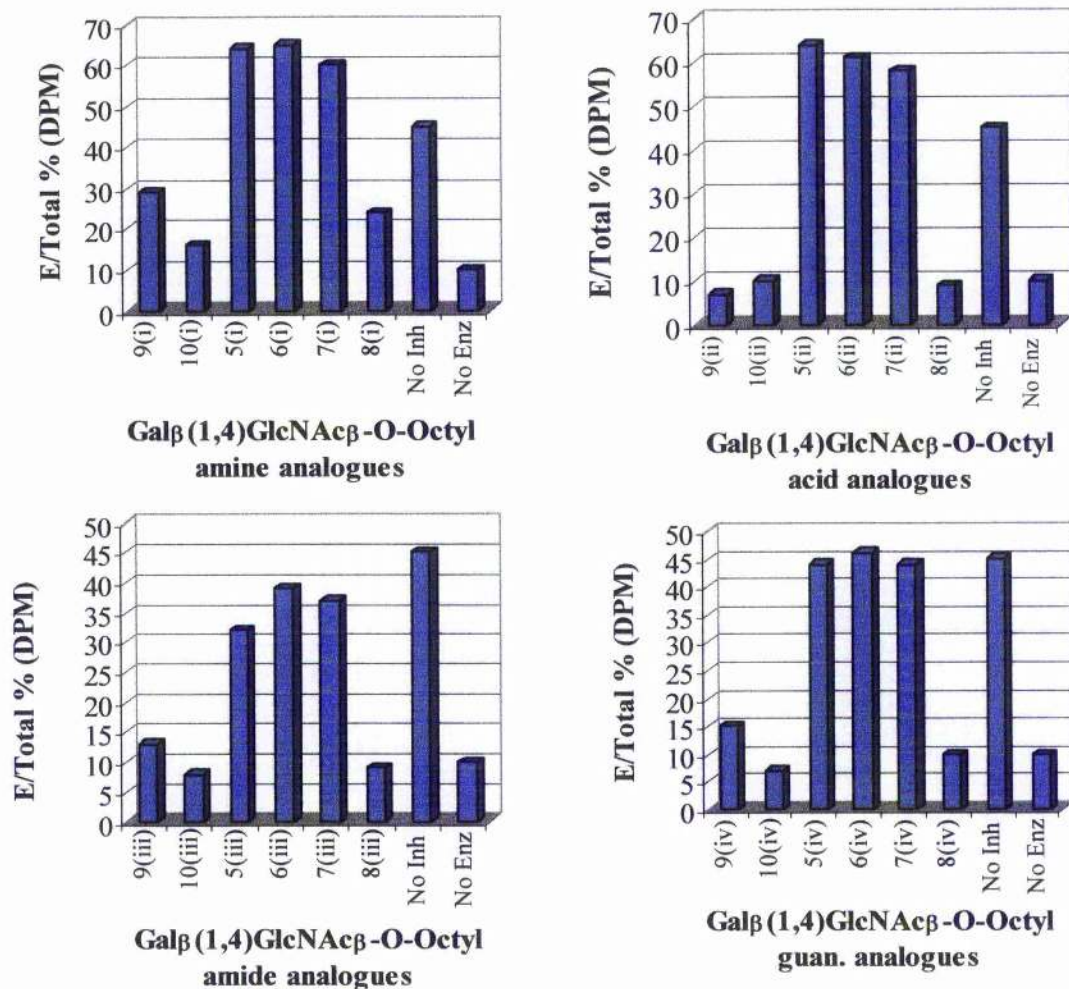
\* The concentration of each analogue = 540  $\mu$ M

### 3.2.2 Modified Gal $\beta$ (1,4)GlcNAc $\beta$ -O-Octyl radiochemical assay

Compounds 5(i,ii,iii,iv)-10(i,ii,iii,iv) (shown before in **Figure 36**) were incubated and assessed radiochemically as before, see page 46 and page 111 (*Pereira et al* 1995, *Vetere et al* 1996). The results were tabulated and plotted, **Figure 38**. These plots represent the result of the radiochemical assay using alternative substrate [compounds 5(i,ii,iii,iv)-10(i,ii,iii,iv)] to lactose. The results of the screen of compounds 5(i,ii,iii,iv)-10(i,ii,iii,iv) may be interpreted as before, i.e. compounds

giving results with values between 0-15 % Elution/Total (DPM) are good *trans*-sialidase substrates.

**Figure 38** The four graphs of radiochemical assay of compounds 5(i,ii,iii,iv)-10(i,ii,iii,iv)



**Legend of Figure 38**

Legend	Compound	Legend	Compound
5(i)	2' Amine-Galβ(1,4)GlcNAcβ-O-Octyl	5(ii)	2' Acid-Galβ(1,4)GlcNAcβ-O-Octyl
6(i)	3' Amine-Galβ(1,4)GlcNAcβ-O-Octyl	6(ii)	3' Acid-Galβ(1,4)GlcNAcβ-O-Octyl
7(i)	4' Amine-Galβ(1,4)GlcNAcβ-O-Octyl	7(ii)	4' Acid-Galβ(1,4)GlcNAcβ-O-Octyl
8(i)	6' Amine-Galβ(1,4)GlcNAcβ-O-Octyl	8(ii)	6' Acid-Galβ(1,4)GlcNAcβ-O-Octyl
9(i)	3 Amine-Galβ(1,4)GlcNAcβ-O-Octyl	9(ii)	3 Acid-Galβ(1,4)GlcNAcβ-O-Octyl
10(i)	6 Amine-Galβ(1,4)GlcNAcβ-O-Octyl	10(ii)	6 Acid-Galβ(1,4)GlcNAcβ-O-Octyl
No Sub	No substrate	No Sub	No substrate
No Enz	No enzyme	No Enz	No enzyme

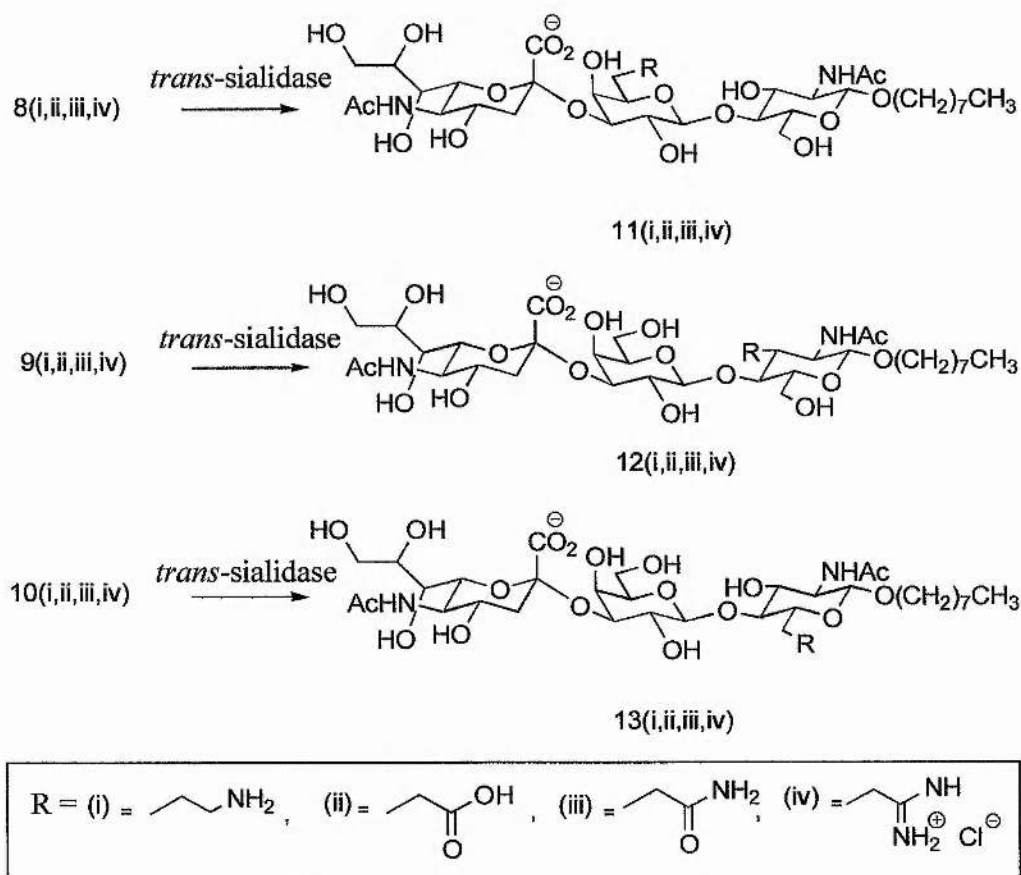


**Legend of Figure 38 cont.**

Legend	Compound	Legend	Compound
5(iii)	2'Amide-Galβ(1,4)GlcNAcβ-O-Octyl	5(iv)	2'Guan.-Galβ(1,4)GlcNAcβ-O-Octyl
6(iii)	3'Amide-Galβ(1,4)GlcNAcβ-O-Octyl	6(iv)	3'Guan.-Galβ(1,4)GlcNAcβ-O-Octyl
7(iii)	4'Amide-Galβ(1,4)GlcNAcβ-O-Octyl	7(iv)	4'Guan.-Galβ(1,4)GlcNAcβ-O-Octyl
8(iii)	6'Amide-Galβ(1,4)GlcNAcβ-O-Octyl	8(iv)	6'Guan.-Galβ(1,4)GlcNAcβ-O-Octyl
9(iii)	3Amide-Galβ(1,4)GlcNAcβ-O-Octyl	9(iv)	3Guan.-Galβ(1,4)GlcNAcβ-O-Octyl
10(iii)	6Amide-Galβ(1,4)GlcNAcβ-O-Octyl	10(iv)	6Guan.-Galβ(1,4)GlcNAcβ-O-Octyl
No Sub	No substrate	No Sub	No substrate
No Enz	No enzyme	No Enz	No enzyme

This study indicates that compounds 8(i,ii,iii,iv), 9(i,ii,iii,iv) and 10(i,ii,iii,iv) can be sialylated by *trans*-sialidase (as expected), but that compounds 5(i,ii,iii,iv), 6(i,ii,iii,iv) and 7(i,ii,iii,iv) are non-sialylable substrates. Compounds 11(i,ii,iii,iv)-13(i,ii,iii,iv), the sialylation products of compounds 8(i,ii,iii,iv), 9(i,ii,iii,iv) and 10(i,ii,iii,iv) are shown below in **Figure 39A**.

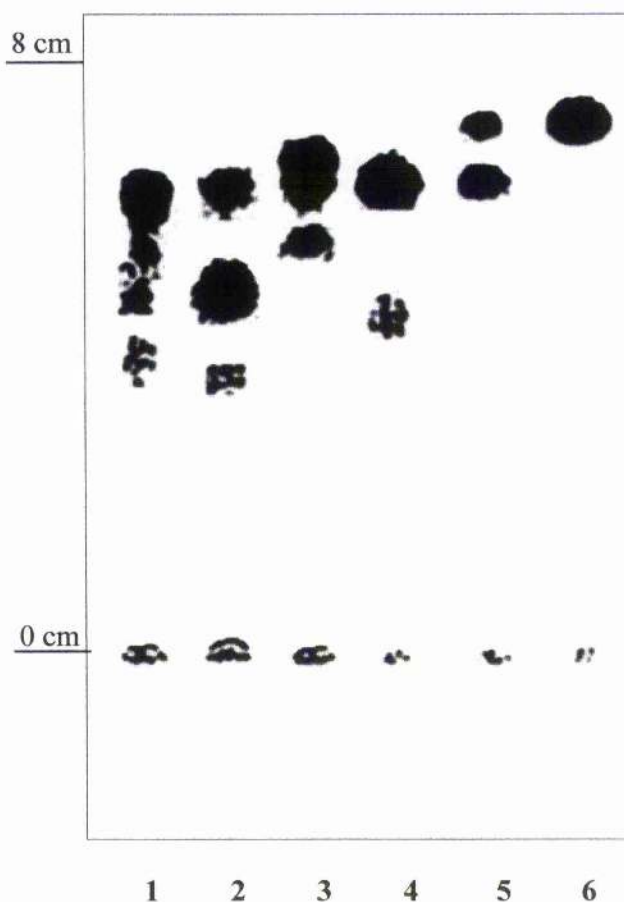
**Figure 39A** Sialylation products of compounds 8(i,ii,iii,iv), 9(i,ii,iii,iv) and 10(i,ii,iii,iv)



### 3.2.3 Potential sialylation of compounds 5(i,ii,iii,iv)-10(i,ii,iii,iv) using Neu5Ac-O-PNP (monitored by T.L.C.)

Compounds 5(i,ii,iii,iv)-10(i,ii,iii,iv) **Figure 36**, page 55, were incubated at 37 °C overnight (approx. 16 hours) with Neu5Ac-O-PNP and *trans*-sialidase (crude), see page 114. The results were recorded by T.L.C. and photographed. An example of sialylation of compounds 10(i,ii,iii,iv) to give 11(i,ii,iii,iv) is shown below in **Figure 39B**.

**Figure 39B** Compounds 11(i,ii,iii,iv)



**Legend of Figure 39B**

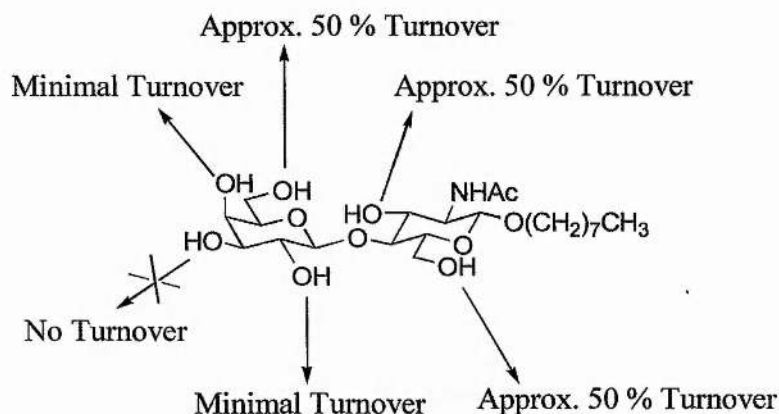
Lane 1	10(i) Incubation, Rf = 0.6, 0.5	Lane 4	10(iv) Incubation, Rf = 0.6, 0.4
Lane 2	10(ii) Incubation, Rf = 0.6, 0.4	Lane 5	Gal $\beta$ (1,4)Glc $\beta$ -O-Octyl Incubation, Rf = 0.7, 0.6
Lane 3	10(iii) Incubation, Rf = 0.6, 0.5	Lane 6	Gal $\beta$ (1,4)Glc $\beta$ -O-Octyl marker, Rf = 0.7

(Only the significant spots are referenced)

This T.L.C. shows all of compounds 8(i,ii,iii,iv) have become sialylated producing a

spot with an  $R_f = 0.5$  and  $0.4$  (approx.). As before modification of the hydroxyl group at position three prime of this sugar renders attachment of sialic acid impossible and hence any modifications at this position render compounds 6(i,ii,iii,iv) non-sialylatable substrates. Modification to the hydroxyl groups at position two prime and four prime again allow the attachment of sialic acid at position three prime, however the turnover is minimal compared to the unmodified turnover at 50 %. Modification of hydroxyl groups at the six prime position of Gal $\beta$ (1,4)GlcNAc $\beta$ -O-Octyl made no significant difference to the turnover, concurrent with the results of the radioactive screen and the study Gal $\beta$ -O-Octyl [compounds 3(i,ii,iii,iv)]. Modification of the hydroxyl groups at position three and six is also tolerated. This relative toleration of substrate modifications of *trans*-sialidase can be compared to the lack of substrate modifications permitted by  $\alpha$ (1,3)GalT (page 56). *trans*-sialidase substrate specificity to compounds 5(i,ii,ii,iv)-10(i,ii,iii,iv) is illustrated below in Figure 40.

**Figure 40** Approximate figures of turnover for *trans*-sialidase product formation from Gal $\beta$ (1,4)GlcNAc $\beta$ -O-Octyl analogues (assessment made by eye)



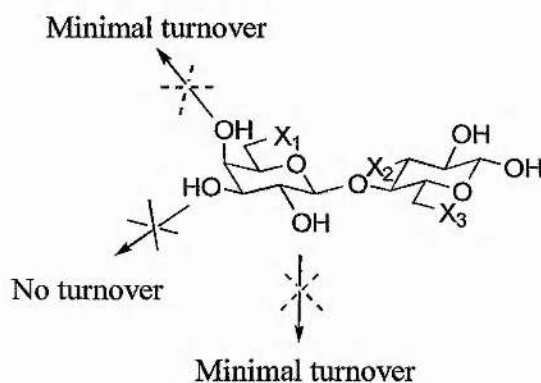
### 3.2.4 Conclusions

The results of the radiochemical assay indicates that modification of the hydroxyl groups at positions 2', 3', 4' (compounds 5(i,ii,ii,iv)-7 (i,ii,iii,iv) (*Hindsgaul et al* 1996)) prevents or prohibits the attachment of sialic acid to Gal $\beta$ (1,4)GlcNAc $\beta$ -O-Octyl. This information reiterates previous findings and indicates that the hydroxyl groups at positions 2', 3' and 4' of Gal $\beta$ (1,4)GlcNAc $\beta$ -O-Octyl are paramount for



sialylation. Modification of the hydroxyl groups at positions 6', 3 and 6 (compounds 8(i,ii,ii,iv)-10(i,ii,iii,iv) (*Hindsgaul et al 1996*)) play a minimal or no role in the enzyme binding and subsequent sialylation. These findings are comparable with the results of *trans*-sialidase incubations (with Neu5Ac-O-PNP) which were assessed by T.L.C., agreeing with previous findings. It may be that the hydroxyl group at the six prime position (position six of galactose) is projecting into space and hence is too far from the binding site to be of consequence. As before it may be possible to incorporate a solid phase linker (*Whittaker et al 1996*) at the 6 prime position to immobilise Gal $\beta$ (1,4)GlcNAc $\beta$ -O-Octyl analogues for exploitation of *trans*-sialidase in organic synthesis. *trans*-Sialidase can also tolerate modifications to the hydroxyl groups at position 3 and 6 the disaccharide unit. This point is shown diagrammatically again in **Figure 41**.

**Figure 41** Diagrammatic representation of key positions required for sialylation by *trans*-sialidase



X<sub>1</sub> = Any substrate of Gal $\beta$ (1,4)GlcNAc $\beta$ -O-Octyl/Gal $\beta$ -O-Octyl screen  
 X<sub>2</sub>/X<sub>3</sub> = Any substrate of Gal $\beta$ (1,4)GlcNAc $\beta$ -O-Octylscreen

## Chapter 4

*trans*-Sialidase substrates  
based on natural surface  
oligosaccharides

## Chapter 4 - Introduction

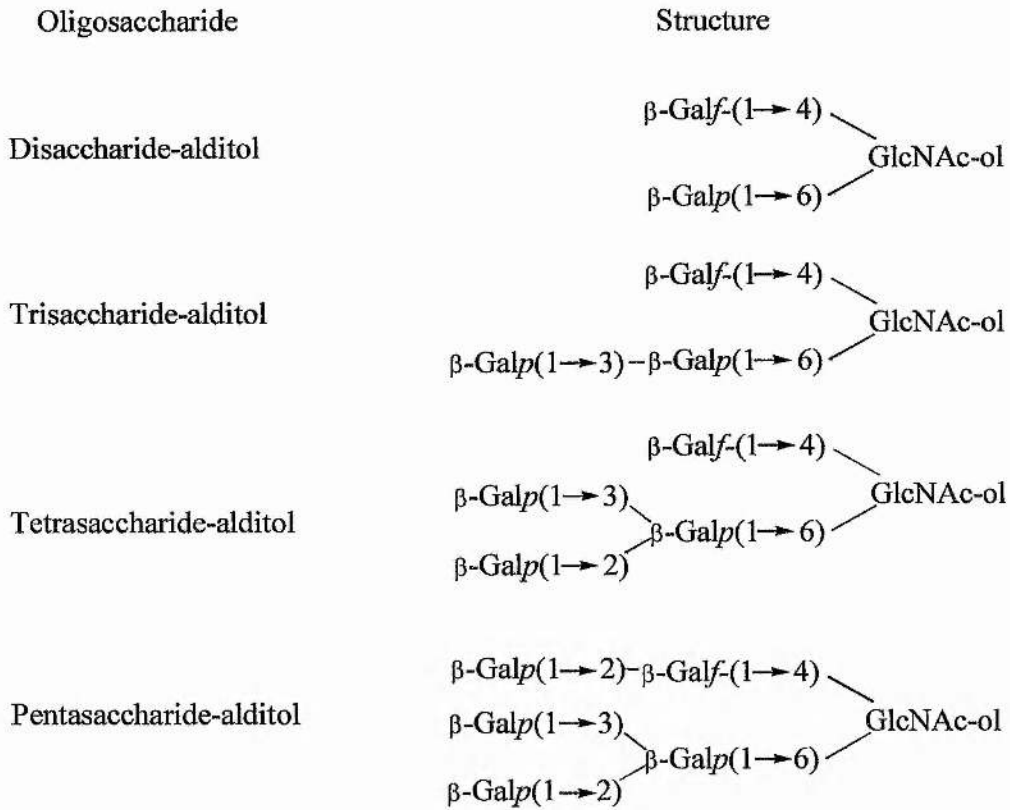
### 4.1 *Trypanosoma cruzi* G-strain (Epimastigotes)

To understand fully the actions of *Trypanosoma cruzi* (G-strain) *trans*-sialidase it is necessary to characterise the cell surface glycoconjugates. This allows an extrapolation to the role of carbohydrates on the parasitic cell surface. The cell surface glycoconjugates from the epimastigote form of *Trypanosoma cruzi* have been analysed by SDS-PAGE. The result of this was a broad band at 38-43 kDa (Previato *et al* 1994). These components are non-sialylated. The oligosaccharide cell surface acceptor moiety of *T. cruzi* (G-strain) consists of GlcNAc units which other oligosaccharides can be joined to give branched structures and are *O*-glycosidically bonded to the amino acids serine or threonine (Previato *et al* 1994).

#### 4.1.2 Characterisation of the oligosaccharides accepting sialic acid

Analysis of the isolated epimastigote showed neutral sugars 57.5 %, hexosamine 16 %, protein 4.5 %, phosphorus 1 %, sialic acid - trace. The sugar region was then digested to reveal the monomers present as follows, galactose 4.8 M, *N*-acetyl glucosamine 1.6 M, mannose 1 M and glucose 0.15 M, (relative molarity) (Previato *et al* 1994). The cell surface glycoproteins were subject to enzymatic digestion and then separated on a Bio-Gel P4 column. This purification gave five oligosaccharide fractions (Previato *et al* 1994). The structures of these fragments were then analysed and evaluated using F.A.B.-MS and G.C. This study revealed the oligosaccharides which are shown in **Figure 42** (Previato *et al* 1994).

**Figure 42** *O*-Glycosidically linked GlcNAc-bound oligosaccharides isolated from 38/43 kDa glycoproteins from epimastigote *T. cruzi* (G-strain) (Previato *et al* 1994).



These fragments are the main acceptors of neuraminic acid on the cell surface of *T. cruzi* (G-strain). They are unusual in that it was suspected that the branched sugar moieties would be *O*-linked to GalNAc and not GlcNAc, since only unsubstituted *O*-linked GlcNAc's had been discovered previously (Previato *et al* 1994). It is suspected that monosaccharide *O*-GlcNAc's have an important role in the cellular pathway regulation. Single *O*-GlcNAc oligosaccharides have also been located in *Trypanosoma brucei* (Haltiwanger *et al* 1992) as well as other parasitic organisms. The GlcNAc end of these units can also be attached to other residues forming three to six units. It is the other end of the chains which give a negative charge (i.e. sialic acid) which is recognised by antibodies and lectins. Sialylated epitopes (Ssp3) are important for monoclonal antibody recognition (Frasch *et al* 1996), cell surface attachment and invasion by *T. cruzi*. Metacyclic trypomastigotes use a sialylated

glycoprotein (35/50 kDa by SDS-page), to invade cells, presumably by an analogous method (Previato *et al* 1994).

The *O*-GlcNAc units of *T. cruzi* G-strain are novel since some consist of branched structures carrying both galactofuranose (Gal-*f*) and galactopyranose (Gal-*p*) substitutions (Previato *et al* 1994).

#### 4.1.3 *Trypanosoma cruzi* (Y-strain)

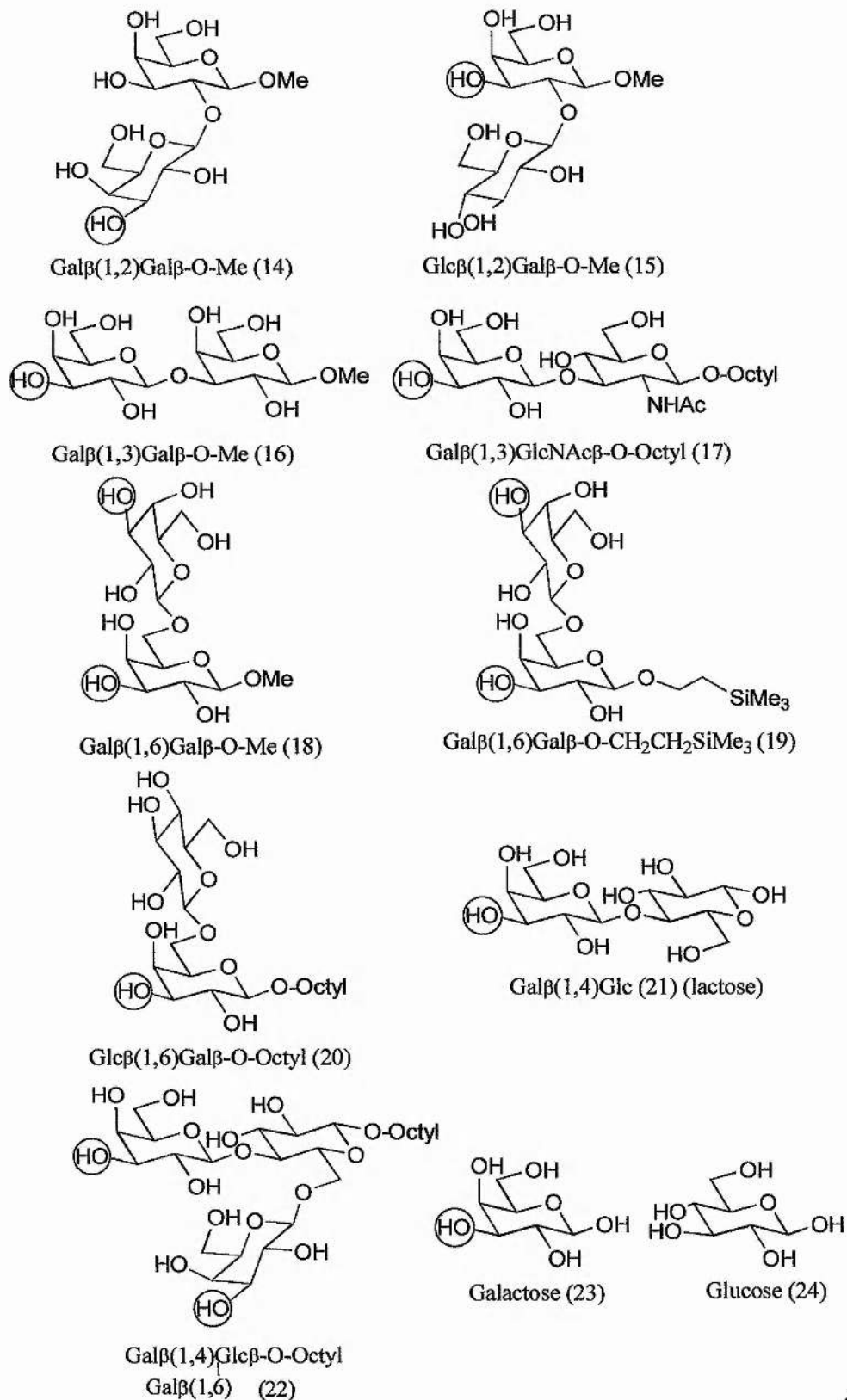
Analysis was carried out on  $\beta$ -eliminated oligosaccharide-alditols. The glycoprotein was reduced using sodium borohydride before separation took place on a Bio-gel P4 column (Previato *et al* 1995). Four fractions were collected, similar to that of *Trypanosoma cruzi* G-strain. The four fractions were characterised and named as Fractions I, II, III and IV (0.3, 5.0, 3.0 and 0.4 relative molar ratio) (Previato *et al* 1995). These fractions were characterised by G.C. and NMR spectroscopy. Fraction I consists of GlcNAc only whereas Fractions II, III and IV comprised of a mixture of GlcNAc-ol, galactose and GalNAc-ol, and each had mono, di and trisaccharides present (Previato *et al* 1995), see **Figure 43**.

**Figure 43** The structures of the *O*-linked oligosaccharides found in *Trypanosoma cruzi* Y-strain (Previato et al 1995)

Oligosaccharide	Structure
Monosaccharide-alditol	$\beta\text{-Galp}(1\rightarrow 3) - \text{GlcNAc-ol}$
	$\beta\text{-Galp}(1\rightarrow 4) - \text{GlcNAc-ol}$
Disaccharide-alditol	$\begin{array}{l} \beta\text{-Galp}(1\rightarrow 3) \\ \beta\text{-Galp}(1\rightarrow 6) \end{array} \begin{array}{l} \diagdown \\ \diagup \end{array} \text{GlcNAc-ol}$
	$\begin{array}{l} \beta\text{-Galp}(1\rightarrow 4) \\ \beta\text{-Galp}(1\rightarrow 6) \end{array} \begin{array}{l} \diagdown \\ \diagup \end{array} \text{GlcNAc-ol}$
	$\begin{array}{l} \beta\text{-Galp}(1\rightarrow 3) \\ \beta\text{-Galp}(1\rightarrow 2) - \beta\text{-Galp}(1\rightarrow 6) \end{array} \begin{array}{l} \diagdown \\ \diagup \end{array} \text{GlcNAc-ol}$
	$\begin{array}{l} \beta\text{-Galp}(1\rightarrow 4) \\ \beta\text{-Galp}(1\rightarrow 2) - \beta\text{-Galp}(1\rightarrow 6) \end{array} \begin{array}{l} \diagdown \\ \diagup \end{array} \text{GlcNAc-ol}$
Trisaccharide-alditol	

Based on these natural fragments, known to be the sites of sialic acid recognition, a variety of disaccharides and trisaccharides have been synthesised, some are shown below **Figure 44** (Kantha and Field 1997).

**Figure 44** A variety of potential disaccharide and trisaccharide substrates for *T. cruzi* trans-sialidase (Kantha and Field 1997) (The circles indicate the potential sites of sialic acid attachment)

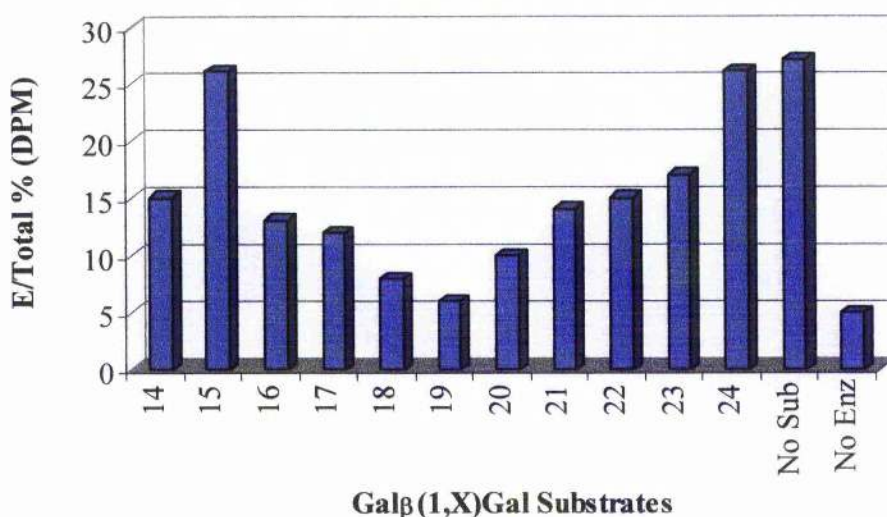


## Chapter 4 – Results and Discussion

### 4.2 Radiochemical assay of all the Gal $\beta$ (1,X)Gal derivatives

The Gal $\beta$ (1,X)Gal derivatives were assayed radiochemically, as before see page 46 and 111 (Pereira *et al* 1995, Vetere *et al* 1996) to assess their capability as *trans*-sialidase substrates. The results were plotted and are shown below in **Figure 45**.

**Figure 45** % E/Total (DPM) of all Gal $\beta$ (1,X)Gal



Legend of **Figure 45**

Gal $\beta$ (1,2)Gal $\beta$ -O-Me (14)	Gal $\beta$ (1,4)[Gal $\beta$ (1,6)Glc] $\beta$ -O-Octyl (21)
Glc $\beta$ (1,2)Gal $\beta$ -O-Me (15)	Gal $\beta$ (1,4)Glc (22)
Gal $\beta$ (1,3)Gal $\beta$ -O-Me (16)	Galactose (23)
Gal $\beta$ (1,3)GlcNAc $\beta$ -O-Octyl (17)	Glucose (24)
Gal $\beta$ (1,6)Gal $\beta$ -O-Me (18)	No inhibitor
Gal $\beta$ (1,6)Gal $\beta$ -O-CH <sub>2</sub> CH <sub>2</sub> SiMe <sub>3</sub> (19)	No enzyme
Glc $\beta$ (1,6)Gal $\beta$ -O-Octyl (20)	

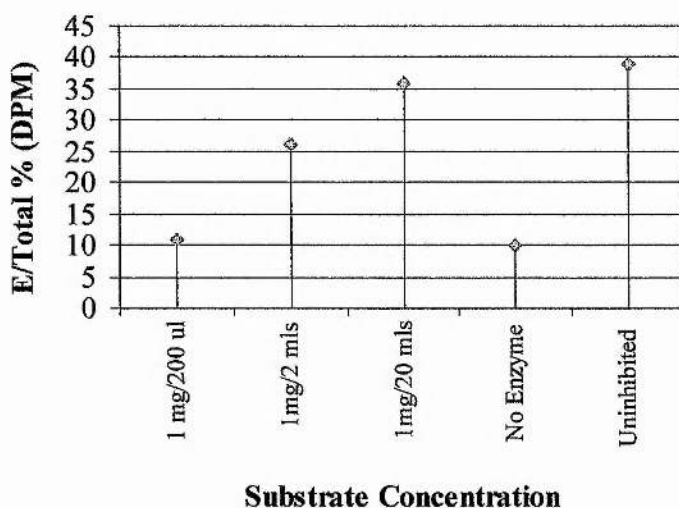
The plotted results above are based on an average of three radioactive assays for all substrates, except for compounds (15) and (19) which are based on an average of four radioactive assays. The results above are an indication of the oligosaccharides which are good substrates of *trans*-sialidase, (Compounds giving results with values between 0-15 % Elution/Total (DPM) are good *trans*-sialidase substrates). As expected glucose is not a substrate.



### 4.3 Multi-sialylation of oligosaccharide containing resin

It is apparent from the radioactive assay, page 68 that it may be possible to sialylate an internal galactose. It may also be possible to sialylate more than one  $\beta$ -galactose moiety, i.e. a terminal galactose as well as an internal galactose (depending of the Gal $\beta$ (1,X) linkage). It is believed that *trans*-sialidase has two galactose binding sites (one in the active site and one in the lectin binding domain, compare to *Micromonospora Viridifaciens* neuraminidase), it may be possible to simultaneously bind two  $\beta$ -galactose moieties. Consequently, this theory was tested using a resin containing many surface galacto-pyranosides was purchased (*Sigma Chemicals Ltd*). The resin, *p*-aminobenzyl-1-thio- $\beta$ -S-galacto-pyranoside was used as a potential acceptor substrate and assayed radiochemically as before. The initial study gave a result suggesting that this resin is comparable with other reliable substrates of *trans*-sialidase from our study, such as Gal $\beta$ (1,3)GlcNAc $\beta$ -O-Octyl and Gal $\beta$ (1,6)Gal. Therefore, a study was carried out radiochemically on this resin using a serial dilution. **Figure 46** shows a plot of the serial dilution of *p*-aminobenzyl-1-thio- $\beta$ -S-galacto-pyranoside.

**Figure 46** *p*-aminobenzyl-1-thio- $\beta$ -S-galacto-pyranoside (substrate) resin (serial dilution)



This graph indicates that *p*-aminobenzyl-1-thio- $\beta$ -S-galacto-pyranoside is a good substrate of *trans*-sialidase.

The binding capacity of the resin was calculated as follows:

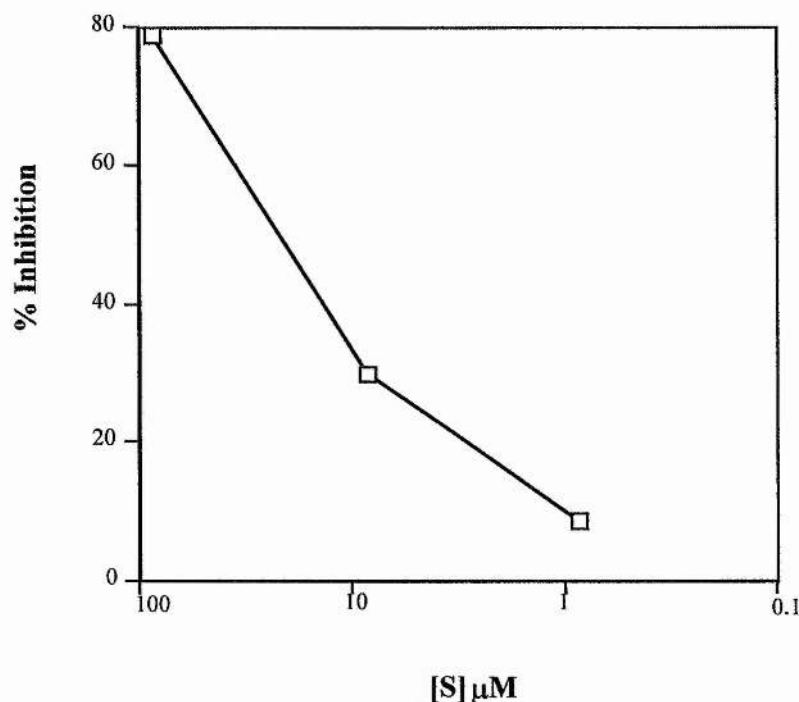
1 ml of resin binds 2 mgs of  $\beta$ -galactosidase (Molecular weight of  $\beta$ -galactosidase, monomer (*E. coli*) = 116 kDa) 1 ml of resin will bind  $1.72 \times 10^{-8}$  mol of protein.

Assuming a ratio of 1 sugar/ 1 enzyme  $\therefore$  1 ml resin contains  $1.72 \times 10^{-8}$  mol sugar.

$$\therefore 1 \text{ ml}/200\mu\text{l} \cong 86 \mu\text{M}, 1 \text{ ml}/2\text{ml} \cong 8.6 \mu\text{M}, 1 \text{ ml}/20\text{ml} \cong 0.86 \mu\text{M}$$

The above data for *p*-aminobenzyl-1-thio- $\beta$ -O-galacto-pyranoside resin was re-plotted to assist the calculation for an  $IC_{50}$  value for this substrate. This plot is shown below in **Figure 47**.

**Figure 47** Concentration of *p*-aminobenzyl-1-thio- $\beta$ -S-galacto-pyranoside versus % inhibition



This plot indicates that *p*-aminobenzyl-1-thio- $\beta$ -S-galacto-pyranoside has  $IC_{50}$  value of  $34 \mu\text{M}$ .

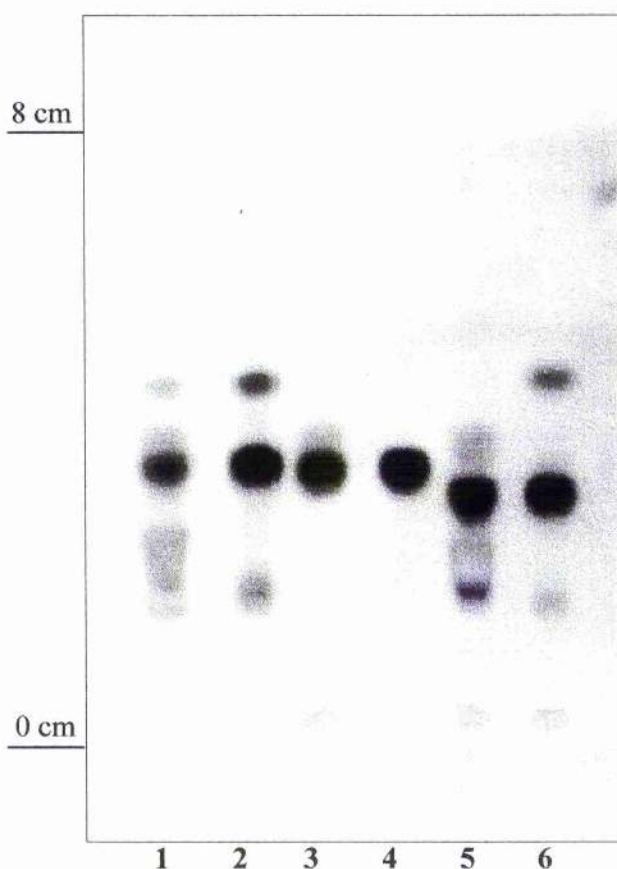
#### **4.4** *trans*-Sialidase catalysed sialylation of di and trisaccharide acceptor substrates

Compounds (14)-(24), **Figure 44**, page 67, were incubated at  $37^\circ\text{C}$  overnight (approx. 16 hours) with Neu5Ac-O-PNP and *trans*-sialidase (crude). The results were recorded on T.L.C. and photographed.

#### 4.4.1 Incubation of Gal $\beta$ (1,2)Gal-O-Me (14), Glc $\beta$ (1,2)Gal $\beta$ -O-Me (15) and Gal $\beta$ (1,3)Gal $\beta$ -OMe (16)

Gal $\beta$ (1,2)Gal $\beta$ -O-Me, Glc $\beta$ (1,2)Gal $\beta$ -O-Me and Gal $\beta$ (1,3)Gal $\beta$ -O-Me were incubated as before, also see page 114. **Figure 48** shows the photograph of the T.L.C. plate. This photograph shows that Gal $\beta$ (1,3)Gal $\beta$ -O-Me and Gal $\beta$ (1,2)Gal $\beta$ -O-Me have been sialylated but Glc $\beta$ (1,2)Gal-O-Me has not. Strong marker solutions show some degradation on storage, although all were purified before experimentation.

**Figure 48** Sialylation of Gal $\beta$ (1,2)Gal-O-Me, Glc $\beta$ (1,2)Gal $\beta$ -O-Me and Gal $\beta$ (1,3)Gal $\beta$ -OMe



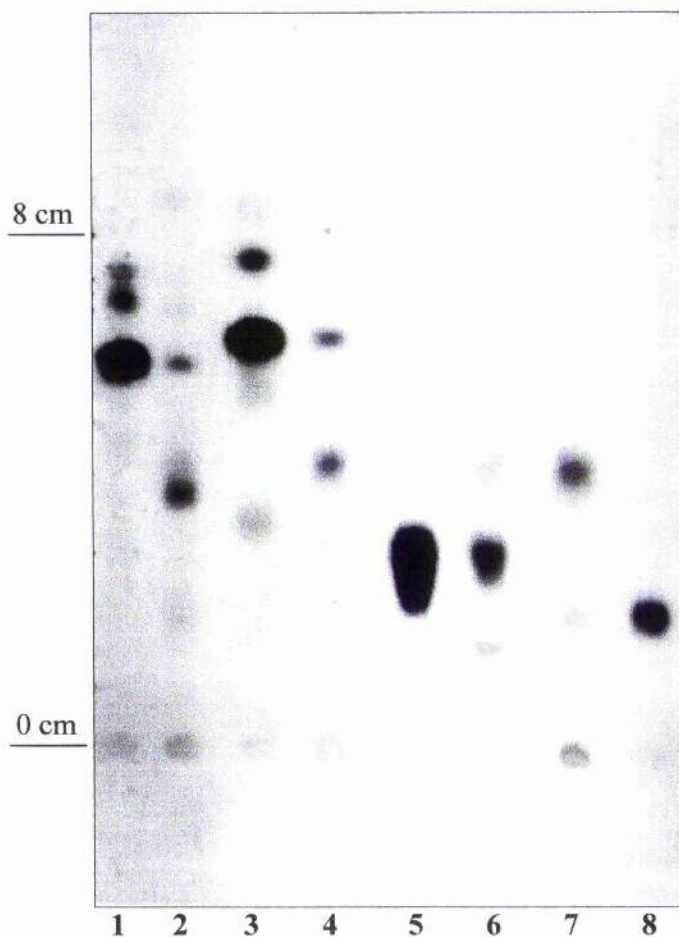
**Legend of Figure 48** (Only Rfs corresponding to the main compound are indicated)

Lane 1 Incubation of Gal $\beta$ (1,3)Gal $\beta$ -O-Me with <i>trans</i> -sialidase, Rf = 0.4, 0.3	Lane 4 Glc $\beta$ (1,2)Gal $\beta$ -O-Me marker, Rf = 0.4
Lane 2 Gal $\beta$ (1,3)Gal $\beta$ -O-Me marker, Rf = 0.4	Lane 5 Incubation of Gal $\beta$ (1,2)Gal $\beta$ -O-Me with <i>trans</i> -sialidase, Rf = 0.4, 0.3
Lane 3 Incubation of Glc $\beta$ (1,2)Gal $\beta$ -O-Me with <i>trans</i> -sialidase, Rf = 0.4	Lane 6 Gal $\beta$ (1,2)Gal $\beta$ -O-Me, Rf = 0.4

#### 4.4.2 Incubation of Gal $\beta$ (1,6)Gal $\beta$ -O-Me (18), Gal $\beta$ (1,6)Gal $\beta$ -O-CH<sub>2</sub>CH<sub>2</sub>SiMe<sub>3</sub> (19) and Glc $\beta$ (1,6)Gal $\beta$ -O-Octyl (20)

A similar experiment was carried out using Gal $\beta$ (1,6)Gal $\beta$ -O-CH<sub>2</sub>CH<sub>2</sub>SiMe<sub>3</sub>, Glc $\beta$ (1,6)Gal $\beta$ -O-Octyl and Gal $\beta$ (1,6)Gal $\beta$ -O-Me as *trans*-sialidase acceptors. **Figure 49** shows the photograph of the T.L.C. plate. This photograph confirms that Gal $\beta$ (1,6)Gal $\beta$ -O-CH<sub>2</sub>CH<sub>2</sub>SiMe<sub>3</sub>, Glc $\beta$ (1,6)Gal $\beta$ -O-Octyl and Gal $\beta$ (1,6)Gal $\beta$ -O-Me have been sialylated. Strong marker solutions show some degradation on storage, although all were purified before experimentation.

**Figure 49** Sialylation of Gal $\beta$ (1,6)Gal $\beta$ -O-CH<sub>2</sub>CH<sub>2</sub>Si(CH<sub>3</sub>)<sub>3</sub>, Glc $\beta$ (1,6)Gal $\beta$ -O-Octyl and Gal $\beta$ (1,6)Gal $\beta$ -O-Me



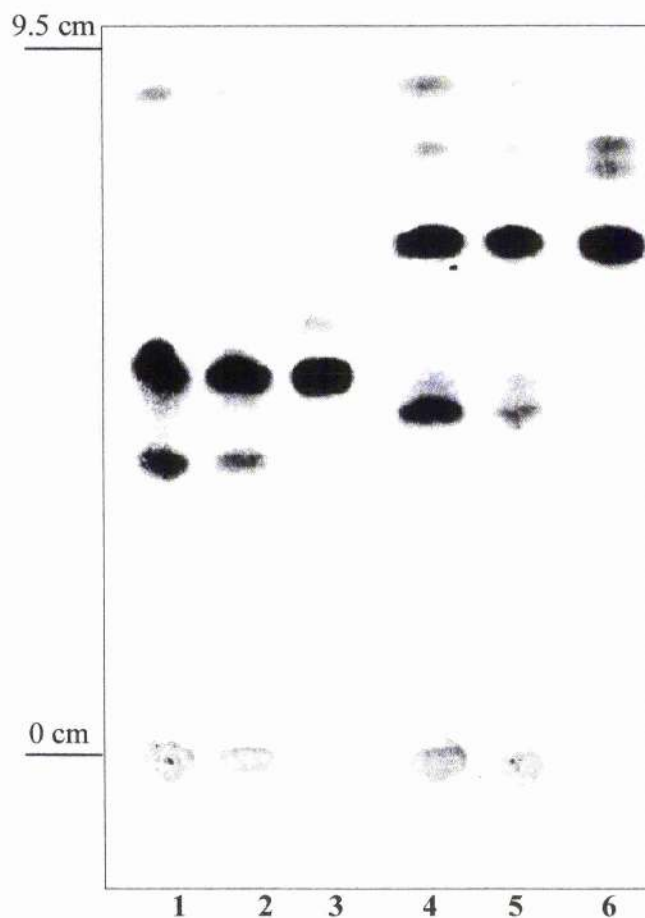
**Legend of Figure 49** (Only Rfs of the main compounds are indicated)

Lane 1 Gal $\beta$ (1,6)Gal $\beta$ -O-CH <sub>2</sub> CH <sub>2</sub> Si(CH <sub>3</sub> ) <sub>3</sub> marker, Rf = 0.5	Lane 5 Gal $\beta$ (1,6)Gal $\beta$ -O-Me, Rf = 0.3
Lane 2 Incubation of Gal $\beta$ (1,6)Gal $\beta$ -O-CH <sub>2</sub> CH <sub>2</sub> Si(CH <sub>3</sub> ) <sub>3</sub> with <i>trans</i> -sialidase, Rf = 0.5, 0.3	Lane 6 Incubation of Gal $\beta$ (1,6)Gal $\beta$ -O-Me with <i>trans</i> -sialidase, Rf = 0.3, 0.1
Lane 3 Glc $\beta$ (1,6)Gal $\beta$ -O-Octyl marker, Rf = 0.5	Lane 7 Incubation lactose with <i>trans</i> -sialidase, Rf = 0.4, 0.2
Lane 4 Incubation of Glc $\beta$ (1,6)Gal $\beta$ -O-Octyl with <i>trans</i> -sialidase, Rf = 0.5, 0.4	Lane 8 Sialyl lactose marker, Rf = 0.2

#### 4.4.3 Incubation of Glc $\beta$ (1,6)Gal $\beta$ -O-Octyl (20) and Gal $\beta$ (1,4)[Gal $\beta$ (1,6)Glc] $\beta$ -O-Octyl (21)

The disaccharide Glc $\beta$ (1,6)Gal $\beta$ -O-Octyl was incubated as before, in parallel with the incubation of a branched trisaccharide, Gal $\beta$ (1,4)[Gal $\beta$ (1,6)Glc] $\beta$ -O-Octyl (*Kartha and Field* 1997). The incubation of Glc $\beta$ (1,6)Gal $\beta$ -O-Octyl is important since the terminal residue is glucose and not galactose, as in all of the previous substrates. **Figure 50** shows a photograph of the T.L.C. plate of this incubation. This incubation was carried out using two concentrations of Neu5Ac-O-PNP, (see legend below for concentrations).

**Figure 50** Sialylation of Gal $\beta$ (1,4)[Gal $\beta$ (1,6)Glc] $\beta$ -O-Octyl and Glc $\beta$ (1,6)Gal $\beta$ -O-Octyl



**Legend of Figure 50**

Lane 1 Incubation of branched lactose (30 mM Neu5Ac-O-PNP), Rf = 0.6, 0.5	Lane 4 Incubation of Glc $\beta$ (1,6)Gal $\beta$ -O-Octyl (30 mM Neu5Ac-O-PNP), Rf = 0.7, 0.4
Lane 2 Incubation of branched lactose (10 mM Neu5Ac-O-PNP), Rf = 0.6, 0.5	Lane 5 Incubation of Glc $\beta$ (1,6)Gal $\beta$ -O-Octyl (10 mM Neu5Ac-O-PNP), Rf = 0.7, 0.4
Lane 3 branched lactose marker, Rf = 0.6	Lane 6 Glc $\beta$ (1,6)Gal $\beta$ -O-Octyl marker, Rf = 0.7, 0.4



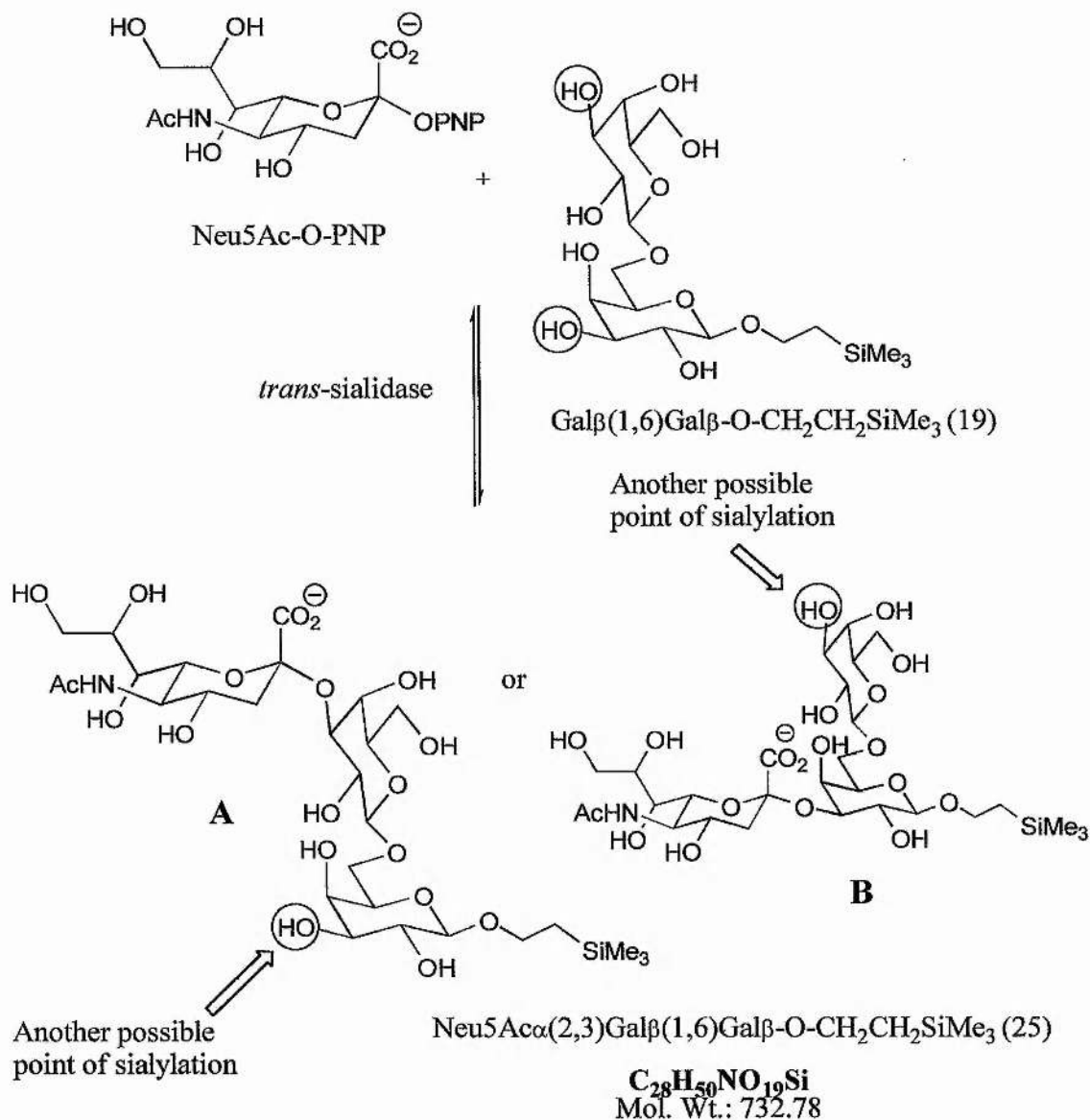
#### 4.5 Sialylation of Gal $\beta$ (1,6)Gal $\beta$ -O-CH<sub>2</sub>CH<sub>2</sub>SiMe<sub>3</sub> (19)

In an attempt to confirm the sialylation of these Gal $\beta$ (1,X)Gal substrates, three of the substrates, Gal $\beta$ (1,6)Gal $\beta$ -O-CH<sub>2</sub>CH<sub>2</sub>SiMe<sub>3</sub>, Gal $\beta$ (1,4)[Gal $\beta$ (1,6)]Glc $\beta$ -O-Octyl and Glc $\beta$ (1,6)Gal $\beta$ -O-Octyl were incubated on a preparative scale. Sialylated products of these incubations were analysed by electrospray-MS. Neu5Ac $\alpha$ (2,3)Gal $\beta$ (1,6)Gal $\beta$ -O-CH<sub>2</sub>CH<sub>2</sub>SiMe<sub>3</sub> and Neu5Ac $\alpha$ (2,3)Glc $\beta$ (1,6)Gal $\beta$ -O-Octyl were also degraded with *C. perfringens* neuraminidase,  $\beta$ -galactosidase and  $\beta$ -glucosidase respectively.

##### 4.5.2 Preparative scale sialylation of Gal $\beta$ (1,6)Gal $\beta$ -O-CH<sub>2</sub>CH<sub>2</sub>SiMe<sub>3</sub> (19)

Gal $\beta$ (1,6)Gal $\beta$ -O-CH<sub>2</sub>CH<sub>2</sub>SiMe<sub>3</sub> was synthesised chemically (*Kartha and Field* 1996). In an attempt to prove the sialylation of this oligosaccharide, already confirmed radiochemically and by T.L.C., the incubation of Gal $\beta$ (1,6)Gal $\beta$ -O-CH<sub>2</sub>CH<sub>2</sub>SiMe<sub>3</sub> was increased to a preparative level of approximately 3 mgs. As before, the sialylation of (19) by *trans*-sialidase is reversible with the sialylated product being a substrate for the back reaction. **Figure 51** illustrates the proposed sialylation of Gal $\beta$ (1,6)Gal $\beta$ -O-CH<sub>2</sub>CH<sub>2</sub>SiMe<sub>3</sub>. A product (approximately 1 mg) was isolated which had the correct assumed R<sub>f</sub> value by T.L.C.

**Figure 51** *trans*-Sialidase sialylation of Gal $\beta$ (1,6)Gal $\beta$ -O-CH<sub>2</sub>CH<sub>2</sub>SiMe<sub>3</sub>

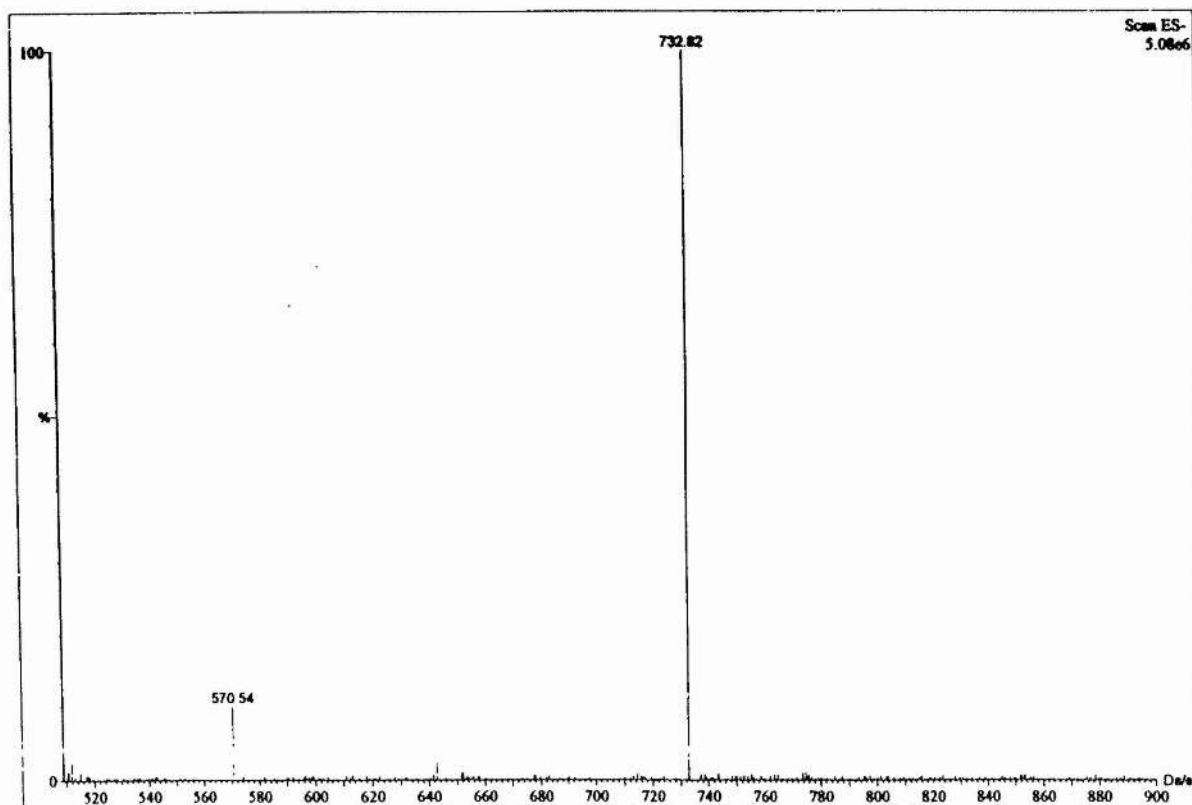


There is two possible sites of sialylation on the Gal $\beta$ (1,6)Gal $\beta$ -O-CH<sub>2</sub>CH<sub>2</sub>SiMe<sub>3</sub> as indicated on **Figure 51**. Consequently there are two possible products from this *trans*-sialidase incubation. The two products are shown above as product A and B. A is the most likely based on previous literature (*Schenkman and Vandkerchove* 1992). However, product B is also a viable proposition which will be discussed later.

#### 4.5.3 Characterisation of Neu5Ac $\alpha$ (2,3)Gal $\beta$ (1,6)Gal $\beta$ -O-CH<sub>2</sub>CH<sub>2</sub>Si(CH<sub>3</sub>)<sub>3</sub> (25) - Electrospray Mass Spectrometry

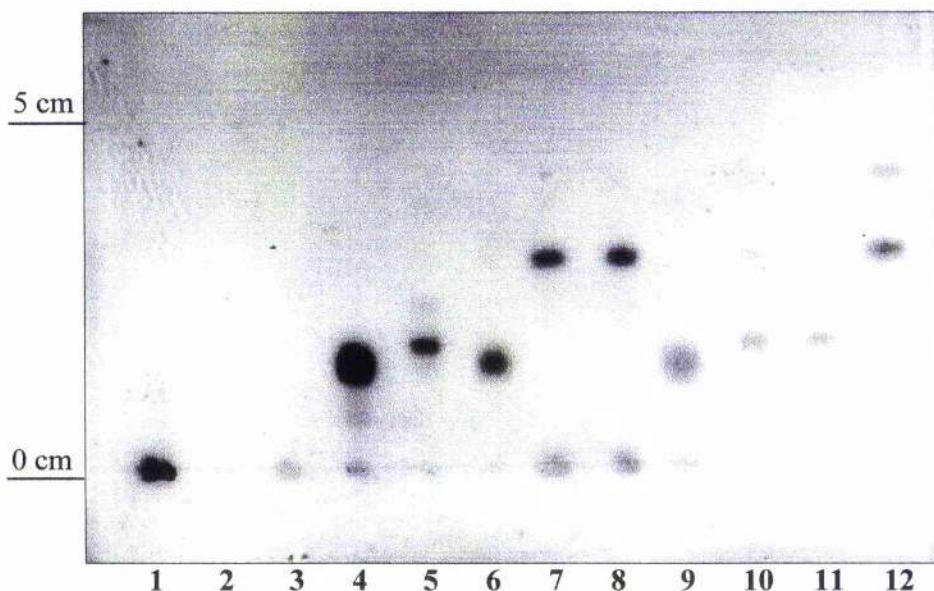
Neu5Ac $\alpha$ (2,3)[Gal $\beta$ (1,6)Gal $\beta$ -O-CH<sub>2</sub>CH<sub>2</sub>Si(CH<sub>3</sub>)<sub>3</sub>] was isolated and subject to Electrospray Mass Spectrometry. The spectrum is shown below in **Figure 52**. The spectrum was run from 510-900 Da/e. The calculated molecular weight for this compound is 732.78. The spectrum shows clearly only one peak at 732.82 Da/e.

**Figure 52** Mass Spectrum of Neu5Ac $\alpha$ (2,3)Gal $\beta$ (1,6)Gal $\beta$ -O-CH<sub>2</sub>CH<sub>2</sub>Si(CH<sub>3</sub>)<sub>3</sub>



**4.5.4 Enzymatic digestion of Neu5Ac $\alpha$ (2,3)Gal $\beta$ (1,6)Gal $\beta$ -O-CH<sub>2</sub>CH<sub>2</sub>SiMe<sub>3</sub> (25)** Neu5Ac $\alpha$ (2,3)Gal $\beta$ (1,6)Gal $\beta$ -O-CH<sub>2</sub>CH<sub>2</sub>SiMe<sub>3</sub> was subjected to systematic enzymatic digestion with  $\beta$ -galactosidase and *C. perfringens* neuraminidase. Shown below in **Figure 53** is the photograph of the enzymatic digestion of Neu5Ac $\alpha$ (2,3)Gal $\beta$ (1,6)Gal $\beta$ -O-CH<sub>2</sub>CH<sub>2</sub>SiMe<sub>3</sub>.

**Figure 53** Systematic enzymatic digestion Neu5Ac $\alpha$ (2,3)Gal $\beta$ (1,6)Gal $\beta$ -O-CH<sub>2</sub>CH<sub>2</sub>SiMe<sub>3</sub> (25)



**Legend of Figure 53**

Lane 1 <i>C. perfringens</i> neuraminidase Marker, Rf = 0	Lane 7 Incubation c, Neu5Ac $\alpha$ (2,3)Gal $\beta$ (1,6)Gal $\beta$ -O-CH <sub>2</sub> CH <sub>2</sub> Si(CH <sub>3</sub> ) <sub>3</sub> with <i>C. perfringens</i> neuraminidase, Rf = 0.5
Lane 2 $\beta$ -galactosidase Marker, Rf = 0	Lane 8 Incubation d, Gal $\beta$ (1,6)Gal $\beta$ -O-CH <sub>2</sub> CH <sub>2</sub> Si(CH <sub>3</sub> ) <sub>3</sub> with <i>C. perfringens</i> neuraminidase, Rf = 0.5
Lane 3 Neuraminic acid Marker, Rf = 0	Lane 9 Incubation e, Neu5Ac $\alpha$ (2,3)Gal $\beta$ (1,6)Gal $\beta$ -O-CH <sub>2</sub> CH <sub>2</sub> Si(CH <sub>3</sub> ) <sub>3</sub> with <i>C. perfringens</i> neuraminidase and $\beta$ -galactosidase, Rf = 0.2
Lane 4 Galactose Marker, Rf = 0.2	Lane 10 Incubation f, Neu5Ac $\alpha$ (2,3)Gal $\beta$ (1,6)Gal $\beta$ -O-CH <sub>2</sub> CH <sub>2</sub> Si(CH <sub>3</sub> ) <sub>3</sub> and buffer only, Rf = 0.5, 0.3
Lane 5 Incubation a, Neu5Ac $\alpha$ (2,3)Gal $\beta$ (1,6)Gal $\beta$ -O-CH <sub>2</sub> CH <sub>2</sub> Si(CH <sub>3</sub> ) <sub>3</sub> with $\beta$ -galactosidase, Rf = 0.3	Lane 11 Neu5Ac $\alpha$ (2,3)Gal $\beta$ (1,6)Gal $\beta$ -O-CH <sub>2</sub> CH <sub>2</sub> Si(CH <sub>3</sub> ) <sub>3</sub> Marker, Rf = 0.3
Lane 6 Incubation b, Gal $\beta$ (1,6)Gal $\beta$ -O-CH <sub>2</sub> CH <sub>2</sub> Si(CH <sub>3</sub> ) <sub>3</sub> with $\beta$ -galactosidase, Rf = 0.2	Lane 12 Gal $\beta$ (1,6)Gal $\beta$ -O-CH <sub>2</sub> CH <sub>2</sub> Si(CH <sub>3</sub> ) <sub>3</sub> Marker, Rf = 0.6, 0.5, 0.1

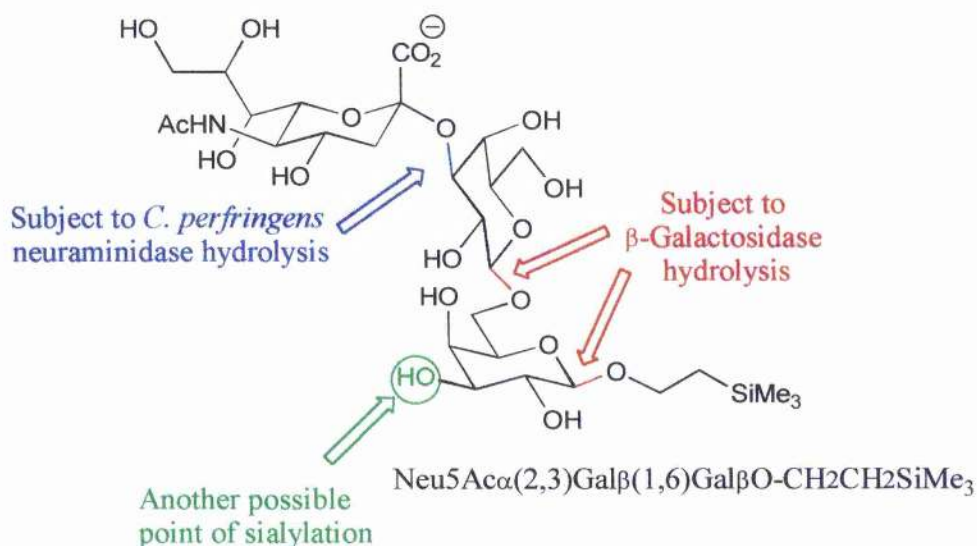
#### 4.5.5 Systematic degradation of Neu5Ac $\alpha$ (2,3)Gal $\beta$ (1,6)Gal $\beta$ -O-CH<sub>2</sub>CH<sub>2</sub>SiMe<sub>3</sub> (25)

Neu5Ac $\alpha$ (2,3)Gal $\beta$ (1,6)Gal $\beta$ -O-CH<sub>2</sub>CH<sub>2</sub>SiMe<sub>3</sub> is not subject to hydrolysis by  $\beta$ -galactosidase (*E. coli*). This is because the Neu5Ac is blocking the enzyme from cleaving the galactose residue and hence the trisaccharide cannot be digested. Cleavage of Gal $\beta$ (1,6)Gal $\beta$ -O-CH<sub>2</sub>CH<sub>2</sub>SiMe<sub>3</sub> by  $\beta$ -galactosidase (*E. coli*) shows the presence of galactose.

Treatment of the sialylated material, Neu5Ac $\alpha$ (2,3)Gal $\beta$ (1,6)Gal $\beta$ -O-CH<sub>2</sub>CH<sub>2</sub>SiMe<sub>3</sub>, by *C. perfringens* neuraminidase yields Gal $\beta$ (1,6)Gal $\beta$ -O-CH<sub>2</sub>CH<sub>2</sub>SiMe<sub>3</sub> as expected, from the removal of Neu5Ac, however neuraminidase has no effect on Gal $\beta$ (1,6)Gal $\beta$ -O-CH<sub>2</sub>CH<sub>2</sub>SiMe<sub>3</sub>. Only after the sialic acid is cleaved from Neu5Ac-X by *C. perfringens* neuraminidase then is it possible for the  $\beta$ -galactosidase to cleave Gal $\beta$ (1,6)Gal $\beta$ -O-CH<sub>2</sub>CH<sub>2</sub>SiMe<sub>3</sub>.

Shown below in **Figure 54** is a diagrammatic representation of the systematic enzyme digestion of Neu5Ac $\alpha$ (2,3)Gal $\beta$ (1,6)Gal $\beta$ -O-CH<sub>2</sub>CH<sub>2</sub>SiMe<sub>3</sub>.

**Figure 54** Diagram of systematic enzyme digestion Neu5Ac $\alpha$ (2,3)Gal $\beta$ (1,6)Gal $\beta$ -O-CH<sub>2</sub>CH<sub>2</sub>SiMe<sub>3</sub> (25)





This suggests the formation of the linear trisaccharide arising from the sialylation of the non-reducing terminal galactose unit, rather than the alternative (literature supported) branched product.

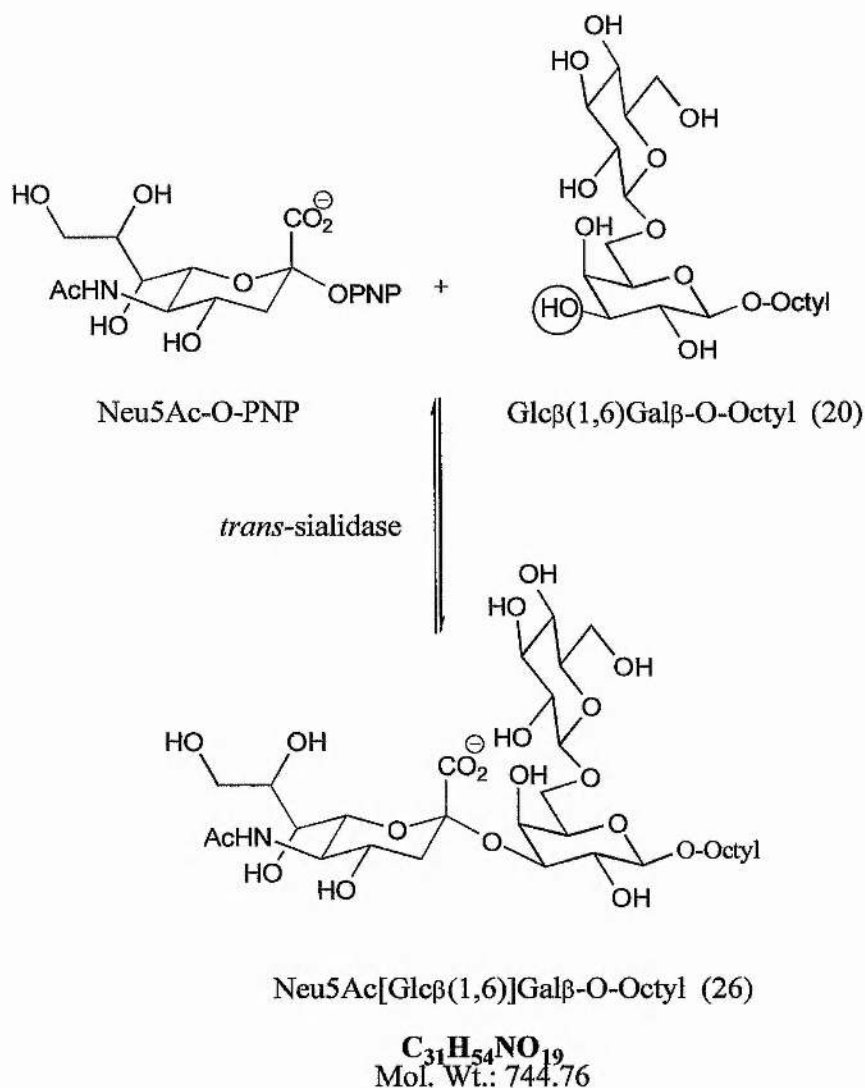
#### 4.6 Sialylation of Glc $\beta$ (1,6)Gal $\beta$ -Octyl (20)

Glc $\beta$ (1,6)Gal $\beta$ -Octyl has been proven to be a good substrate of *trans*-sialidase. This is possibly as a result of the orientation of the galactose moiety at the 6 position. This is a significant result, since only the sialylation of terminal galactose residues has been reported in the literature.

##### 4.6.2 Preparative scale sialylation of Glc $\beta$ (1,6)Gal $\beta$ -O-Octyl (20)

In an attempt to prove the sialylation of Glc $\beta$ (1,6)Gal $\beta$ -O-Octyl, the incubation of this sugar was increased to a preparative level of approximately 3 mgs. Since the sialylation of oligosaccharides by *trans*-sialidase is a reversible reaction and the products of the reaction are substrates for the back reaction, as well as the fact that the sialylated sugars are unstable, this was a difficult task. However a product (approximately 1.5 mg) was isolated which had the assumed correct R<sub>f</sub> value by T.L.C. The proposed sialylation of Glc $\beta$ (1,6)Gal $\beta$ -O-Octyl by *trans*-sialidase is shown below in **Figure 55**.

**Figure 55 Sialylation of Glc $\beta$ (1,6)Gal $\beta$ -Octyl (20)**

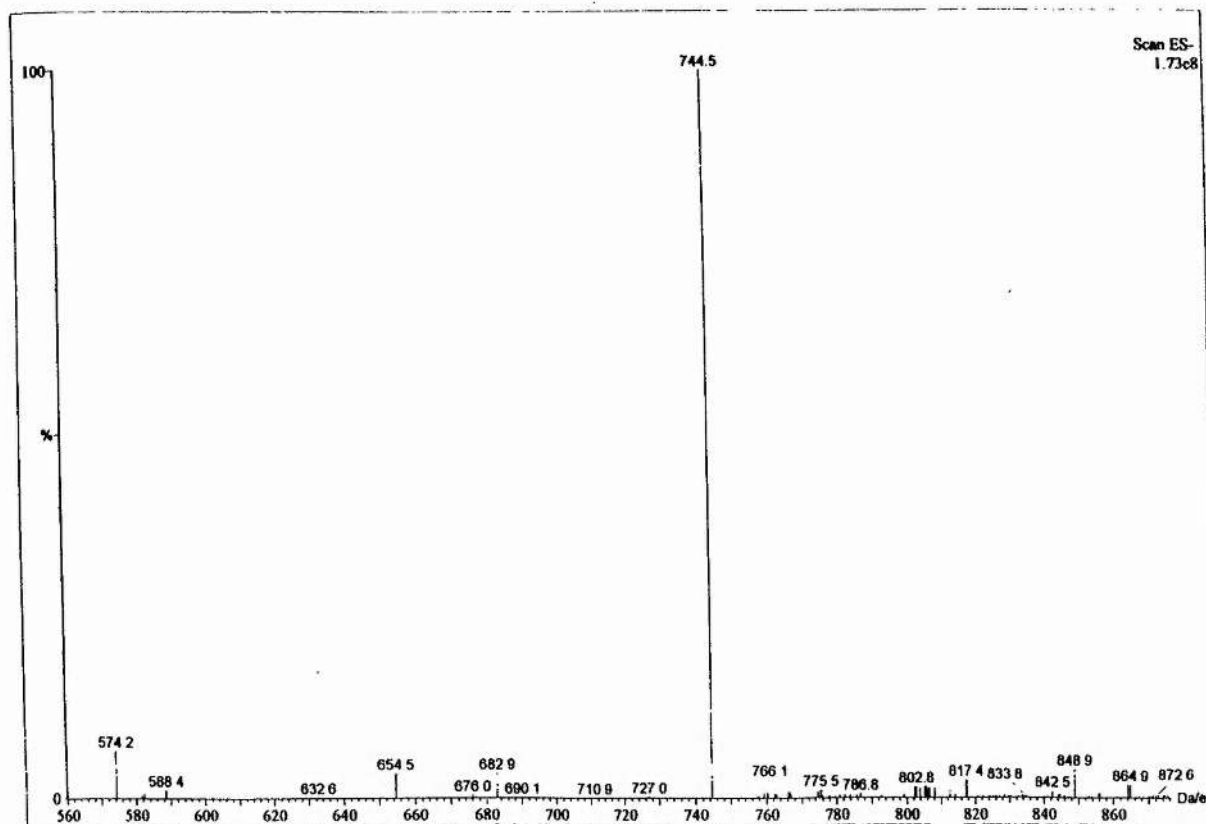


#### 4.6.3 Analysis of Neu5Ac $\alpha$ (2,3)[Glc $\beta$ (1,6)]Gal $\beta$ -O-Octyl (26) - Electrospray Mass Spectrometry

The compound was subject to Electrospray Mass Spectrometry. The spectrum was run from 500-900 Da/e. The calculated molecular weight for this compound is 744.76. The spectrum shows clearly only one peak at 745 Da/e. This corresponds to Neu5Ac $\alpha$ (2,3)[Glc $\beta$ (1,6)]Gal $\beta$ -O-Octyl. Shown below in **Figure 56** is the mass spectrum.



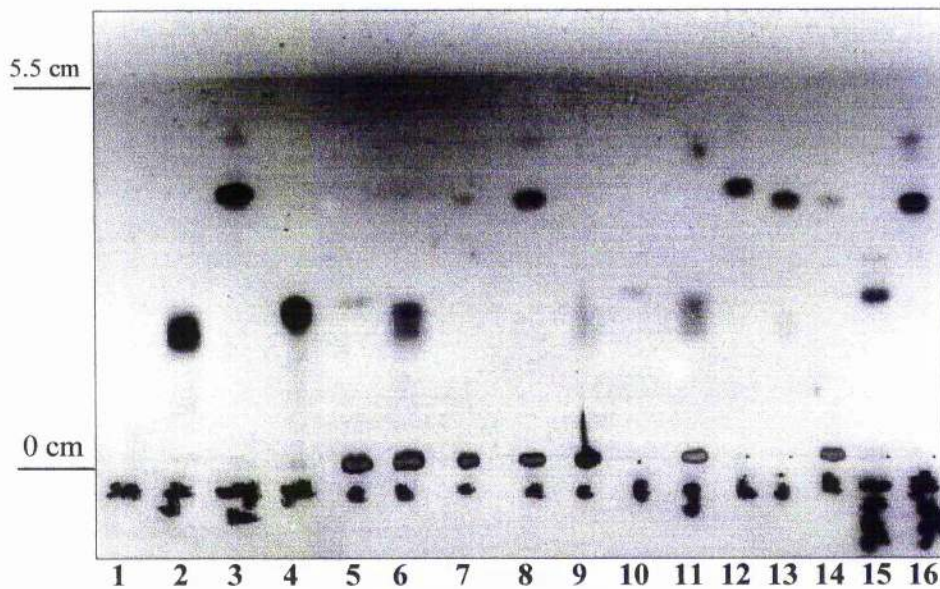
**Figure 56** Mass spectrum of Neu5Ac $\alpha$ (2,3)[Glc $\beta$ (1,6)]Gal $\beta$ -O-Octyl (26)



#### 4.6.4 Systematic enzymatic digestion Neu5Ac $\alpha$ (2,3)[Glc $\beta$ (1,6)]Gal $\beta$ -O-Octyl (26)

Neu5Ac $\alpha$ (2,3)[Glc $\beta$ (1,6)]Gal $\beta$ -O-Octyl was isolated and then subjected to systematic enzymatic digestion using  $\beta$ -glucosidase (*Caldocellum saccharolyticum*),  $\beta$ -glucosidase [almond extract (both crude and 98 % pure)],  $\beta$ -galactosidase (*E. coli*) and neuraminidase (*C. perfringens*). **Figure 57** shows a photograph of the T.L.C. plate of the enzymatic digestion of Neu5Ac $\alpha$ (2,3)[Glc $\beta$ (1,6)]Gal $\beta$ -O-Octyl.

**Figure 57** Systematic enzymatic digestion Neu5Ac $\alpha$ (2,3)[Glc $\beta$ (1,6)]Gal $\beta$ -O-Octyl (26)



**Legend of Figure 57**

Lane 1 Neu5Ac Marker, Rf = 0	Lane 9 Incubation e, Neu5Ac $\alpha$ (2,3)[Glc $\beta$ (1,6)]Gal $\beta$ -O-Octyl with <i>C. perfringens</i> neuraminidase, and $\beta$ -glucosidase, Rf = 0.4 (smeared)
Lane 2 Glucose Marker, Rf = 0.4	Lane 10 Incubation f, Neu5Ac $\alpha$ (2,3)[Glc $\beta$ (1,6)]Gal $\beta$ -O-Octyl, Rf = 0.4
Lane 3 Octyl lactoside Marker, Rf = 0.7	Lane 11 Incubation g, Octyl lactoside with $\beta$ -galactosidase, Rf = 0.4
Lane 4 Galactose Marker, Rf = 0.4	Lane 12 Incubation h, Octyl lactoside with $\beta$ -glucosidase, Rf = 0.6
Lane 5 Incubation a, Neu5Ac $\alpha$ (2,3)[Glc $\beta$ (1,6)]Gal $\beta$ -O-Octyl with $\beta$ -glucosidase, Rf = 0.4	Lane 13 Incubation j, Glc $\beta$ (1,6)Gal $\beta$ -O-Octyl with <i>C. perfringens</i> neuraminidase and $\beta$ -galactosidase (grade VIII), Rf = 0.6
Lane 6 Incubation b, Glc $\beta$ (1,6)Gal $\beta$ -O-Octyl with $\beta$ -glucosidase, Rf = 0.3	Lane 14 Incubation k, Neu5Ac $\alpha$ (2,3)[Glc $\beta$ (1,6)]Gal $\beta$ -O-Octyl with <i>C. perfringens</i> neuraminidase and $\beta$ -galactosidase Rf = 0.6
Lane 7 Incubation c, Neu5Ac $\alpha$ (2,3)[Glc $\beta$ (1,6)]Gal $\beta$ -O-Octyl with <i>C. perfringens</i> neuraminidase, Rf = 0.6	Lane 15 Neu5Ac $\alpha$ (2,3)[Glc $\beta$ (1,6)]Gal $\beta$ -O-Octyl Marker, Rf = 0.5, 0.4
Lane 8 Incubation d, Glc $\beta$ (1,6)Gal $\beta$ -O-Octyl with <i>C. perfringens</i> neuraminidase, Rf = 0.6	Lane 16 Glc $\beta$ (1,6)Gal $\beta$ -O-Octyl Marker, Rf = 0.7

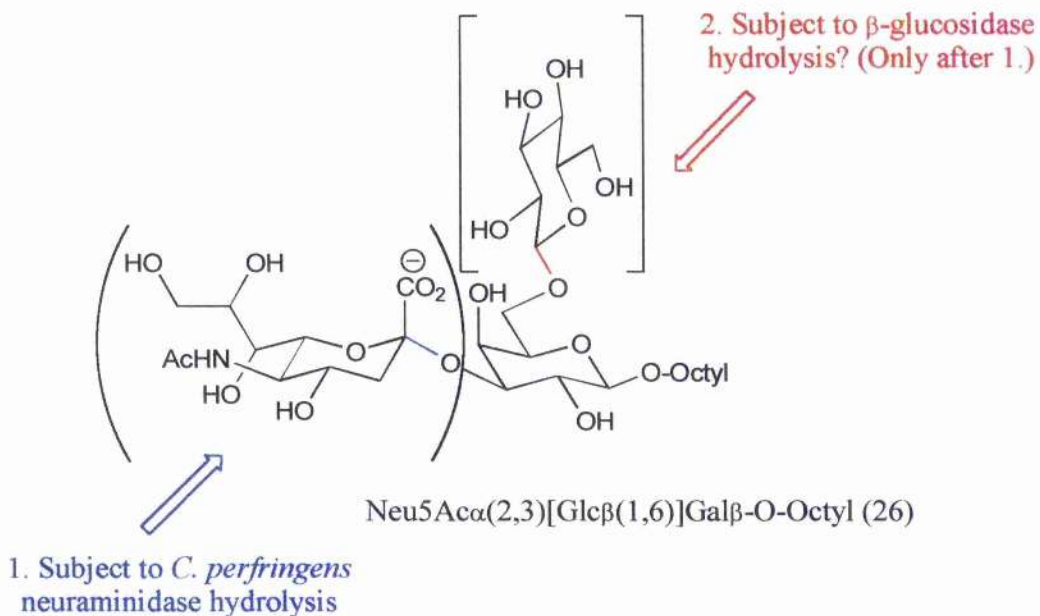
**4.6.5 Treatment of Neu5Ac $\alpha$ (2,3)[Glc $\beta$ (1,6)]Gal $\beta$ -O-Octyl (26) with *C. perfringens* neuraminidase and  $\beta$ -glucosidase**

Neu5Ac $\alpha$ (2,3)[Glc $\beta$ (1,6)]Gal $\beta$ -O-Octyl is not subject to hydrolysis by  $\beta$ -glucosidase (crude, almonds). This does not indicate that Neu5Ac is attached to glucose, (since there is no literature precedent for this). It is more likely that the branched trisaccharide (26), is too large for the  $\beta$ -glucosidase binding site, and hence is not digested. An attempt to degrade (26) by alternative  $\beta$ -glucosidases was also examined, (see page 86) but was also unsuccessful.

*C. perfringens* neuraminidase will remove sialic acid to give Glc $\beta$ (1,6)Gal $\beta$ -O-Octyl. Further degradation of Glc $\beta$ (1,6)Gal $\beta$ -O-Octyl by  $\beta$ -glucosidase followed by  $\beta$ -galactosidase produces glucose and galactose. Neuraminidase has no effect on the Glc $\beta$ (1,6)Gal $\beta$ -O-Octyl (expected).

Treatment of Glc $\beta$ (1,6)Gal $\beta$ -O-Octyl with  $\beta$ -galactosidase leaves Glc $\beta$ (1,6)Gal $\beta$ -O-Octyl unchanged, as expected. A diagrammatic illustration of possible sites and sequence of enzymatic digestion is shown below in **Figure 58**.

**Figure 58 Digestion of Neu5Ac $\alpha$ (2,3)[Glc $\beta$ (1,6)]Gal $\beta$ -O-Octyl (26) by *C. perfringens* neuraminidase and  $\beta$ -glucosidase**



#### 4.6.6 Digestion of Neu5Ac $\alpha$ (2,3)[Glc $\beta$ (1,6)]Gal $\beta$ -O-Octyl (26) by other $\beta$ -glucosidases

Neu5Ac $\alpha$ (2,3)[Glc $\beta$ (1,6)]Gal $\beta$ -O-Octyl was tested for susceptibility by another  $\beta$ -glucosidase to establish whether or not it was only resistant to only  $\beta$ -glucosidase (crude, almonds) and to hopefully establish the point of attachment of sialic acid. (26) was assayed with  $\beta$ -glucosidase (*Caldocellum saccharolyticum*). This study indicated that  $\beta$ -glucosidase (*Caldocellum saccharolyticum*) is not able to digest (26) [similar to  $\beta$ -glucosidase (almonds)] and gave no information as to the point of attachment of Neu5Ac.

#### 4.7 Sialylation of Gal $\beta$ (1,4)[ $\beta$ Gal(1,6)]Glc $\beta$ -O-Octyl (21)

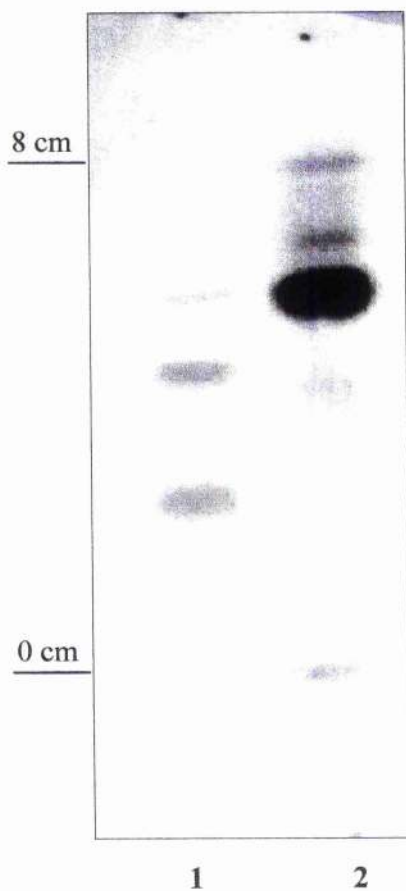
The sialylation of Gal $\beta$ (1,4)[ $\beta$ Gal(1,6)]GlcNAc $\beta$ -O-Octyl has previously been illustrated, see **Figure 50**, page 75. Gal $\beta$ (1,4)[ $\beta$ Gal(1,6)]Glc $\beta$ -O-Octyl was synthesised chemically (*Kartha and Field 1997*), to reflect one of the naturally occurring trisaccharide fragments of *Trypanosoma cruzi*. [All of the naturally occurring oligosaccharide fragments (both human and insect form) are shown in **Figures 42 and 43**, pages 64 and 66]. Hence the sialylation and characterisation of Neu5Ac $\alpha$ (2,3)Gal $\beta$ (1,4)[ $\beta$ Gal(1,6)]Glc $\beta$ -O-Octyl is important in the mapping of the enzyme binding site.

##### 4.7.2 Preparative scale sialylation of Gal $\beta$ (1,4)[ $\beta$ Gal(1,6)]Glc $\beta$ -O-Octyl (21)

In an attempt to prove this sialylation, the incubation of Gal $\beta$ (1,4)[ $\beta$ Gal(1,6)]Glc $\beta$ -O-Octyl was increased to a preparative level of approximately 3 mgs. As before, the sialylation of this sugar by *trans*-sialidase is reversible with the sialylated product being a substrate for the back reaction, hence isolation is difficult. A product (approximately 1 mg) was isolated. By T.L.C. the second sialylated product was recognisable. A photograph was taken to record the second product visible by T.L.C. This is shown below in **Figure 59**.



**Figure 59** Di-sialylation of Gal $\beta$ (1,4)[ $\beta$ Gal(1,6)]GlcNAc $\beta$ -O-Octyl (21)

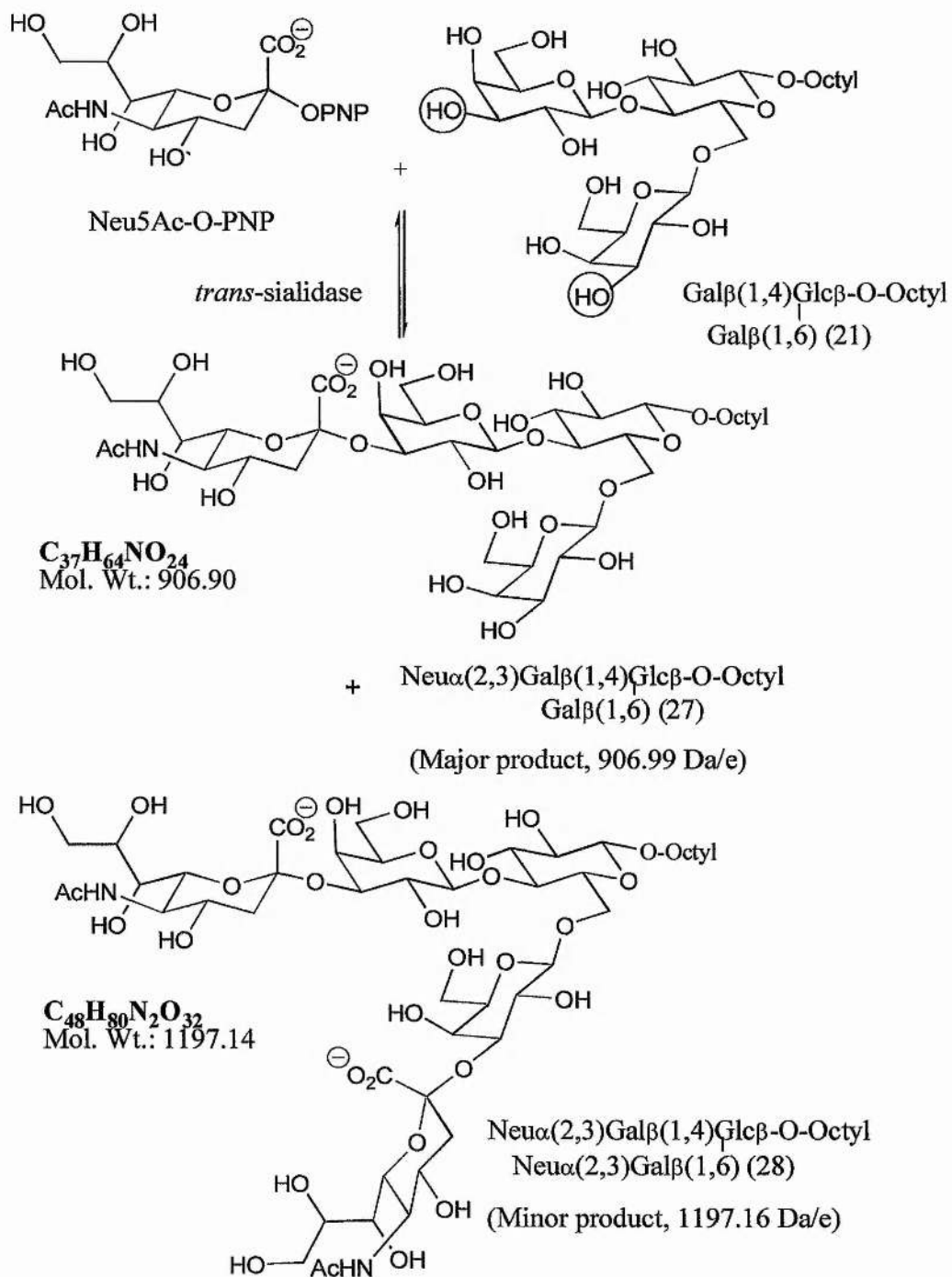


**Legend of Figure 59**

Lane 1 Sialylation of Gal $\beta$ (1,4)[ $\beta$ Gal(1,6)]Glc $\beta$ -O-Octyl Rf = 0.4, 0.2	Lane 2 Gal $\beta$ (1,4)[ $\beta$ Gal(1,6)]Glc $\beta$ -O-Octyl Rf = 0.5
--	--

Shown below in **Figure 60** is the proposed enzymatic sialylation of Gal $\beta$ (1,4)[ $\beta$ Gal(1,6)]Glc $\beta$ -O-Octyl.

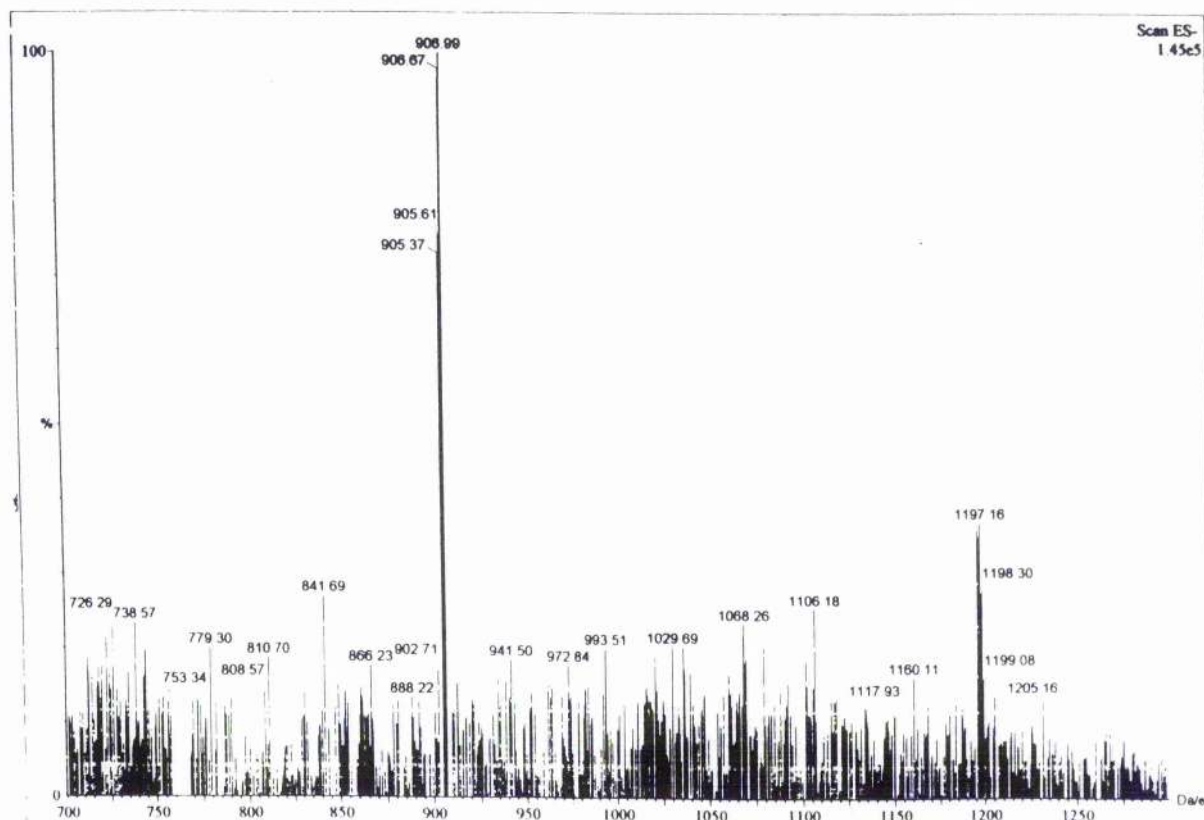
**Figure 60 Sialylation of Gal $\beta$ (1,4)[ $\beta$ Gal(1,6)]Glc $\beta$ -O-Octyl (21)**



#### 4.7.3 Analysis of sialylated-(2,3)Gal $\beta$ (1,4)[ $\beta$ Gal(1,6)]Glc $\beta$ -O-Octyl (27) and (28) - Electrospray Mass Spectrometry

The compound was subject to Electrospray Mass Spectrometry. The spectrum is shown below in **Figure 61**. The spectrum was run from 700-1300 Da/e. (However it should have been from 550 to observe the di-charged species at 598.57 Da/e. There are clearly two peaks as expected by T.L.C., these are located at 906.99 and 1197.16 Da/e, corresponding to the mono (27) and di-sialylated (28) Gal $\beta$ (1,4)[ $\beta$ Gal(1,6)]Glc $\beta$ -O-Octyl. By MS there are two products, one located at 1197.16 and the other at 906.99, approximately 290.27 Da/e apart. The molecular weight of Neu5Ac is 308.26 (subtracting OH = 17.01) leaves 291.25. (The peak height at 1197.16 is smaller than expected, since this is the singularly charged species. It is suspected that there will be a much larger peak at 598.57).

**Figure 61** Mass Spectrum of sialylated-Gal $\beta$ (1,4)[ $\beta$ Gal(1,6)]Glc $\beta$ -O-Octyl (27) and (28)





## 4.8 Conclusions

Based on the natural *Trypanosoma cruzi* cell surface sialic acid acceptors, a variety of oligosaccharides, compounds (14)-(21) were chemically synthesised (Kantha 1997). These compounds were subject to a radiochemical assay, to assess their potential as substrates (Pereira *et al* 1995, Vetere *et al* 1996). Compounds (14) and (16)-(21) were found to be sialylatable substrates. This indicates that *trans*-sialidase has very little linkage specificity or size specificity. These findings concur with the results recorded by T.L.C.

The sialylation of compounds (19), (20) and (21) indicate that it is possible to modify the hydroxyl group at position 6 of galactose-X acceptors i.e. *trans*-sialidase will permit even another monosaccharide at position 6 without any negative effects on sialylation. This result agrees with the sialylation of compounds 3(i,ii,iii,iv) and 8(i,ii,iii,iv) from previous studies. The lack of specificity of *trans*-sialidase towards the hydroxyl group at position six of the terminal (or otherwise)  $\beta$ -galactose could tolerate significant modification. As described before, this could encompass a solid-phase linker to exploit this enzyme in oligosaccharide chemistry (Whittaker *et al* 1996).

The sialylation of *p*-aminobenzyl-1-thio- $\beta$ -S-galacto-pyranoside resin (Sigma Chemicals Ltd) (confirmed radiochemically) indicates that it is possible to sialylate more than one neighbouring galactose moiety. This result is compounded with the formation of compound (28) which was proved by T.L.C. and radiochemically before characterisation by electrospray-mass spectrometry.

Sialylation of an internal non-reducing galactose (20) has been carried out successfully. The product (26) was confirmed radiochemically and by T.L.C. before being isolated and characterised by electrospray-mass spectrometry and enzymatic digestion. This result is novel and could be exploited in synthetic oligosaccharide chemistry, to possibly sialylate other internal  $\beta$ -gal residues.

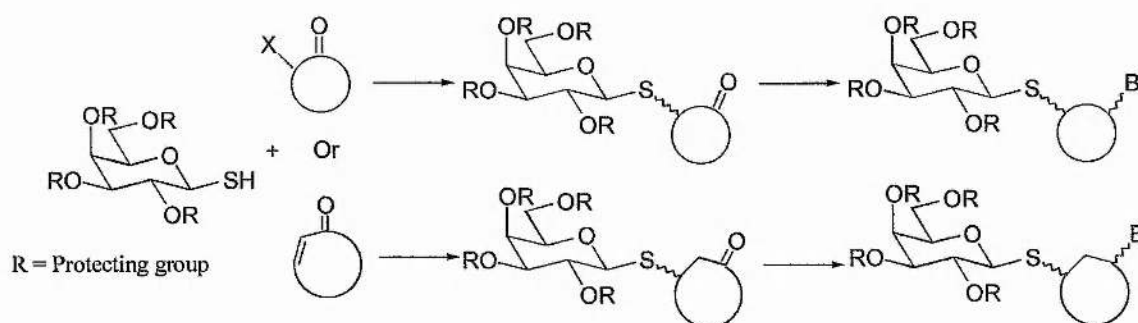
# Chapter 5

*trans*-Sialidase substrate  
recognition of modified  
Gal $\beta$ -S-X analogues

## 5.1 Substituted Gal $\beta$ -S-X analogues

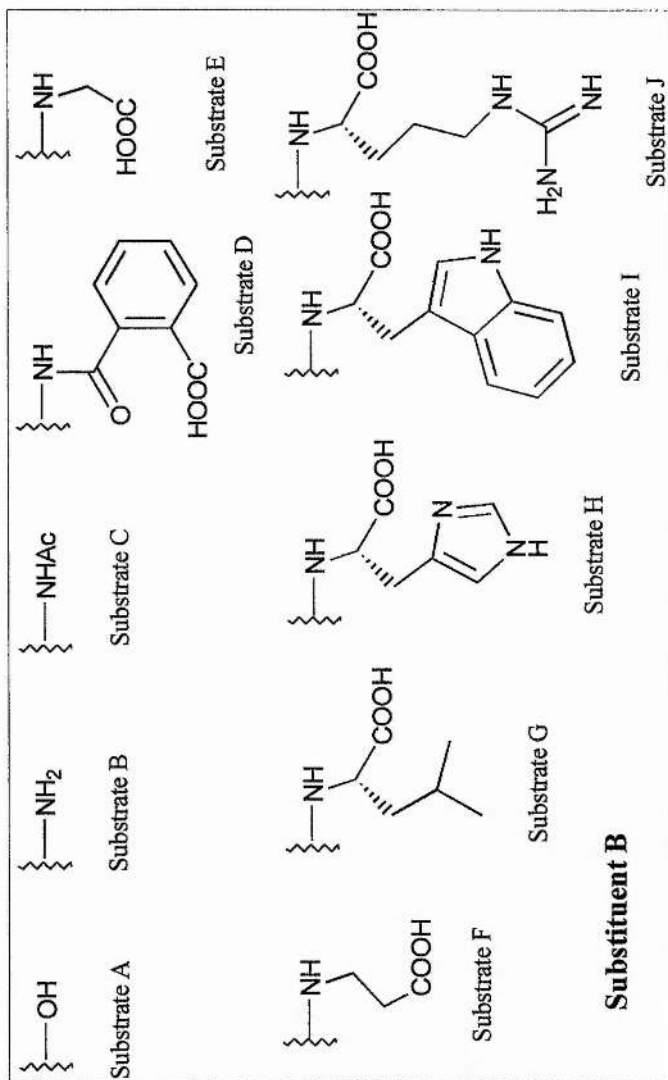
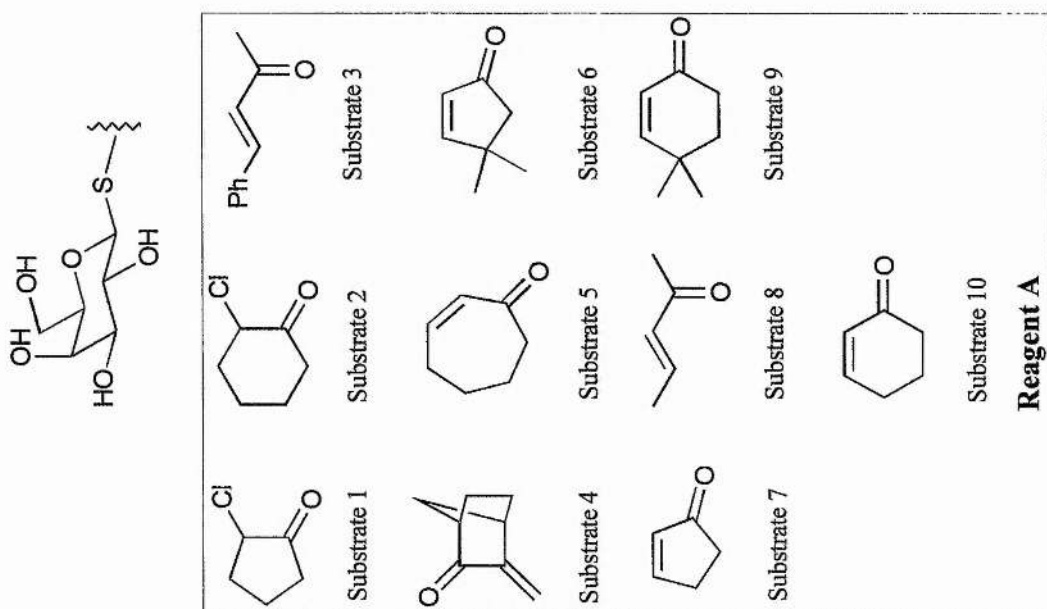
Characterisation of the enzyme binding site and its recognition of terminal galactose, was carried out using a library of modified sugars. A library of modified thiol galactose sugars was obtained from Ole Hindsgaul's laboratory, Alberta, Canada. These compounds had been synthesised for the purpose of a study of cholera toxin 1998. This basic sugar skeleton reacted twice with a variety of substituents as outlined in **Figure 62**.

**Figure 62** General scheme for the formation of the library of Gal $\beta$ -S-X oligosaccharides



The first reaction (Michael addition) was carried out using substrates 1-10. The second reaction (Imine formation) then followed using substrates A-J. Gal $\beta$ -SH and all of the compounds which it was reacted with are shown below in **Figure 63**.

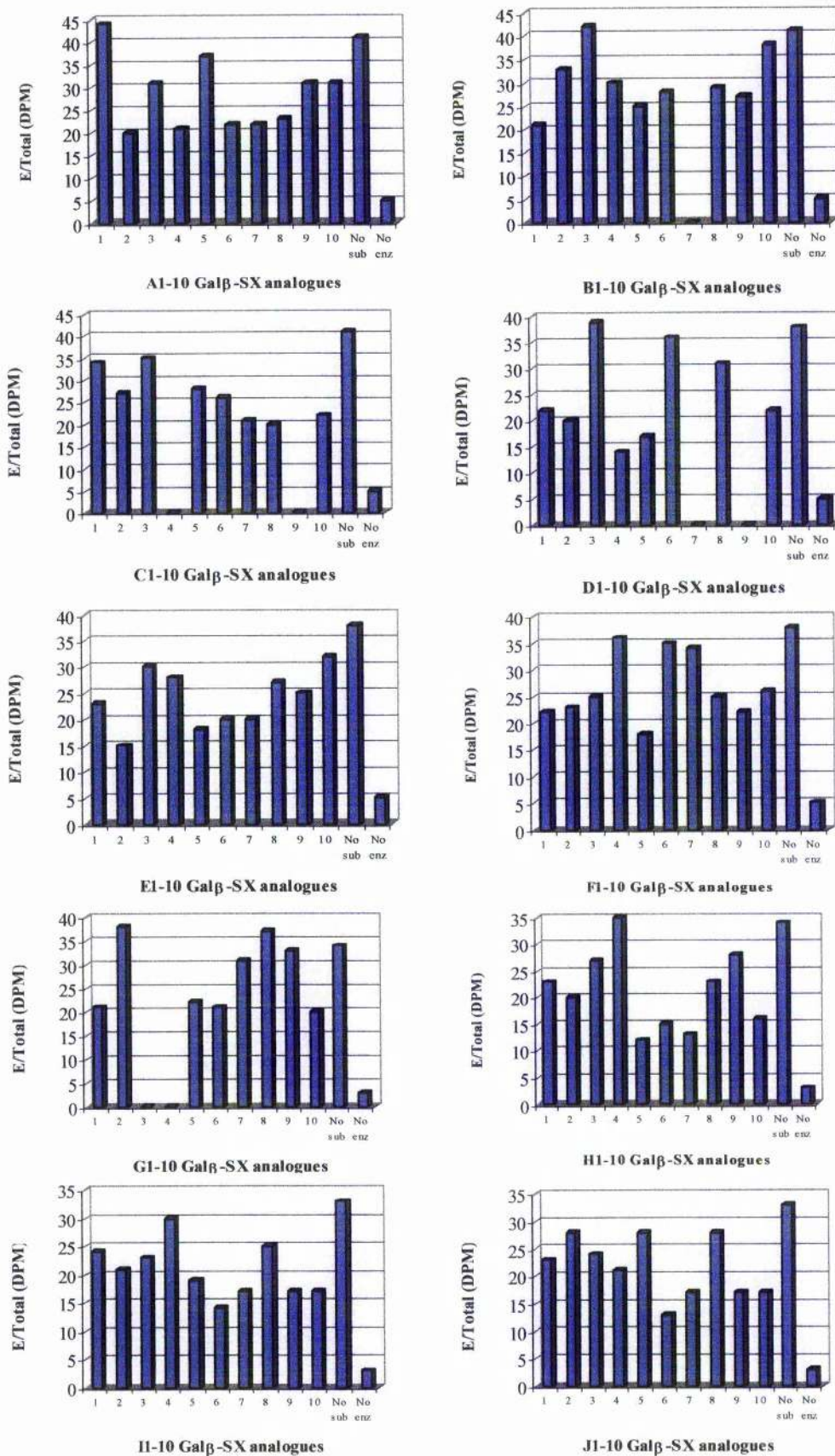
**Figure 63** Reactions of Gal $\beta$ -S-X analogues



## 5.2 Gal $\beta$ -S-X radiochemical assay

Each of the 100 Gal $\beta$ -S-X analogues (compounds A1-J10) was assayed radiochemically (*Pereira et al 1995, Vetere et al 1996*). The graphs below in **Figure 64** represent all of the Gal $\beta$ -S-X oligosaccharides incubated. The results may be interpreted as before, i.e. a value of 0-15 % elution/total represents a good substrate, whereas >35 % represents a non-substrate. In this screen the columns above with E/Total % = 0 represents a substrate which was unavailable. The results are based on a radioactive assay which was carried out twice.

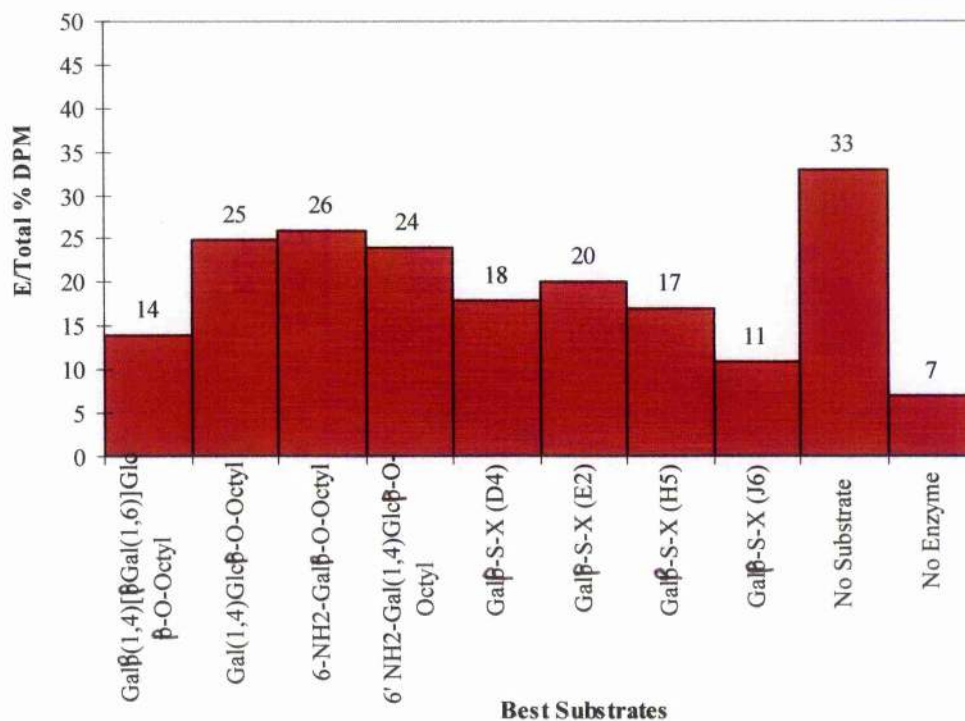
**Figure 64** The complete substituted Gal $\beta$ -S-X oligosaccharide library





It is apparent that from these plots that some of these compounds are particularly good substrates for *trans*-sialidase. However there seems to be no particular pattern to the substrate specificity. The above data can confirm that *trans*-sialidase is an excellent sialyl transferase, having the capability to exploit many diverse oligosaccharides. The best substrates of this library were incubated again radiochemically (Pereira *et al* 1995, Vetere *et al* 1996) with the best substrates from all of the other screens and the results plotted as before. The results are shown below in **Figure 65**.

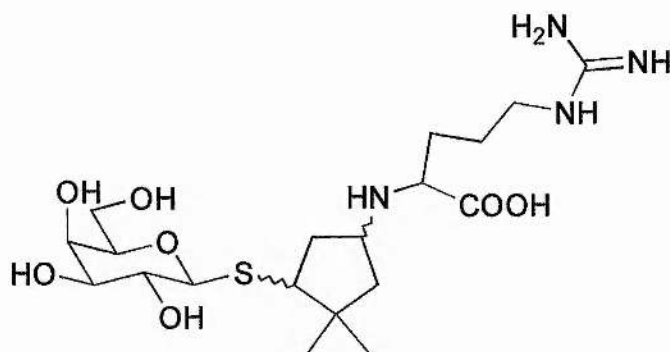
**Figure 65** Graph of the best *trans*-sialidase substrates



J6 was selected as the best substrate of this library and was subject to a serial dilution. The structure of this compound is illustrated below, in **Figure 66**.



**Figure 66** The best substrate of the substituted Gal $\beta$ -S-X oligosaccharide library, J6

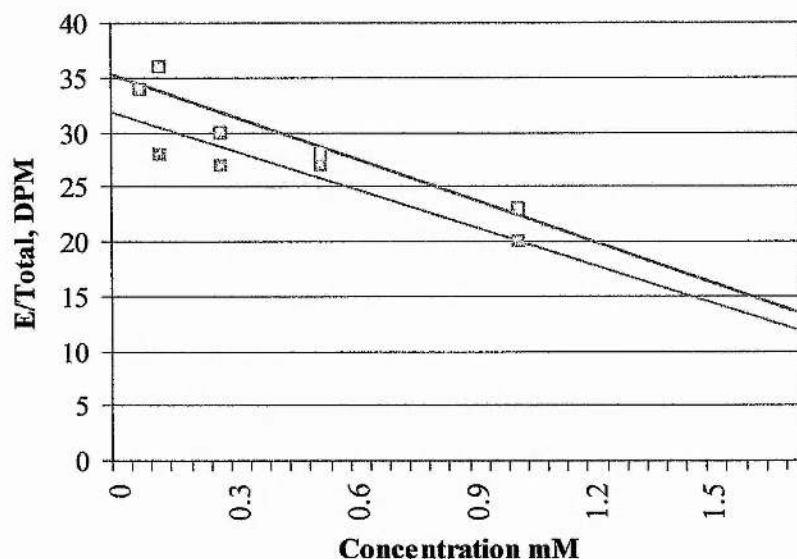


Only one of the four possible stereoisomers is shown above.

### 5.3 Serial dilution of J6 and Gal $\beta$ (1,4)[ $\beta$ Gal(1,6)]Glc $\beta$ -O-Octyl (21)

A serial dilution was carried out from 1 ml to 50  $\mu$ l in order to calculate IC<sub>50</sub> values for substrates of *trans*-sialidase. J6 and Gal $\beta$ (1,4)[ $\beta$ Gal(1,6)]Glc $\beta$ -O-Octyl were selected as the substrates which gave the best % turnover. **Figure 67** shows the graph of substrate J6 in comparison to Gal $\beta$ (1,4)[ $\beta$ Gal(1,6)]Glc $\beta$ -O-Octyl.

**Figure 67** Graph of J6 and Gal $\beta$ (1,4)[ $\beta$ Gal(1,6)]Glc $\beta$ -O-Octyl % turnover comparison



The blue line is Gal $\beta$ (1,4)[ $\beta$ Gal(1,6)]Glc $\beta$ -O-Octyl and Red line is J6.

From this graphical illustration, IC<sub>50</sub> values are estimated based no enzyme/substrate present giving a value of 5 % (Elution/Total, DPM) and no substrate present giving a turnover of 35 % and 33 % for J6 and Gal $\beta$ (1,4)[ $\beta$ Gal(1,6)]Glc $\beta$ -O-Octyl (Elution/Total) respectively, (Therefore 5 % = 0 and 35 % or 33 % = 100).

J6 IC<sub>50</sub> = 1.62 mM and Gal $\beta$ (1,4)[ $\beta$ Gal(1,6)]Glc $\beta$ -O-Octyl IC<sub>50</sub> = 1.55 mM

As these substrates both have a considerable size requirement, it is obvious that either the side chains are oriented such that they are in space, or the enzyme binding site is larger enough to accommodate this size.

#### 5.4 Conclusions

This study of structurally diverse Gal $\beta$ -S-X analogues was comprehensive in its assessment of *trans*-sialidase as a potential oligosaccharide. Of the 100+ galactose-based diastereoisomer acceptor substrates analysed (compounds A1-J10), greater than 75 % served as *trans*-sialidase substrates. The results of this and previous studies indicate that *trans*-sialidase is a versatile reagent for sialyl-glycoconjugate synthesis.

The best acceptor substrate of the 100 Gal $\beta$ -SX analogues was found to be compound J6. J6 contains a large aliphatic side chain containing one carboxylic acid group and a guanidino group at its tail. From this study it is not possible to confirm whether the charged tail is significant for improved *trans*-sialidase substrate specificity. However, it is probably more likely that *trans*-sialidase more generally, has a large size requirement, as suggested from previous findings (19), (20), (21) and also J6. A serial dilution was carried out using both J6 and (21) to allow IC<sub>50</sub> values to be measured. The values for 50 % inhibitor are as follows, J6 IC<sub>50</sub> = 1.62 mM and (21) IC<sub>50</sub> = 1.55 mM.

# Chapter 6

# Experimental

## A.1 List of Suppliers

### Amersham Life Sciences

- [<sup>14</sup>C]Lactose

### Amicon

- 50 kDa *Centricon* filters
- Coomassie brilliant blue

### BioRad

- SDS-Polyacrylamide "Ready" gels
- Reverse-phase Silica

### Fisher Scientific (bulk reagents and supplies)

- Na<sub>2</sub>CO<sub>3</sub>
- NH<sub>4</sub>OAc
- (NH<sub>4</sub>)<sub>2</sub>SO<sub>4</sub>
- MeOH, CHCl<sub>3</sub>
- Imidazole
- AgNO<sub>3</sub>
- CH<sub>3</sub>COOH
- H<sub>3</sub>PO<sub>4</sub>
- Na<sub>2</sub>S<sub>2</sub>O<sub>3</sub>
- Thin Layer Chromatography Plate (Whatman, K6F Silica Gel 60Å, 20 cm 20 cm, thickness 250 μm)

### Merek

- Optiphase Scintillation Cocktail

### Qiagen

- Ni<sup>2+</sup> NTA chelation affinity resin

### Sigma

- A25 Sephadex anion exchange resin
- β-galactosidase (*E. coli*) E.C. 3.2.1.23 (G5635)
- β-glucosidase (Almonds, Crude) E.C. 3.2.1.21 (G 0395)
- β-glucosidase (Almonds, purified) E.C. 3.2.1.21 (G 4511)
- β-glucosidase (*Caldocellum saccharolyticum*) E.C. 3.2.1.21 (G 6906)
- Neuraminidase (*C. perfringens*) E.C. 3.2.1.18 (N 2876)

## **Sigma (Cont.)**

- Trizma (HCl, 99 % pure)
- HEPES (Na salt, 99.5 % pure)
- MES (Monohydrate, >99.5 % pure)
- *p*-Aminobenzyl-1-thio- $\beta$ -S-galacto-pyranosidase
- D-Lactose (Monohydrate)
- D-Galactose (99 %)
- D-Glucose (anhydrous, 99.5 %)
- LB Broth, Miller
- LB Agar, Miller
- Ampicillin
- Kanamycin Monosulfate
- Sodium Phosphate
- Lysozyme
- EDTA
- *DNase* 1
- $\beta$ -mercaptoethanol
- Bovine Serum Albumin

## **Toronto Research Chemicals**

- 2,3-dehydro-2-deoxy-Neu5Ac

## **Waters**

C<sup>18</sup> *Sep-Pac* reverse-phase resin cartridges

### **Source of recombinant *trans*-sialidase**

*E. coli* culture expressing recombinant *trans*-sialidase protein was sent from Sergio Schenkman's Laboratory at the Department of Cell Biology, Escola Paulista de Medicina, Sao Paulo, Brazil. This 70 kDa construct contains the catalytic head region and incorporates a hexa-histidine tag at the C-terminus. This protein was isolated using standard molecular biological techniques and then purified. The hexa-histidine tag aided the separation of the enzyme by nickel affinity chromatography. This enzyme has been purified to a single band by SDS-PAGE (silver stain), see Appendix 1 for full purification details, *Schenkman et al* 1997). It was found, however that the purified material was less stable than crude material. It was found that crude lysate had sufficient enzymatic activity and increased stability. Hence crude material was used for all of the subsequent studies.

### ***trans*-Sialidase donor and acceptor substrates**

Unless otherwise stated the carbohydrate donor and acceptor substrates for all of the biological assays, as well as the Gal $\beta$ (1,X)Gal acceptor substrates were synthetically made "in house" by *K. P. R. Kartha*.



## 6.1 Assay development

All of the following assays were carried out using a variety of substrates and with either *trans*-sialidase and *C. perfringens* neuraminidase (or both).

The experimental procedure was the same for all experiments, and is as follows: all of the components were incubated together at 37 °C for the time indicated. The reaction was quenched with 1 ml of Na<sub>2</sub>CO<sub>3</sub> (100 mM) pH 10, before the absorption was measured. In some cases the assay was carried out in duplicate or triplicate. In these cases an average best represented the absorption results.

### 6.1.2 Spectrophotometric assay of *trans*-sialidase and *C. perfringens* neuraminidase

*trans*-Sialidase and *C. perfringens* neuraminidase were assayed using Neu5Ac-O-PNP as a substrate and lactose as an acceptor. The incubation included 0.1 units of *C. perfringens* neuraminidase or an undetermined amount of *trans*-sialidase. Although no formal calculation was made on the activity of *trans*-sialidase, the level of activity was comparable with the other neuraminidase in all cases. All of the assay components, including concentrations, are listed below in Table 4.

**Table 4** *trans*-sialidase and *C. perfringens* neuraminidase assay components

Component	Stock Conc.	Volume 50 µl
Neu5Ac-O-PNP	5 mM	10
Lactose (or H <sub>2</sub> O)	5 mM	10
HEPES buffer	150 mM	10
H <sub>2</sub> O	-	10
<i>C. perfringens</i> neuraminidase or <i>trans</i> -sialidase	See above	10

The results of the assay were tabulated and are shown below in Table 5 -

**Table 5 Comparison of *trans*-sialidase and *C. perfringens* neuraminidase reaction rates**

Incubation	$\Delta A_{400}$ (After 30 Mins)
Control	0.05
<i>trans</i> -sialidase (-) lactose	0.06
<i>trans</i> -sialidase (+) lactose	0.14
<i>C. perfringens</i> neuraminidase (-) lactose	0.58
<i>C. perfringens</i> neuraminidase (+) lactose	0.62

This study indicates that *C. perfringens* neuraminidase is a hydrolase, and that the presence of an acceptor such as lactose makes no significant difference. However there is a significant difference when an acceptor such as lactose is added to the *trans*-sialidase incubation. This confirms that *trans*-sialidase is preferentially a transferase.

### 6.1.3 Comparison of *trans*-sialidase transferase and hydrolase activities

Since Neu5Ac-O-PNP was not a particularly good donor substrate for our purposes a coupled assay was developed, replacing Neu5Ac-O-PNP with Neu5Ac $\alpha$ (2,3)Gal $\beta$ -O-PNP. This would require the introduction of a  $\beta$ -galactosidase.

#### 6.1.3.2 First coupled assay for *trans*-sialidase using lactose as an acceptor

Since *trans*-sialidase is both a transferase and a hydrolase a new coupled assay incorporating both these reactions was developed. This coupled assay uses Neu5Ac $\alpha$ (2,3)-Gal $\beta$ -O-PNP as a donor substrate and lactose as an acceptor sugar.  $\beta$ -Glucosidase which also possessed some  $\beta$ -galactosidase activity, was used to hydrolyse the resulting Gal $\beta$ -O-PNP bond. This assay was buffered at pH 6.5. The assay components are outlined below in **Table 6**.

**Table 6 Comparison of *trans*-sialidase transferase and hydrolase assay (mark I) components**

Component	Stock Conc.	Volume 50 $\mu$ l
Neu5Ac-O-PNP or Neu5Ac $\alpha$ (2,3)-Gal $\beta$ -O-PNP	5 mM	10
Lactose (or H <sub>2</sub> O)	5 mM	10
HEPES buffer	150 mM	10
H <sub>2</sub> O	-	10
<i>trans</i> -sialidase or <i>C. perfringens</i> neuraminidase	See above	10

These components were assayed as before and the results are shown below in **Table 7**.

**Table 7 Comparison of *trans*-sialidase transferase and hydrolase activities (mark I)**

Incubation	$\Delta A_{400}$ (After 30 Mins)
<i>trans</i> -sialidase (-) lactose (Neu5Ac-PNP)	0.06
<i>trans</i> -sialidase (+) lactose (Neu5Ac-PNP)	0.14
<i>trans</i> -sialidase (-) lactose (Neu5Ac-Gal-PNP)	0.23
<i>trans</i> -sialidase (+) lactose (Neu5Ac-Gal-PNP)	0.47

#### 6.1.4 Comparison of *C. perfringens* neuraminidase activity with and without acceptor

A similar assay was carried out using the same components as before but with *C. perfringens* neuraminidase assay was carried out utilising both Neu5Ac-O-PNP and Neu5Ac $\alpha$ (2,3)Gal $\beta$ -O-PNP. The results of the *C. perfringens* neuraminidase assay were tabulated and are shown below in **Table 8**.

**Table 8 Comparison of *C. perfringens* neuraminidase with and without acceptor**

Incubation	$\Delta A_{400}$ ( 30 Mins)
Control ( <i>C. perfringens</i> neuraminidase)	0
<i>C. perfringens</i> neuraminidase (-) lactose (Neu5Ac-PNP)	0.58
<i>C. perfringens</i> neuraminidase (+) lactose (Neu5Ac-PNP)	0.62
<i>C. perfringens</i> neuraminidase (-) lactose (Neu5Ac-Gal-PNP)	0.46
<i>C. perfringens</i> neuraminidase (+) lactose (Neu5Ac-Gal-PNP)	0.47

### 6.1.5 Coupled assay for *trans*-sialidase using Gal $\beta$ (1,3)GlcNAc $\beta$ -O-Octyl as an acceptor (mark II)

As outlined on page 34, it was found that the acidic pH of the *trans*-sialidase coupled spectrophotometric assay was creating a problem. The coupled assay was adapted to overcome this problem. The pH was increased which resulted in a new  $\beta$ -galactosidase being used and hence another acceptor was selected which was unsusceptible to  $\beta$ -galactosidase activity. It was found that Gal $\beta$ (1,3)GlcNAc $\beta$ -O-Octyl was a reliable acceptor substrate which was not subject to enzymatic degradation. Consequently a study was carried out on *trans*-sialidase using variable concentrations of donor substrate, in the presence and absence of an acceptor to optimise assay conditions. A control was also carried out to monitor the background hydrolysis rate. The assay components are shown below in Table 9.

**Table 9** Coupled assay for *trans*-sialidase assay components (mark II)

Component	Stock Conc.	Volume 50 $\mu$ l
Neu $\alpha$ (2,3)Gal $\beta$ -O-PNP	5 mM	10
Gal $\beta$ (1,3)GlcNAc $\beta$ -O-Octyl	5 mM	10
$\beta$ -galactosidase ( <i>E. coli</i> )	80 units	10
HEPES buffer	150 mM	10
<i>trans</i> -sialidase and <i>C. perfringens</i> neuraminidase	As before	10

The components were assayed as before and the results of the incubation are shown below in Table 10.

**Table 10** Results of coupled assay for *trans*-sialidase (mark II)

Incubation	$\Delta A_{400}$ (After 30 Mins)
Control ( <i>trans</i> -sialidase)	0.01
<i>trans</i> -sialidase (-) acceptor	0.19
<i>trans</i> -sialidase (+) lactose	0.38
<i>trans</i> -sialidase (+) Gal $\beta$ (1,3)GlcNAc $\beta$ -O-Octyl	0.47

This table shows that Gal $\beta$ (1,3)GlcNAc $\beta$ -O-Octyl is a significantly better acceptor than lactose.

### 6.1.6 Spectrophotometric coupled assay (mark II) using a variable concentration of donor substrate (Neu $\alpha$ (2,3)Gal $\beta$ -O-PNP)

These incubations were repeated several times with various concentrations of substrate and a representative average was calculated of each. The results are as follows in Table 11.

**Table 11** *trans*-sialidase assay (mark II): variable concentrations of donor substrate with and without acceptor (After 30 Mins)

Substrate concentration	$\Delta A_{400}$ (+ ) 5 mM Gal $\beta$ (1,3)GlcNAc $\beta$ -O-Octyl	$\Delta A_{400}$ (-) 5 mM Gal $\beta$ (1,3)GlcNAc $\beta$ -O-Octyl
1 mM	0.08	0.06
2 mM	0.25	0.08
3 mM	0.27	0.09
4 mM	0.41	0.08
5 mM	0.51	0.14

#### 6.1.6.2 $K_m$ and $V_{max}$ for *trans*-sialidase

The  $K_m$  and  $V_{max}$  values were estimated for *trans*-sialidase based on enzyme incubations. *trans*-Sialidase was incubated 37 °C, for 30 minutes, with 5 mM - 25 mM stock concentrations of Neu5Ac- $\alpha$ -2,3-Gal- $\beta$ -O-PNP (Donor substrate) and with and without 5 mM (stock) Gal- $\beta$ -1,3-GlcNAc-O-Octyl.

Using these figures, Tables 12 and 13 and using the Beer-Lambert Law ( $A = \epsilon cl$ ) we can construct a Lineweaver-Burk double reciprocal plot. The molar extinction co-efficient for *p*-nitrophenol = 18 300 M<sup>-1</sup> cm<sup>-1</sup> (absorption 400 nm) (Byers *et al* 1985). For example, *trans*-sialidase (transferase), 1 mM concentration gives a value of  $v$  as follows:

Since  $A = \epsilon cl$ ,  $0.078 = 18\,300cl$ ,

$c = 4.26 \mu\text{M}$  in 1 ml

i.e. 4.26 nmoles of PNP produced in 30 minutes (incubation time)

$\therefore 0.142 \text{ nmol/min}$

**Table 12**  $1/[S]$  and  $1/v$  values for *trans*-sialidase, the transferase

Substrate Concentration, [S]	$1/[S] \text{ mM}^{-1}$	$\Delta A_{400}$ (-) Acceptor*	$v$ $\text{nM min}^{-1}$	$1/v$ $\text{min nM}^{-1}$
1 mM	1	0.08	0.14	7.04
2 mM	0.5	0.25	0.46	2.17
3 mM	0.33	0.27	0.49	2.04
4 mM	0.25	0.41	0.74	1.34
5 mM	0.2	0.51	0.92	1.08

\* Each substrate concentration was repeated three times. The errors in the assay are approximately +/- 10 %.

**Table 13**  $1/[S]$  and  $1/v$  values for *trans*-sialidase, the hydrolase

Substrate Concentration, [S]	$1/[S] \text{ mM}^{-1}$	$\Delta A_{400}$ (-) Acceptor*	$v$ $\text{nM min}^{-1}$	$1/v$ $\text{min nM}^{-1}$
1 mM	1	0.06	0.11	9.35
2 mM	0.5	0.08	0.15	6.80
3 mM	0.33	0.09	0.17	5.78
4 mM	0.25	0.08	0.15	6.71
5 mM	0.2	0.14	0.26	3.85

\* Each substrate concentration was repeated three times. The errors in the assay are approximately +/- 10 %.

### 6.1.7 Incubation of *trans*-sialidase and *C. perfringens* neuraminidase with 2,3-dehydro-2-deoxy-Neu5Ac

*trans*-Sialidase and *C. perfringens* neuraminidase were incubated with 2,3-dehydro-2-deoxy-Neu5Ac. This acts as an inhibitor of *C. perfringens* neuraminidase, but not *trans*-sialidase. Again this was incubated in our assay system (same conditions as before) with *C. perfringens* neuraminidase and *trans*-sialidase and the relative turnover rate calculated. Shown below in **Table 14** is a comparison of relative enzymatic activity of *C. perfringens* neuraminidase and *trans*-sialidase with disaccharide substrate and 2,3-dehydro-2-deoxy-Neu5Ac present.

**Table 14** Assay components of spectrophotometric inhibitor study on *trans*-sialidase and *C. perfringens* neuraminidase

Component	Stock Conc.	Volume 50 $\mu$ l
2,3-dehydro-2-deoxy-Neu5Ac	5 mM	10
H <sub>2</sub> O	-	10
Gal $\beta$ (1,3)GlcNAc $\beta$ -O-Octyl	5 mM	10
HEPES buffer	150 mM	10
<i>trans</i> -sialidase and <i>C. perfringens</i> neuraminidase	As before	10

The assay results are shown below in **Table 15**

**Table 15** Results of the spectrophotometric inhibitor study on *trans*-sialidase and *C. perfringens* neuraminidase

Incubation	$\Delta A_{400}$ (After 30 Mins)
<i>trans</i> -sialidase	0.33
<i>trans</i> -sialidase + Inhibitor	0.35
<i>C. perfringens</i> neuraminidase	0.37
<i>C. perfringens</i> neuraminidase + Inhibitor	0.02

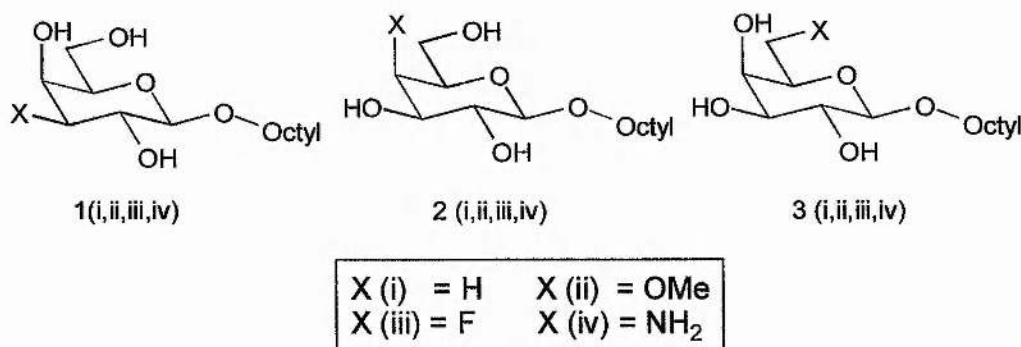
These results indicate that 2,3-dehydro-2-deoxy-Neu5Ac is an inhibitor of *C. perfringens* neuraminidase but not of *trans*-sialidase. This indicates that *trans*-sialidase could possibly proceed through a different intermediate.



## 6.2 Sialylation of Gal $\beta$ -O-Octyl analogues

The diagram below, **Figure 30** (shown before on page 46) shows the three positions which have been synthetically modified.

**Figure 30** Synthetically substituted Gal $\beta$ -O-Octyl library (Lowary *et al* 1993)



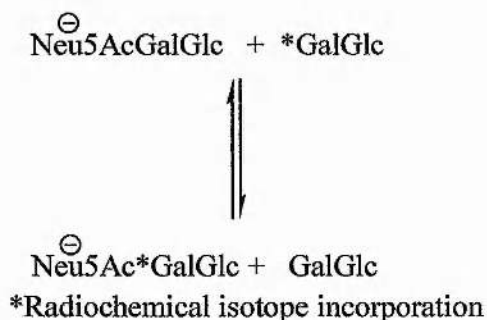
### 6.2.2 Radiochemical assay of Gal $\beta$ -O-Octyl analogues (Lowary *et al* 1993)

All of the above substrates were assayed radiochemically (Pereira *et al* 1995, Vetere *et al* 1996) (page 48). The experimental procedure is outlined below.

### 6.2.3 Synthetically substituted Gal $\beta$ -O-Octyl radiochemical incubations

The radiochemical assay employed monitors the incorporation of [<sup>14</sup>C] lactose and results in the formation of anionic radiolabelled Neu5Ac\*GalGlc. This incorporation process shown below in **Figure 21** (see before, page 32).

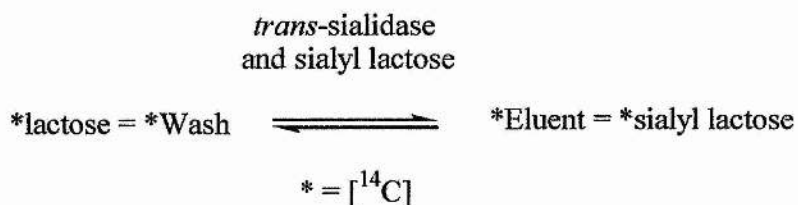
**Figure 21** Incorporation of [<sup>14</sup>C] lactose



In this assay (with no alternative substrate present), *trans*-sialidase will reversibly transfer sialic acid from sialyl lactose to [<sup>14</sup>C] lactose. The charged material can be separated from uncharged material by anion exchange chromatography as follows:

The assay mixture is loaded onto A25 resin (*Sigma Chemical Ltd*) and washed with water to remove all non-sialylated material (wash). The resin is then eluted with  $\text{NH}_4\text{OAc}$  (eluent).

Since *trans*-sialidase is a reversible sialyl transferase (provided the substrate/acceptor concentrations are equal and an equilibrium is established) the total number of radioactive counts in wash and the eluent should be approximately equal, thus:



If a better *trans*-sialidase substrate is added to the assay to compete with  $[^{14}\text{C}]$  lactose, this will result in the unsialylated  $[^{14}\text{C}]$  lactose being washed off the resin with  $\text{H}_2\text{O}$  and hence the radioactive counts in the eluent will be significantly smaller. In some cases the alternative substrate is unsuitable for *trans*-sialidase to transfer sialic acid onto, hence the radioactive result will mirror that of no substrate present. In this assay (with no alternative substrate), *trans*-sialidase will reversibly transfer sialic acid from sialyl lactose to  $[^{14}\text{C}]$  lactose. Hence this results in the total number of radioactive counts in the wash and the eluent being approximately equal. If a better *trans*-sialidase substrate is added to compete with  $[^{14}\text{C}]$  lactose, this will result in the unsialylated  $[^{14}\text{C}]$  lactose being washed off and hence the radioactive counts in the eluent will be significantly smaller. In some cases the alternative substrate is unsuitable for *trans*-sialidase to transfer sialic acid onto, hence the radioactive result will mirror that of no substrate present. The incubation was set up as follows:

**Table 16 Modified Gal $\beta$ -Octyl compound library radiochemical assay components**

Volume	Component
10 $\mu$ l	HEPES (250 mM, pH7.0)
10 $\mu$ l	[ $^{14}$ C] Gal $\beta$ (1,4)Glc (0.02 $\mu$ Ci)
10 $\mu$ l	Neu5Ac $\alpha$ (2,3)Gal $\beta$ (1,4)Glc (1 mM)
10 $\mu$ l	<i>trans</i> -sialidase
10 $\mu$ l	H $_2$ O or alternative substrate

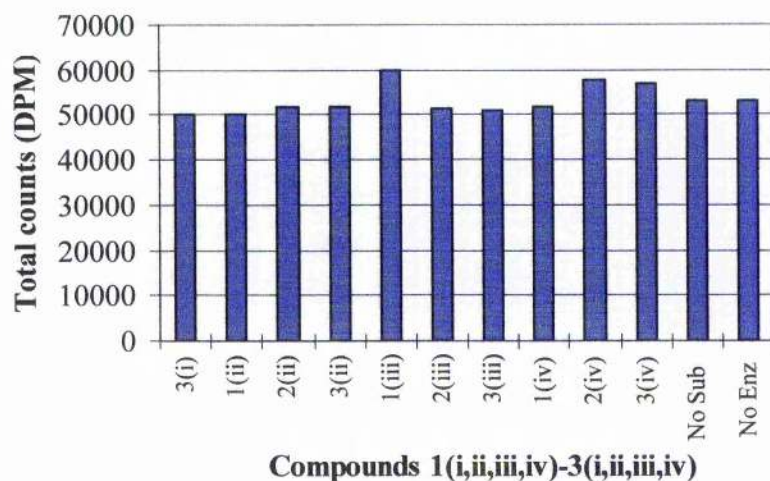
These samples were incubated at 37 °C for 30 mins. 1 ml of H $_2$ O was then added before the incubation was loaded onto 0.5 mls of A25 Sephadex (Anion exchange resin), pre-swollen. The resin was then washed with 2 x 1 ml H $_2$ O before elution with 2 x 1 ml NH $_4$ OAc. All samples were collected and 8 mls of scintillation fluid (*Optiphase*) was added. The samples were then vortexed fully to ensure correct mixing before counting. (Each sample is counted for 5 mins). The assay was repeated twice times.

**Table 17 Substituted Gal $\beta$ -Octyl compound library radioactive Screen (All Numbers are in DPM)**

Substrate	Wash	Elution	Total	E/Total %
1(i)	30325	19864	50190	40
2(i)	34558	15867	50425	31
3(i)	40645	9332	49977	19
1(ii)	27805	22214	50019	44
2(ii)	37547	14272	51818	28
3(ii)	48006	3729	51735	7
1(iii)	40645	19439	60084	32
2(iii)	39311	12199	51511	24
3(iii)	44894	5981	50875	12
1(iv)	25587	26358	51945	51
2(iv)	35834	21895	57729	38
3(iv)	42372	14749	57121	26
No substrate	26269	26950	53210	51
No enzyme	55736	2756	52980	5

Shown below in **Figure 68** is a plot of the total counts of each compound 1(i,ii,iii,iv)-3(i,ii,iii,iv)

**Figure 68** Graph of total radioactive counts (DPM) of each substituted Gal $\beta$ -O-Octyl analogues



### 6.3 Gal $\beta$ -O-Octyl analogue incubations (using Neu5Ac-O-PNP as a substrate)

Compounds 1(i,ii,iii,iv)-3(i,ii,iii,iv) (Lowary *et al* 1993), shown above (see before, **Figure 30**, page 46) were incubated with *trans*-sialidase as follows:

**Table 18** Assay components of Gal $\beta$ -O-Octyl analogue incubations, monitored by T.L.C.

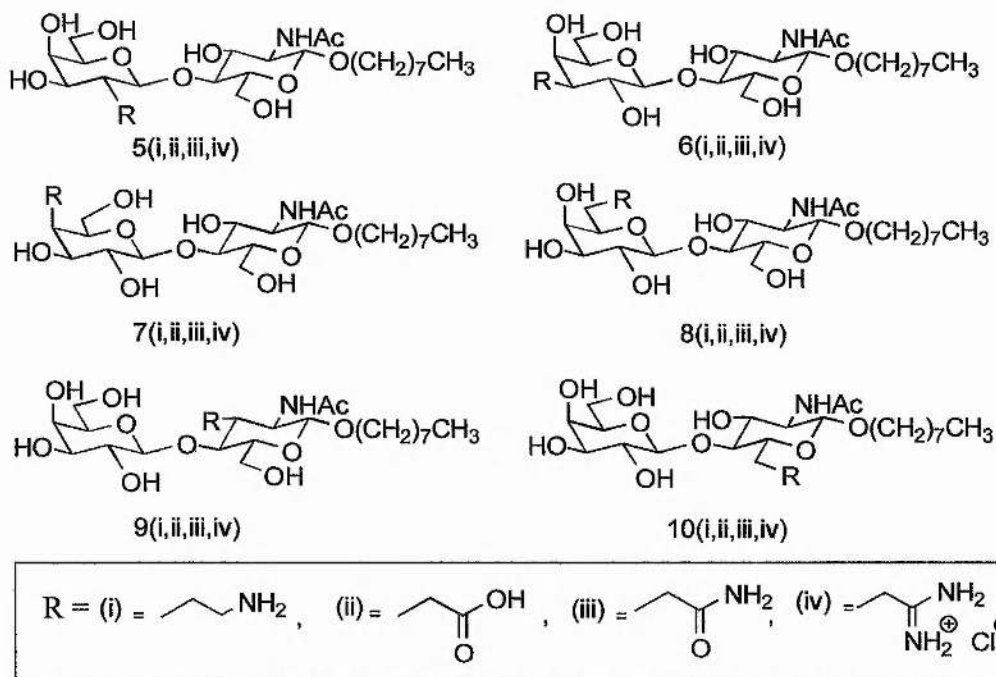
Concentration	Component
5 mg/ml (Approx.)	<i>trans</i> -sialidase (1 ml)
5 mM	Neu5Ac-OPNP
1 mM	Modified Gal $\beta$ -O-Octyl
250 mM	HEPES (1 ml, pH 7.3)

The incubations were set up and left overnight, (~16 H) at 37 °C. 2 x 1  $\mu$ l of each was loaded onto a T.L.C. plate and run in the solvent system CHCl<sub>3</sub>:MeOH:H<sub>2</sub>O (120:85:20). The T.L.C. plate shows all of the modified 6 position octyl-galactoses have been sialylated.

### 6.3.2 Modified Gal $\beta$ (1,4)GlcNAc $\beta$ -O-Octyl library

The following 24 Gal $\beta$ (1,4)GlcNAc $\beta$ -O-Octyl substrates (also see **Figure 36**, page 55), shown in **Figure 36**, were obtained from O. Hindsgaul's Laboratory, Alberta, Canada.

**Figure 36** 24 Substituted Gal $\beta$ (1,4)GlcNAc $\beta$ -O-Octyl library (*Hindsgaul et al* 1996)



### 6.3.3 Gal $\beta$ (1,4)GlcNAc $\beta$ -O-Octyl analogues radiochemical assay

The radiochemical assay was set up as before (*Pereira et al* 1995, *Vetere et al* 1996), see pages 48 and 111. Shown below in **Table 19** is the total radioactive assay counts. The assay was repeated twice.

**Table 19 Amine substituted Gal $\beta$ (1,4)GlcNAc $\beta$ -O-Octyl analogues, radioactive screen (All Numbers are in DPM)**

Compound	Wash/DPM	Elution/DPM	Total/DPM	% E/Total
9(i)	34005	13804	47809	29
10(i)	40679	7470	48149	16
5(i)	18062	31486	49548	64
6(i)	17621	31954	49574	65
7(i)	18215	27737	45952	60
8(i)	36565	11850	48414	24
No substrate	28132	22835	51213	45
No enzyme	48388	5103	53491	9

**Table 20 Acid substituted Gal $\beta$ (1,4)GlcNAc $\beta$ -O-Octyl analogues, radioactive screen (All Numbers are in DPM)**

Compound	Wash/DPM	Elution/DPM	Total/DPM	% E/Total
9(ii)	73884	5506	79390	7
10(ii)	44541	4826	49367	10
5(ii)	17740	30991	48731	64
6(ii)	19235	29435	48670	61
7(ii)	21172	28845	50017	58
8(ii)	42682	3981	46664	9
No substrate	28132	22835	51213	45
No enzyme	48388	5103	53491	9



**Table 21 Amide substituted Gal $\beta$ (1,4)GlcNAc $\beta$ -O-Octyl analogues, radioactive screen (All Numbers are in DPM)**

Compound	Wash/DPM	Elution/DPM	Total/DPM	% E/Total
9(iii)	44899	6520	51419	13
10(iii)	46389	4177	50566	8
5(iii)	29225	21573	50798	32
6(iii)	31635	19874	51509	39
7(iii)	32984	19163	52148	37
8(iii)	46586	4353	50940	9
No substrate	28132	22835	51213	45
No enzyme	48388	5103	53491	9

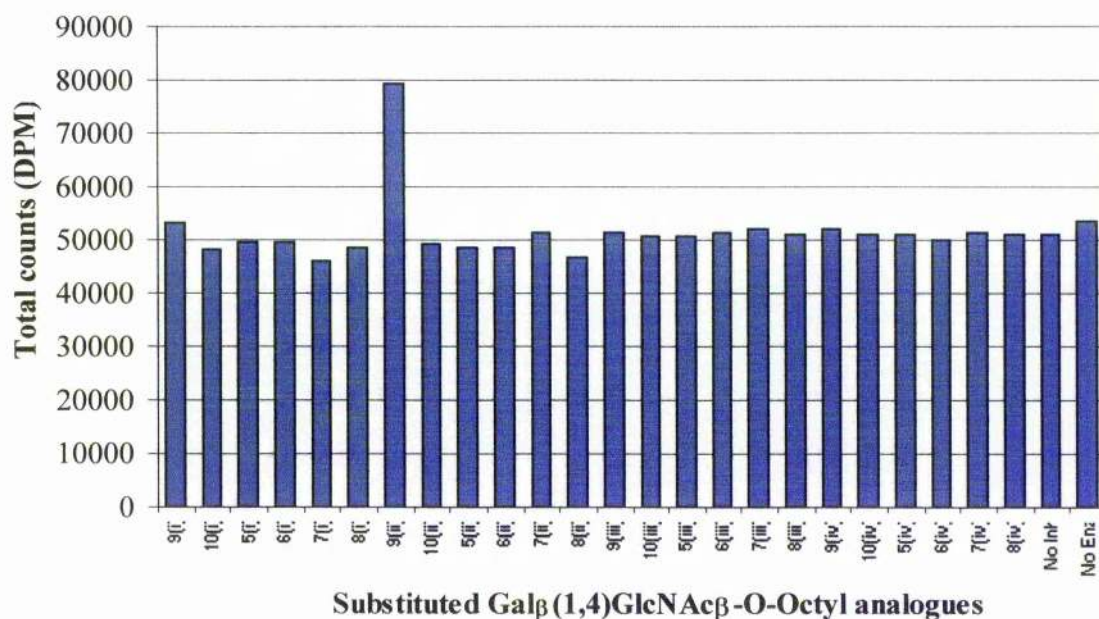
**Table 22 Guanidino substituted Gal $\beta$ (1,4)GlcNAc $\beta$ -O-Octyl analogues, radioactive screen (All Numbers are in DPM)**

Compound	Wash/DPM	Elution/DPM	Total/DPM	% E/Total
9(iv)	43960	8055	52015	15
10(iv)	47382	3542	50924	7
5(iv)	28355	22592	50947	44
6(iv)	31357	18806	50163	46
7(iv)	28476	22785	51262	44
8(iv)	46109	5103	51212	10
No substrate	28132	22835	51213	45
No enzyme	48388	5103	53491	9

Shown below in **Figure 69** is a plot of the total radioactive counts for each compound, 5(i,ii,iii,iv) -10(i,ii,iii,iv).



**Figure 69** Graph of total counts of Gal $\beta$ (1,4)GlcNAc $\beta$ -O-Octyl analogues radiochemical assay



#### 6.3.4 Substituted Gal $\beta$ (1,4)GlcNAc $\beta$ -O-Octyl incubation using Neu5Ac-PNP as a substrate (observed by T.L.C.)

Each of the 24 substrates were incubated with *trans*-sialidase as before, see pages 48 and 111 and loaded onto a T.L.C. plate. They were run in the solvent system CHCl<sub>3</sub>:MeOH:H<sub>2</sub>O (120:85:20). The T.L.C. plate showed that all of the six prime modified Gal $\beta$ (1,4)GlcNAc $\beta$ -O-Octyl have been sialylated.

#### 6.4 Radiochemical assay of all Gal $\beta$ (1,X)Gal analogues (compounds (14)-(21))

The radiochemical assay was set up as before, see pages 48 and 111, using compounds (14)-(21), shown on page 67, (Pereira *et al* 1995, Vetere *et al* 1996).

**Table 23** is an average of the results shown in **Table 24** and **Table 25**, which are also shown below.

**Table 23** Average % E/Total (DPM) of all Gal $\beta$ (1,X)Gal (All Numbers are in DPM)

Substrate	% E/Total	Substrate	% E/Total
A Gal $\beta$ (1,2)Gal $\beta$ -O-Me	15	H Gal $\beta$ (1,4)[Gal $\beta$ (1,6)Glc] $\beta$ -O-Octyl	14
B Glc $\beta$ (1,2)Gal $\beta$ -O-Me	26	I Gal $\beta$ (1,4)Glc	15
C Gal $\beta$ (1,3)Gal $\beta$ -O-Me	13	J Galactose	17
D Gal $\beta$ (1,3)GlcNAc $\beta$ -O-Octyl	12	K Glucose	26
E Gal $\beta$ (1,6)Gal $\beta$ -O-Me	8	L No inhibitor	27
F Gal $\beta$ (1,6)Gal $\beta$ -O-CH <sub>2</sub> CH <sub>2</sub> SiMe <sub>3</sub>	6	M No enzyme	5
G Glc $\beta$ (1,6)Gal $\beta$ -O-Octyl	10		

**Table 24** Total counts of Gal $\beta$ (1,X)Gal (compounds (14)-(21)) radioactive screen (All Numbers are in DPM)

Substrate	Wash	Elution	Total	E/Total %
Galactose	41034	8363	49397	17
Glucose	35981	12846	48829	26
Gal $\beta$ (1,2)Gal $\beta$ -OMe	41276	7718	48994	16
Gal $\beta$ (1,3)Gal $\beta$ -OMe	43263	6717	49980	13
Gal $\beta$ (1,6)Gal $\beta$ -OMe	45486	3478	48964	7
Gal $\beta$ (1,4)Glc	41013	7228	48241	15
No Inhibitor	35471	13112	48584	27
No Enzyme	46425	2300	48724	5

**Table 25 Total counts of Gal $\beta$ (1,X)Gal (compounds (14)-(21)) radioactive screen (All Numbers are in DPM)**

Substrate	Wash	Elution	Total	% E/Total
Gal $\beta$ (1,2)Gal $\beta$ -OMe	50152	7364	57516	13
Glc $\beta$ (1,2)Gal $\beta$ -OMe	40602	14260	54861	26
Gal $\beta$ (1,3)GlcNAc $\beta$ -Octyl	49642	7080	56722	12
Gal $\beta$ (1,6)Gal $\beta$ -OMe	49958	4450	54407	8
Gal $\beta$ (1,6)Gal $\beta$ -OCH <sub>2</sub> CH <sub>2</sub> Si(CH <sub>3</sub> ) <sub>3</sub>	53035	3301	56336	6
Glc $\beta$ (1,6)Gal $\beta$ -Octyl	49152	5647	54799	10
Gal $\beta$ (1,4)[Gal $\beta$ (1,6)Glc] $\beta$ -O-Octyl	32121	7615	39736	14
No substrate	36029	19772	55801	35
No enzyme	54479	1923	56402	328

#### 6.4.1.2 Sialylation of *p*-aminobenzyl-1-thio- $\beta$ -S-galacto-pyranoside (multi-pyranoside) resin

The results shown in **Table 23** indicate the possibility of sialylation of an internal b-galactose moiety. Consequently, a radioactive assay was carried out using *p*-aminobenzyl-1-thio- $\beta$ -S-galacto-pyranoside resin (*Sigma Chemicals Ltd*). This was to assess the possibility of multi-sialylation of oligosaccharides by *trans*-sialidase. This resin was found to be a good substrate of *trans*-sialidase and consequently a serial dilution was carried out. The result of this study is shown below in **Table 26**.

**Table 26 Serial dilution of *p*-aminobenzyl-1-thio- $\beta$ -S-galacto-pyranoside**

<i>p</i> -aminobenzyl-1-thio- $\beta$ -S-galacto-pyranoside Conc.	Wash	Elution	Total	E/Total %
1 ml/200 $\mu$ l	35879	5385	41264	13
1ml/2 mls	27783	11541	39324	29
1ml/20 mls	28593	16121	44714	36
No substrate	26020	16493	42513	39
No Enzyme	39145	2424	41569	6

Using this data, we can construct Table 27 and calculate the % inhibition. A plot of log [I] versus % inhibition was then constructed.

**Table 27 Relative inhibition of *p*-aminobenzyl-1-thio- $\beta$ -S-galactopyranoside**

Substrate Conc.	$\mu$ M	E/Total %	Minus Background	% Activity	% Inhibition
1 ml/200 $\mu$ l	86	13	7	21	79
1ml/2 mls	8.6	29	23	70	30
1ml/20 mls	0.86	36	30	91	9
No substrate	-	39	33	-	-
No Enzyme	-	6	-	-	-

#### 6.4.2 Incubation of Gal $\beta$ (1,X)Gal analogues (compounds (14)-(21)) with Neu5Ac-PNP (observed by T.L.C.)

Each of the Gal $\beta$ (1,X)Gal substrates (compounds (14)-(21)) were incubated with *trans*-sialidase as before, see page 114 and loaded onto a TLC plate. The plates were run in the solvent system CHCl<sub>3</sub>:MeOH:H<sub>2</sub>O (120:85:20). The results in each case were recorded and photographed.

#### 6.4.3 Incubation of Gal $\beta$ (1,2)Gal-O-Me, Glc $\beta$ (1,2)Gal $\beta$ -O-Me and Gal $\beta$ (1,3)Gal $\beta$ -O-Me

This T.L.C. plate shows that Gal $\beta$ (1,3)Gal $\beta$ -O-Me has become sialylated, producing a spot with an R<sub>f</sub> = 0.3. Gal $\beta$ (1,2)Gal $\beta$ -O-Me has also been sialylated, producing a spot with an R<sub>f</sub> = 0.3. The T.L.C. also indicates that Glc $\beta$ (1,2)Gal $\beta$ -O-Me has in no way been sialylated.

#### 6.4.4 Incubation of Gal $\beta$ (1,6)Gal $\beta$ -O-CH<sub>2</sub>CH<sub>2</sub>Si(CH<sub>3</sub>)<sub>3</sub>, Glc $\beta$ (1,6)Gal $\beta$ -O-Octyl and Gal $\beta$ (1,6)Gal $\beta$ -O-Me

A similar experiment was carried out using Gal $\beta$ (1,6)Gal $\beta$ -O-CH<sub>2</sub>CH<sub>2</sub>Si(CH<sub>3</sub>)<sub>3</sub>, Glc $\beta$ (1,6)Gal $\beta$ -O-Octyl and Gal $\beta$ (1,6)Gal $\beta$ -O-Me substrates. This T.L.C. shows that Gal $\beta$ (1,6)Gal $\beta$ -O-Me has become sialylated, producing a spot with an R<sub>f</sub> = 0.3. Glc $\beta$ (1,6)Gal $\beta$ -O-Octyl has also been sialylated, producing a spot with an R<sub>f</sub> = 0.4.

The T.L.C. also indicates that Gal $\beta$ (1,6)Gal $\beta$ -O-Me has also been sialylated, producing a spot with an Rf = 0.1.

#### **6.4.5 Incubation of Gal $\beta$ (1,4)[Gal $\beta$ (1,6)Glc] $\beta$ -O-Octyl and Glc $\beta$ (1,6)Gal $\beta$ -O-Octyl**

This T.L.C. indicates that (with both 30 mM and 10 mM) Gal $\beta$ (1,4)[Gal $\beta$ (1,6)Glc] $\beta$ -O-Octyl has become sialylated producing a spot with an Rf = 0.5 and Glc $\beta$ (1,6)Gal $\beta$ -O-Octyl has become sialylated, producing a spot with an Rf = 0.4.

#### **6.4.6 3 mg Preparative Scale Synthesis of Neu5Ac $\alpha$ (2,3)Gal $\beta$ (1,6)Gal $\beta$ -O-CH<sub>2</sub>CH<sub>2</sub>Si(CH<sub>3</sub>)<sub>3</sub>**

3 mgs of Gal $\beta$ (1,6)Gal $\beta$ -O-CH<sub>2</sub>CH<sub>2</sub>Si(CH<sub>3</sub>)<sub>3</sub> was incubated with 20 mgs of Neu5Ac-O-PNP. 4 mls of crude *trans*-sialidase (approximately 5 mgs/ml) was added and the reaction mixture was buffered with 2 mls HEPES (250 mM, pH 7.3). The incubation was heated to 37 °C and left for 16 hours. By T.L.C. two spots (i.e. product and starting material) were present using CHCl<sub>3</sub>:MeOH:H<sub>2</sub>O (120:85:20).

#### **6.4.7 Purification of Neu5Ac $\alpha$ (2,3)Gal $\beta$ (1,6)Gal $\beta$ -O-CH<sub>2</sub>CH<sub>2</sub>Si(CH<sub>3</sub>)<sub>3</sub>**

The product was then isolated on A25 sephadex anion exchange resin. The sialylated product was eluted with 1 M NH<sub>4</sub>OAc. The product was then separated further using *Sep-Pac* reverse-phase resin cartridges. The cartridges were first washed with H<sub>2</sub>O before the product being eluted in 100% MeOH. Approximately 1.0 mgs of sialylated material was isolated. The product was then characterised by electrospray MS and enzymatic digestion.

#### **6.4.8 Characterisation of Neu5Ac $\alpha$ (2,3)Gal $\beta$ (1,6)Gal $\beta$ -O-CH<sub>2</sub>CH<sub>2</sub>Si(CH<sub>3</sub>)<sub>3</sub> - Electrospray Mass Spectrometry**

The spectrum shows clearly only one peak at 732.82 Da/e corresponding to Neu5Ac $\alpha$ (2,3)Gal $\beta$ (1,6)Gal $\beta$ -O-CH<sub>2</sub>CH<sub>2</sub>Si(CH<sub>3</sub>)<sub>3</sub>. The calculated molecular weight for this compound is 732.78.

#### **6.4.9 Enzymatic digestion of Neu5Ac $\alpha$ (2,3)Gal $\beta$ (1,6)Gal $\beta$ -O-CH<sub>2</sub>CH<sub>2</sub>Si(CH<sub>3</sub>)<sub>3</sub>**

Neu5Ac $\alpha$ (2,3)Gal $\beta$ (1,6)Gal $\beta$ -O-CH<sub>2</sub>CH<sub>2</sub>Si(CH<sub>3</sub>)<sub>3</sub> was subjected to systematic enzymatic digestion  $\beta$ -galactosidase (*E. coli*) and neuraminidase (*C. perfringens*).



All incubations were carried out in MES (pH 5.5 50  $\mu$ l), and heated to 37 °C overnight. The incubation mixtures (a-f) were loaded onto a T.L.C. plate. They were run in the solvent system  $\text{CHCl}_3:\text{MeOH}:\text{H}_2\text{O}$  (120:85:20).

Incubation a indicates that  $\text{Neu5Ac}\alpha(2,3)\text{Gal}\beta(1,6)\text{Gal}\beta\text{-O-CH}_2\text{CH}_2\text{Si}(\text{CH}_3)_3$  is not subject to hydrolysis by  $\beta$ -galactosidase as the trisaccharide has not changed on T.L.C. This is because the Neu5Ac is blocking the enzyme from cleaving the galactose residue and hence the trisaccharide cannot be digested.

Incubation b shows quite clearly the cleavage of the  $\text{Gal}\beta(1,6)\text{Gal}\beta\text{-O-CH}_2\text{CH}_2\text{Si}(\text{CH}_3)_3$  and the presence of galactose.

Incubation c shows the presence of starting material,  $\text{Gal}\beta(1,6)\text{Gal}\beta\text{-O-CH}_2\text{CH}_2\text{Si}(\text{CH}_3)_3$  (as well as possibly Neu5Ac, very difficult to observe by T.L.C.), as expected from the removal of Neu5Ac by *C. perfringens* neuraminidase.

Incubation d shows only  $\text{Gal}\beta(1,6)\text{Gal}\beta\text{-O-CH}_2\text{CH}_2\text{Si}(\text{CH}_3)_3$  (as expected). Neuraminidase has no effect on the  $\text{Gal}\beta(1,6)\text{Gal}\beta\text{-O-CH}_2\text{CH}_2\text{Si}(\text{CH}_3)_3$ .

Incubation e shows galactose. As proven from incubation a and b, only after the sialic acid is cleaved by *C. perfringens* neuraminidase is it possible for the  $\beta$ -galactosidase to cleave  $\text{Gal}\beta(1,6)\text{Gal}\beta\text{-O-CH}_2\text{CH}_2\text{Si}(\text{CH}_3)_3$ . The smear at the base line is indicative of sialic acid.

Incubation f shows the sialylated  $\text{Glc}\beta(1,6)\text{Gal}\beta\text{-O-Octyl}$  which is unchanged.

#### **6.4.10 3 mg Preparative Scale Synthesis of $\text{Neu5Ac}\alpha(2,3)[\text{Glc}\beta(1,6)]\text{Gal}\beta\text{-O-Octyl}$**

$\text{Glc}\beta(1,6)\text{Gal}\beta\text{-O-Octyl}$  was first purified to one spot by T.L.C. on reverse-phase silica. The product was eluted in a gradient of 100 % MeOH.

3 mgs of  $\text{Glc}\beta(1,6)\text{Gal}\beta\text{-O-Octyl}$  was then incubated with 20 mgs of  $\text{Neu5Ac-O-PNP}$ . 4 mls of crude *trans*-sialidase (approximately 5 mgs/ml) was added and the reaction mixture was buffered with 2 mls HEPES (250 mM, pH 7.3). The incubation was heated to 37 °C and left for 16 hours. By T.L.C. two spots were present using  $\text{CHCl}_3:\text{MeOH}:\text{H}_2\text{O}$  (120:85:20).

#### 6.4.11 Purification of Neu5Ac $\alpha$ (2,3)[Glc $\beta$ (1,6)]Gal $\beta$ -O-Octyl

The product was then isolated on reverse-phase silica. A gradient of 0-100% MeOH (In 25 % increments) was carried out. The product was isolated at 50 % MeOH. The product was then subject to further purification on A25 sephadex anion exchange resin. The sialylated product was eluted with 1 M NH<sub>4</sub>OAc. Approximately 1.5 mgs of sialylated material was isolated. This product was then characterised by electrospray MS and enzymatic digestion.

#### 6.4.12 Analysis of Neu5Ac $\alpha$ (2,3)[Glc $\beta$ (1,6)]Gal $\beta$ -O-Octyl - Electrospray Mass Spectrometry

The spectrum shows clearly only one peak at 745 Da/e. This corresponds to Neu5Ac $\alpha$ (2,3)[Glc $\beta$ (1,6)]Gal $\beta$ -O-Octyl (calculated molecular weight 744.76).

#### 6.1.14 Systematic enzymatic digestion Neu5Ac $\alpha$ (2,3)[Glc $\beta$ (1,6)]Gal $\beta$ -O-Octyl

Neu5Ac $\alpha$ (2,3)[Glc $\beta$ (1,6)]Gal $\beta$ -O-Octyl was subjected to systematic enzymatic digestion using  $\beta$ -glucosidase (*Caldocellum saccharolyticum*), (Almonds),  $\beta$ -galactosidase and *C. perfringens* neuraminidase. All incubations were carried out in (pH 5.5, 50  $\mu$ l), and heated to 37 °C over night. The incubation mixtures (a-k) were loaded onto a T.L.C. plate. They were run in the solvent system CHCl<sub>3</sub>:MeOH:H<sub>2</sub>O (120:85:20).

Incubation a indicates that Neu5Ac $\alpha$ (2,3)[Glc $\beta$ (1,6)]Gal $\beta$ -O-Octyl is not subject to hydrolysis by  $\beta$ -galactosidase as the trisaccharide has not changed on T.L.C. This may be for a number of reasons. It is not indicative that the Neu5Ac is attached to the galactose residue, (since there is no literature president for this). It is more likely that the branched trisaccharide is too bulky for the enzyme, and hence cannot be digested.

Incubation b shows quite clearly the cleavage of the Glc $\beta$ (1,6)Gal $\beta$ -O-Octyl and the presence of glucose. (Since glucose and galactose have very similar R<sub>f</sub> values, it is very difficult to distinguish between the two).

Incubation c shows the presence of starting material, Glc $\beta$ (1,6)Gal $\beta$ -O-Octyl (as well as possibly Neu5Ac, very difficult to observe by T.L.C.), as expected from the removal of Neu5Ac by *C. perfringens* neuraminidase.



Incubation d shows only  $\text{Glc}\beta(1,6)\text{Gal}\beta\text{-O-Octyl}$  (as expected). Neuraminidase has no effect on the  $\text{Glc}\beta(1,6)\text{Gal}\beta\text{-O-Octyl}$ .

Incubation e shows glucose (and galactose). As proven from incubation a and b, only after the sialic acid is cleaved by *C. perfringens* neuraminidase is it possible for the  $\beta$ -glucosidase to cleave  $\text{Glc}\beta(1,6)\text{Gal}\beta\text{-O-Octyl}$ . The smear at the base line is indicative of sialic acid.

Incubation f shows the sialylated  $\text{Glc}\beta(1,6)\text{Gal}\beta\text{-O-Octyl}$  which is unchanged.

Incubation g shows a comparison of the digestion of an oligosaccharide  $\text{Gal}\beta(1,4)\text{Glc}\beta\text{-O-Octyl}$ . After treatment with  $\beta$ -galactosidase (crude) galactose and glucose-octyl.

Incubation h shows no cleavage as expected between octyl lactoside and  $\beta$ -glucosidase.  $\beta$ -glucosidase can only cleave the glucose unit when the galactose is removed (some trace of  $\beta$ -galactosidase, present in  $\beta$ -glucosidase may hydrolyse).

Incubation j contains  $\text{Glc}\beta(1,6)\text{Gal}\beta\text{-O-Octyl}$  and  $\beta$ -galactosidase. As expected the major product is  $\text{Glc}\beta(1,6)\text{Gal}\beta\text{-O-Octyl}$  (unchanged).

Incubation k contains the following  $\text{Neu5Ac}\alpha(2,3)[\text{Glc}\beta(1,6)]\text{Gal}\beta\text{-O-Octyl}$ , *C. perfringens* neuraminidase and  $\beta$ -galactosidase. The neuraminidase has removed the sialic acid to give  $\text{Glc}\beta(1,6)\text{Gal}\beta\text{-O-Octyl}$ . This is the major product.

**6.1.15 3 mg Preparative Scale Synthesis of  $\text{Neu5Ac}\alpha(2,3)\text{Gal}\beta(1,4)[\beta\text{Gal}(1,6)]\text{Glc}\beta\text{-O-Octyl}$**

$\text{Gal}\beta(1,4)[\beta\text{Gal}(1,6)]\text{Glc}\beta\text{-O-Octyl}$  was first purified to one spot by T.L.C. on reverse-phase silica. The product was eluted in a gradient of 75 % MeOH.

3 mgs of  $\text{Gal}\beta(1,4)[\beta\text{Gal}(1,6)]\text{Glc}\beta\text{-O-Octyl}$  were then incubated with 20 mgs of  $\text{Neu5Ac-O-PNP}$ . 4 mls of crude *trans*-sialidase (approximately 5 mgs/ml) was added and the reaction mixture was buffered with 2 mls HEPES (250 mM, pH 7.3). The incubation was heated to 37 °C and left for 16 hours. By T.L.C. two spots were present using  $\text{CHCl}_3:\text{MeOH}:\text{H}_2\text{O}$  (120:85:20).

#### **6.4.16 Incubation of Gal $\beta$ (1,4)[ $\beta$ Gal(1,6)]Glc $\beta$ -O-Octyl**

The T.L.C. plate clearly indicates two points of sialylation of Gal $\beta$ (1,4)[ $\beta$ Gal(1,6)]Glc $\beta$ -O-Octyl located with Rf s = 0.4, 0.2.

#### **6.4.17 Purification of Neu5Ac $\alpha$ (2,3)Gal $\beta$ (1,4)[ $\beta$ Gal(1,6)]Glc $\beta$ -O-Octyl**

The product was then isolated by chromatography (gravity) on reverse-phase silica. A gradient of 0-100% MeOH (In 25 % increments) was carried out. The product was isolated at 50 % MeOH. The product was then subject to further purification on A25 sephadex anion exchange resin. The sialylated product was eluted with 1 M NH<sub>4</sub>OAc. Approximately 1.0 mgs of sialylated material was isolated. The product was then characterised by electrospray-MS.

#### **6.4.18 Analysis of Neu5Ac $\alpha$ (2,3)Gal $\beta$ (1,4)[ $\beta$ Gal(1,6)]Glc $\beta$ -O-Octyl - Electrospray Mass Spectrometry**

There are clearly two peaks as expected by T.L.C., these are located at 906.99 and 1197.16 Da/e, corresponding to the mono and di-sialylated Gal $\beta$ (1,4)[ $\beta$ Gal(1,6)]Glc $\beta$ -O-Octyl.

## 6.5 Gal $\beta$ -SX analogue library radiochemical assay

The radiochemical assay was set up and carried out on compounds A1-J10 (twice), as before (*Pereira et al 1995, Vetere et al 1996*), see pages 48 and 111. **Tables 28-37** show the total radioactive counts in each assay.

**Table 28 Radioactive screen A1-A10 (All Numbers are in DPM)**

Modified substrates	Wash	Elution	Total	E/Total %
A1	16900	13013	29913	44
A2	24233	6108	30342	20
A3	20285	8921	29206	31
A4	24082	6493	30575	21
A5	18791	11191	29982	37
A6	23314	6766	30080	22
A7	23124	6699	29823	22
A8	22817	6978	29795	23
A9	20503	9305	29808	31
A10	20494	9262	29758	31
No substrate	16586	11637	28223	41
No enzyme	27931	1364	29295	5

**Table 29 Radioactive screen B1-B10 (All Numbers are in DPM)**

Modified Substrates	Wash	Elution	Total	E/Total %
B1	23121	6261	29389	21
B2	18807	9170	27978	33
B3	17503	12650	30153	42
B4	20763	9027	29790	30
B5	22340	7583	29923	25
B6	21490	8462	29952	28
B7	0	0	0	0
B8	21124	8737	29860	29
B9	21454	7838	29292	27
B10	18612	11329	29942	38
No substrate	16586	11637	28223	41
No enzyme	27931	1364	29295	5

**Table 30 Radioactive screen C1-C10 (All Numbers are in DPM)**

Modified Substrates	Wash	Elution	Total	E/Total %
C1	22164	11638	33802	34
C2	21587	8153	29740	27
C3	18762	10202	28964	35
C4	0	0	0	0
C5	21186	8339	29525	28
C6	21309	7501	28810	26
C7	21082	5512	26594	21
C8	24094	6077	30172	20
C9	0	0	0	0
C10	22949	6455	29405	22
No substrate	16586	11637	28223	41
No enzyme	27931	1364	29295	5

**Table 31 Radioactive screen D1-D10 (All Numbers are in DPM)**

Modified Substrates	Wash	Elution	Total	E/Total %
D1	23119	6567	29686	22
D2	22123	5616	27739	20
D3	17121	10903	28024	39
D4	23645	3847	27492	14
D5	24941	5176	30116	17
D6	19024	10560	29584	36
D7	0	0	0	0
D8	19381	8651	28033	31
D9	0	0	0	0
D10	24094	6600	30694	22
No substrate	18717	11398	30115	38
No enzyme	29451	1462	30913	5

**Table 32 Radioactive screen E1-E10 (All Numbers are in DPM)**

<b>Modified Substrates</b>	<b>Wash</b>	<b>Elution</b>	<b>Total</b>	<b>E/Total %</b>
E1	22236	6625	28861	23
E2	27784	5007	32791	15
E3	20382	8583	28965	30
E4	21403	8460	29863	28
E5	24802	5276	30078	18
E6	24277	6125	30401	20
E7	24231	6200	30431	20
E8	22223	8155	30378	27
E9	20511	6882	27393	25
E10	20226	9331	29557	32
No substrate	18717	11398	30115	38
No enzyme	29451	1462	30913	5

**Table 33 Radioactive screen F1-F10 (All Numbers are in DPM)**

<b>Modified Substrates</b>	<b>Wash</b>	<b>Elution</b>	<b>Total</b>	<b>E/Total %</b>
F1	24943	6840	31783	22
F2	24377	7330	31707	23
F3	23047	7858	30906	25
F4	19287	10791	30079	36
F5	25189	5528	30717	18
F6	20082	10820	30902	35
F7	20384	10658	31042	34
F8	22693	7754	30447	25
F9	23232	6646	29878	22
F10	22437	7884	30321	26
No substrate	18717	11398	30115	38
No enzyme	29451	1462	30913	5

**Table 34 Radioactive screen G1-G10 (All Numbers are in DPM)**

Modified Substrates	Wash	Elution	Total	E/Total %
G1	25439	6751	32190	21
G2	18947	11782	30729	38
G3	0	0	0	0
G4	0	0	0	0
G5	25661	7286	32947	22
G6	23393	6182	29575	21
G7	22273	9815	32089	31
G8	20150	11980	32129	37
G9	21791	10907	32698	33
G10	28211	7169	35380	20
No substrate	21725	10903	32628	34
No enzyme	34097	986	35083	3

**Table 35 Radioactive screen H1-H10 (All Numbers are in DPM)**

Modified Substrates	Wash	Elution	Total	E/Total %
H1	23342	7011	30354	23
H2	24400	6165	30565	20
H3	22364	8330	30694	27
H4	19778	10451	30229	35
H5	27410	3671	31082	12
H6	31073	5588	36661	15
H7	36849	5376	42225	13
H8	32476	9622	42098	23
H9	26938	10355	37293	28
H10	36847	7073	43920	16
No substrate	21725	10903	32628	34
No enzyme	34097	986	35083	3

**Table 36 Radioactive screen I1-I10 (All Numbers are in DPM)**

Modified Substrates	Wash	Elution	Total	E/Total %
I1	30844	9917	40761	24
I2	31592	8569	40162	21
I3	30009	8732	38741	23
I4	24790	10831	35621	30
I5	32522	7499	40021	19
I6	38223	6350	44573	14
I7	32843	6844	39687	17
I8	29213	9724	38937	25
I9	33018	6769	39779	17
I10	32267	6405	38672	17
No substrate	27036	13023	40059	33
No enzyme	42846	1229	44075	3

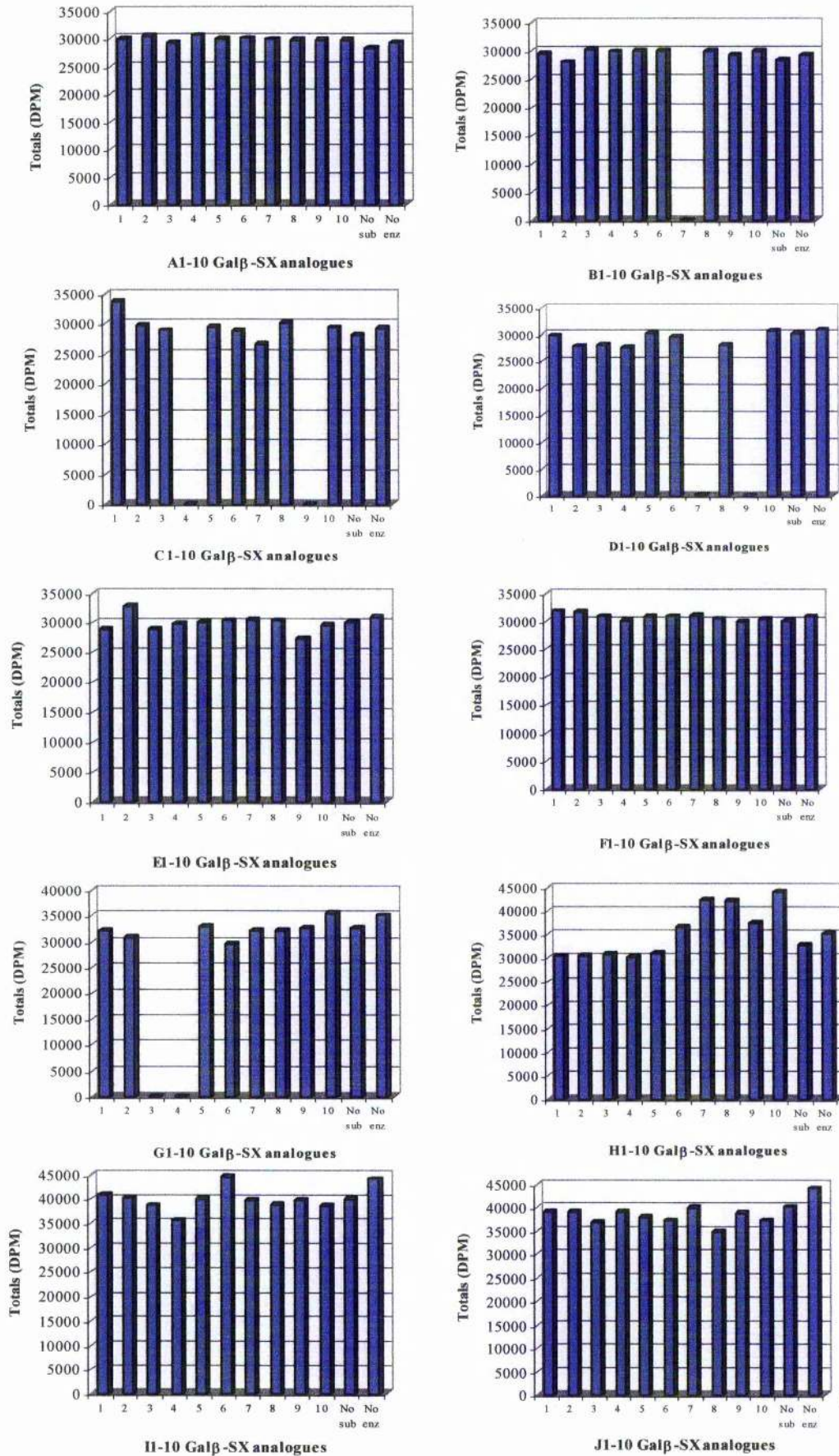
**Table 37 Radioactive screen J1-J10 (All Numbers are in DPM)**

Modified Substrates	Wash	Elution	Total	E/Total %
J1	30237	8903	39140	23
J2	28205	10753	38959	28
J3	27973	8703	36676	24
J4	30637	8356	38993	21
J5	27423	10550	37972	28
J6	32352	4856	37207	13
J7	33195	6806	40001	17
J8	24948	9930	34878	28
J9	31996	6741	38738	17
J10	30946	6294	37240	17
No substrate	27036	13023	40059	33
No enzyme	42846	1229	44075	3

Shown below in **Figure 70** are the graphs of total counts of radioactivity, observed in screens A1-J10 inclusive.



**Figure 70** Total radioactive counts of Gal $\beta$ -SX analogue library



## 6.6 Best substrates from Gal $\beta$ -SX analogue radioactive screen

The best substrate of the radioactive screen encompassing compounds A1-J10 were selected and assayed again to ascertain the best substrate of the group. **Table 38** shows the result of this assay.

**Table 38 Best substrates from Gal $\beta$ -SX analogue radioactive screen**

Sample	Wash	Elution	Total	% E/Total
D4	40030	8848	48878	18
E2	37760	9500	47260	20
H5	38061	7786	45847	17
J6*	41491	5204	46695	11
Control	31369	15376	46745	33
No enzyme	44189	3399	47588	7

\*Best substrate, use for serial dilution later

## 6.7 Serial dilution of Gal $\beta$ (1,4)[ $\beta$ Gal(1,6)]Glc $\beta$ -Octyl (21) radioactive screen

As Gal $\beta$ (1,4)[ $\beta$ Gal(1,6)]Glc $\beta$ -Octyl (21) proved to be the best substrate of the Gal $\beta$ (1,X)gal assay, this compound was subject to a serial dilution to calculate IC<sub>50</sub> for this substrate. After dilution, the resultant concentrations were assessed radiochemically, as before, page 48 and 111. The total counts of this radioactive assay are shown below in **Table 39**.

**Table 39 Serial dilution of Gal $\beta$ (1,4)[ $\beta$ Gal(1,6)]Glc $\beta$ -Octyl radioactive screen (Serial Dilution)**

Gal $\beta$ (1,4)[ $\beta$ Gal(1,6)]Glc $\beta$ -Octyl Concentration	Wash	Elution	Total	% E/Total
1 mM	32729	7973	40254	20
0.5 mM	30618	11374	41993	27
0.25 mM	27552	10218	37770	27
0.1 mM	29784	11747	41531	28
0.05 mM	27295	13919	41214	34
No substrate	26402	14123	40525	35
No enzyme	37363	3894	41257	9

## 6.8 Serial dilution of J6 (Gal $\beta$ -SX analogue) radioactive screen

Since J6 was determined as the best substrate of the radiochemical assessment of the Gal $\beta$ -S-X analogues, a serial dilution was carried out on this compounds and the resultant concentrations assessed radiochemically. The total counts of this radioactive assay are shown below in **Table 40**.

**Table 40** Serial dilution of J6 (Gal $\beta$ -SX analogue) radioactive screen

<b>J6 (Gal<math>\beta</math>-SX analogue) concentration</b>	<b>Wash</b>	<b>Elution</b>	<b>Total</b>	<b>% E/Total</b>
1 mM	32188	9350	41538	23
0.5 mM	30599	11919	42518	28
0.25 mM	27187	11397	38583	30
0.1 mM	26431	14907	41337	36
0.05 mM	26900	14026	40926	34
No substrate	26402	14123	40525	35
No enzyme	37363	3894	41257	9

# Chapter 7

## Conclusions and Further work

### 7.1 *trans*-Sialidase isolation and purification

Recombinant *Trypanosoma cruzi* *trans*-sialidase over-expressed in *E. coli* was grown in media and the protein isolated. It was purified by anion exchange and affinity chromatography to the level of a single band on a silver stained SDS gel(see appendix 1).

### 7.2 *trans*-Sialidase assay development

A rapid reliable spectrophotometric coupled assay has also been developed for the purpose of measuring the activity of *trans*-sialidase during purification. This assay analyses both the hydrolysis and transferase activities of *trans*-sialidase. Using this assay it is possible to conclude that *trans*-sialidase is preferentially a transferase.

### 7.3 Radioactive screening of *trans*-sialidase potential substrates

Studies have been carried out on three mutually exclusive sets of synthetic saccharide derivatives to map substrate recognition by the enzyme. Synthetic fragments of the natural branched oligosaccharide substrates have also been incorporated into these studies.

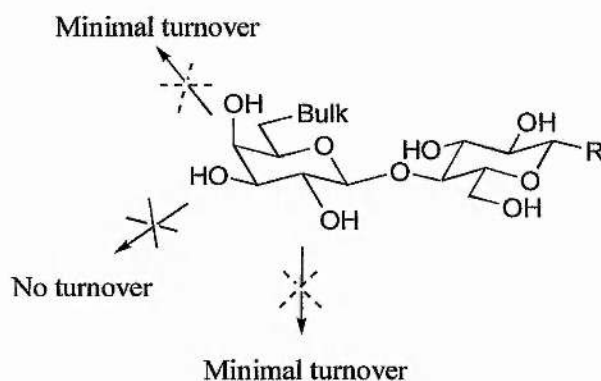
### 7.4 Screening of Gal $\beta$ -O-Octyl and Gal $\beta$ GlcNAc $\beta$ -O-Octyl analogues

The radiochemical assessment of Gal $\beta$ -O-Octyl analogues and Gal $\beta$ GlcNAc $\beta$ -O-Octyl analogues indicate that modification of the hydroxyl groups at positions 2 and 4 on the terminal galactose results in minimum turnover only. Also modification of the hydroxyl group at position 3 rendered the substrate unsialylable (as expected). However the hydroxyl group at position 6 seems to be unimportant for sialylation and may be modified extensively.

The hydroxyl groups of the internal sugar (of disaccharide) may also be altered in many ways, the presence of the second sugar unit seeming to increase the substrate efficacy. These points are summarised in **Figure 71** below.

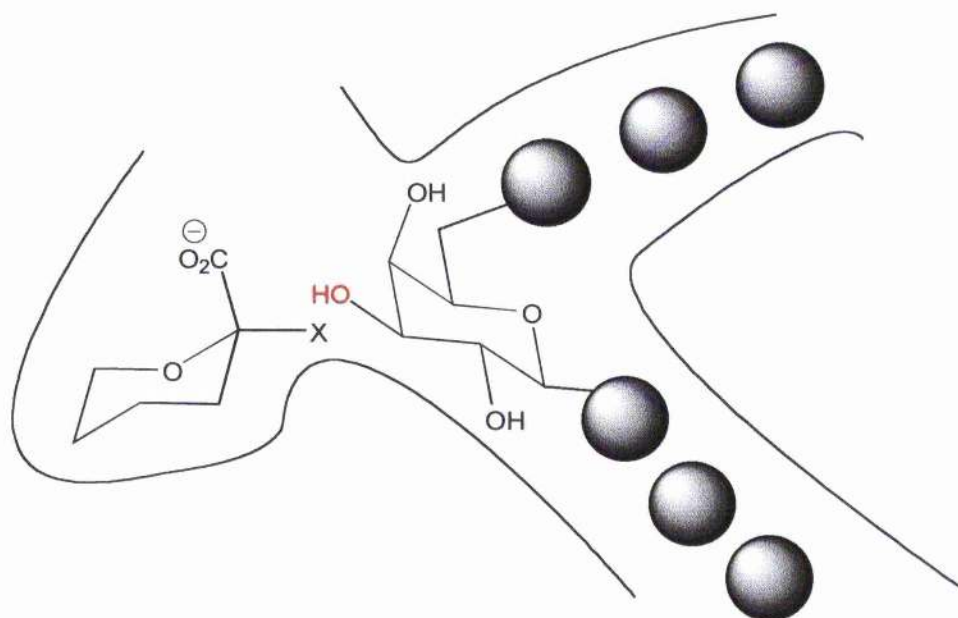


**Figure 71** Modifications to saccharides which influence *trans*-sialidase sialyl transfer



Radiochemical assay results using fragments of the natural substrates have also given interesting findings. It has been possible to sialylate  $\text{Glc}\beta(1,6)\text{Gal}\beta\text{-O-Octyl}$ . This is important since it has been well documented in the literature that it has only been possible to sialylate terminal galactose residues (*Schenkman and Vandekerckhove* 1992). Our conclusions have not fully indicated where *trans*-sialidase has attached the sialic acid, but have conclusively shown that the substrate has been sialylated. (See mass spectrum, **Figure 56**, page 75). It is highly likely that the sialic acid has been attached to the internal galactose, since all prior studies have shown glucose to be a non-substrate. This does, however, indicate that the active site of *trans*-sialidase has the capacity to hold another monosaccharide at the six position of galactose (as well as an anomeric octyl chain). **Figure 72A** shows a possible general model of the *trans*-sialidase active site with the orientation of the substrate,  $\text{Gal}\beta(1,6)\text{X}$ .

**Figure 72A** *trans*-sialidase binding site showing the possible orientation of the substrate Gal $\beta$ (1,6)X



The hydroxyl shown in red is the point of attachment of sialic acid. This model of *trans*-sialidase is supported by the confirmation of the di-sialylation of Gal $\beta$ (1,4)[ $\beta$ Gal(1,6)]GlcNAc $\beta$ -O-Octyl (see mass spectrum, **Figure 61**, page 81). This result suggests that it is possible to sialylate an internal galactose.

### 7.5 Chemo-enzymatic synthesis

Gal $\beta$ (1,4)[ $\beta$ Gal(1,6)]GlcNAc $\beta$ -O-Octyl, Glc $\beta$ (1,6)Gal $\beta$ -O-Octyl and Gal $\beta$ (1,6)Gal $\beta$ -O-CH<sub>2</sub>-CH<sub>2</sub>-Si(CH<sub>3</sub>)<sub>3</sub> were sialylated using *trans*-sialidase preparatively, indicating the potential of *trans*-sialidase for chemo-enzymatic synthesis. Each of these compounds were isolated and their structures confirmed by mass spectrometry. Gal $\beta$ (1,4)[ $\beta$ Gal(1,6)]GlcNAc $\beta$ -O-Octyl and Glc $\beta$ (1,6)Gal $\beta$ -O-Octyl were also subject to enzymatic digestion.



## 7.6 Further work

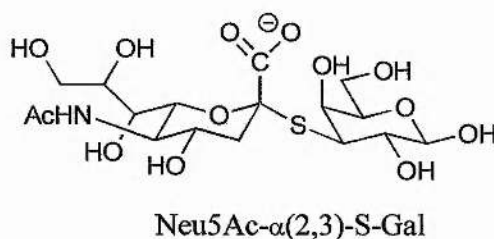
### *trans*-sialidase in organic synthesis

Sialylation of trisaccharides such as  $\text{Glc}\beta(1,\text{X})\text{Glc}\beta(1,6)\text{Gal}\beta\text{-O-Octyl}$  or  $\text{R-Gal}\beta(1,\text{X})\text{Gal}\beta\text{-O-Octyl}$  (where X = any linkage and R = any other large moiety) should give more information about the size of the active site of *trans*-sialidase and exploit further the  $\alpha(2,3)$  sialyl acid transfer potential use of this enzyme in carbohydrate synthesis.

### Inhibitor development

Development of inhibitors to *trans*-sialidase could use an -S- linked donor substrate, i.e.  $\text{Neu5Ac-}\alpha(2,3)\text{-S-Gal}$  or analogues of this general structure, shown below in **Figure 72B**.

**Figure 72B**  $\text{Neu5Ac-}\alpha(2,3)\text{-S-Gal}$



This structure should be likely to act as a Neu5Ac donor for *trans*-sialidase since it incorporates the Neu5Ac-S-Gal bond, which should be less susceptible to sialyl transferase.

# Appendix

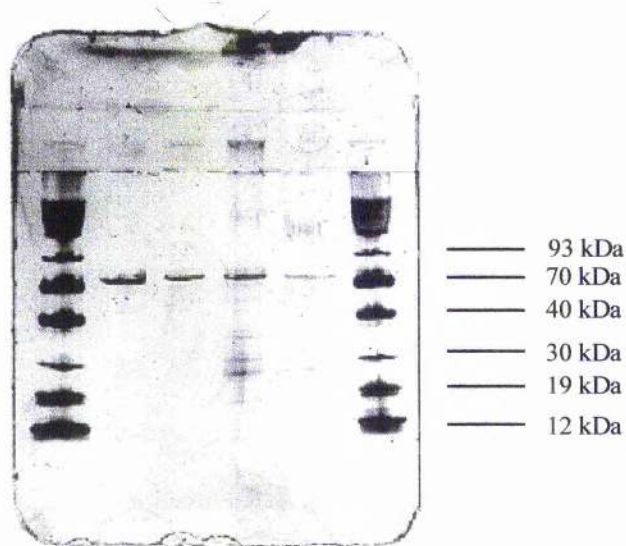
## Appendix 1

### A1 *trans*-Sialidase purification

Purification has encompassed two (and in some cases three) purification steps. We have successfully achieved a very high level of purity, with an equally high level of activity. The biggest problem has been a lack of material.

Our first purification protocol was modified to incorporate Ni<sup>2+</sup>-NTA resin (Hochuli *et al* 1987) as an initial column purification step. This column was adapted for the HPLC system. This was successful in increasing the level of purity of the material and speed. This has been confirmed, giving a single band on an SDS-Page silver stained gel at 69 kDa, **Figure 73**.

**Figure 73** SDS-Gel of purified *trans*-sialidase



The first nickel step provides such a good separation, as it is based on the chelation of two histidine residues (attached to the protein) with nickel cations immobilised in the resin. This column is eluted with imidazole.

Material that was recovered from this nickel purification step was first dialysed into tris (50 mM), pH 8, (to get rid of the imidazole) and concentrated on a 50 kDa cut off filter, before being loaded on to an anion exchange (HQ) column.

This column employs a salt gradient to elute the protein. As this is a high-velocity column, it gives a very fast separation, as illustrated below in **Table 41**.

**Table 41** Average protein purification table

Purification Step	Protein Conc.	$\Delta_{400}$ nm (10 Mins)
1. Initial lysis	64.0 mgs	.1
2. Ni-NTA HPLC (Fraction 1)	10.2 mgs	.12
3. Ni-NTA HPLC (Fraction 2)	4.8 mgs	.09*
4. <i>Centricon 50</i>	5.8 mgs	.12
5. HQ 20S HPLC (Fraction 1)	120 $\mu$ gs	.15
6. HQ 20S HPLC (Fraction 2)	180 $\mu$ gs	.09

\*This fraction was not purified any further.

### **A1.2 Protein purification protocol - small culture preparation**

A single bacterial colony was removed from an agar plate and transferred into sterile LB broth, inoculated with ampicillin (100  $\mu$ g/ml) and kanamycin monosulphate (25  $\mu$ g/ml). The culture was then grown in an incubator at 37 °C with gentle agitation (150 RPM), until it reached an optical density of 0.6. This culture was then transferred into 6x 2 L shake flasks, containing LB Miller broth (500 mls, sterile) and inoculated with ampicillin and kanamycin monosulphate as before. The bacteria was grown at 37 °C, with agitation of 175 RPM again until it reached an OD of 0.6. At this point the culture was induced with IPTG (1 mM), the temperature reduced to 25 °C and the agitation reduced to 150 RPM. The cells were left in the incubator for 16 hours approximately. The broth was spun down at 6198 g (6,000 RPM), 4 °C, for 20 mins and the pellets collected.

### **A1.3 Cell Lysis**

The wet cells were removed and the weight recorded before being re-suspended in 50 mM sodium phosphate, 300 mM NaCl, and 50 mM imidazole buffer pH 8 (sonication buffer). Lysozyme (1 mg/ml) and EDTA (2 mM) was added and the solution which was left to stir at 4 °C for 30 mins. The cells were then sonicated (6x 30 second bursts). *DNase 1* (5  $\mu$ g/ml) was added to the solution which was allowed to stir for a further 15 mins at 4 °C. After this time, the material was spun down at

27167 g (15,000 RPM), 4 °C for 20 mins. The supernatant was removed and the volume recorded.

#### **A1.4 Ni<sup>2+</sup>-NTA column purification**

Ni<sup>2+</sup> NTA beads were added to the culture (1 mls per 1 L, previously adjusted to pH 8). The beads were then washed with 4x bead volumes of lysis buffer (sodium phosphate (50 mM), NaCl (350 mM), and imidazole (20 mM), pH 8.1) to remove the storage material. The protein was added to the beads and shaken. This was left for 1 hour before being drained off and tested for activity. As the supernatant was no longer active, it was assumed that *trans*-sialidase had bound to the resin. The resin was then washed with buffer (sodium phosphate(50 mM), and NaCl (350 mM), pH 8.1). This process used 10x bead volume and it was repeated 4x. The washes were checked by uv spectrophotometry. When there was no further imidazole reading, the beads were eluted with buffer containing sodium phosphate (50 mM), NaCl (100 mM), and imidazole (800 mM), pH 8.1. This used 1x bead volume and was repeated 3x. The protein was assayed for activity and Bradford reagent used to establish the protein concentration, (*Scopes* 1994). The protein was dialysed immediately to remove the imidazole.

##### **A1.4.2 Ni<sup>2+</sup> NTA column purification (HPLC)**

Ni<sup>2+</sup> NTA beads were packed into a column that has been adapted to fit the HPLC system. It was first equilibrated with 2 column volumes of wash buffer, sodium phosphate (50 mM), NaCl (300 mM), pH 8. The protein was loaded on, washed and then eluted with sodium phosphate (50 mM), NaCl (100 mM) and imidazole (500 mM) buffer pH 8. The protein was collected and dialysed immediately.

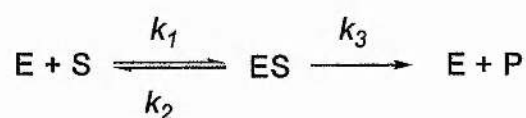
#### **A1.5 Anion exchange chromatography**

The protein was loaded onto the column with a flow rate of about 6 CV per min. The buffer used was trisma (50 mM) pH 8 and NaCl (4 M). A salt gradient was conducted from 0 to 4000 mM. The protein eluted at approximately NaCl (200 mM) assayed for activity and protein concentration.

## Appendix 2

### A2 Kinetic properties of many enzymes

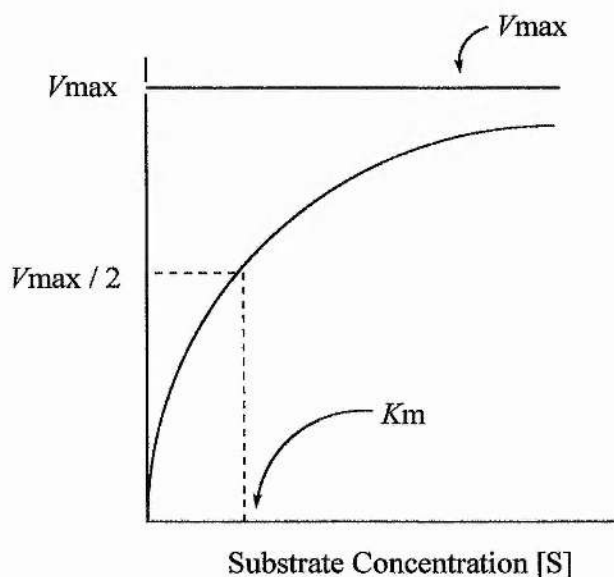
In general the catalysis rate,  $v$ , of an enzyme is dependant on the concentration of the substrate  $[S]$ , present, where  $V$  is the number of moles of product formed per second.  $v$  is directly proportional to  $[S]$ , when  $[S]$  is small, with a fixed amount of enzyme, but at a high  $[S]$ ,  $v$  is almost independent of  $[S]$ . These properties are accounted for by the Michaelis-menten model. The simplest expression that accounts for enzyme kinetics is as follows –



Where E = Enzyme, S = Substrate, ES = Enzyme substrate complex, P = Product

and  $k_R$  are rate constants. It is assumed that at the initial stage of the reaction, i.e. when the concentration of the product is low, that none of the product reverts to the substrate. The rate of production of product at this stage is governed by  $k_3$ . This is shown in **Figure 74**, below.

**Figure 74** Reaction velocity as a function of substrate concentration



The expression is -

$$v = k_3[ES]$$

We can express [ES] in known terms -

$$\text{Rate of formation of ES} = k_1[E][S]$$

$$\text{And the Rate of breakdown of ES} = (k_2 + k_3)[ES]$$

In a steady state, the concentration of reactants and products are changing, but the concentrations of the intermediates is the same i.e.

$$k_1[E][S] = (k_2 + k_3)[ES]$$

by rearrangement

$$[ES] = \frac{[E][S]}{(k_2 + k_3)/k_1}$$

Or by defining  $K_m$ , the Michaelis-Menten constant

$$K_m = \frac{k_2 + k_3}{k_1} = \frac{[E][S]}{[ES]}$$

The assumption is that the substrate concentration is significantly greater than the enzyme concentration, and that the concentration of enzyme is given by

$$[E] = [E_T] - [ES]$$

Where  $E_T$  is the total enzyme concentration present. So by substitution of [E] gives

$$K_m = \frac{([E_T] - [ES])[S]}{[ES]}$$

Solving with respect to [ES] gives

$$[ES] = \frac{k_3 [E_T][S]}{K_m + [S]}$$



Since  $V_{\max} = k_3 [E_T]$  by substitution it is possible to obtain the following Michaelis-Menten equation:

$$v = V_{\max} \frac{[S]}{[S] + K_m}$$

When  $[S] = K_m$ , and  $v = V_{\max}$ , i.e.  $K_m$  is equal to the substrate concentration at which the reaction rate is half of its maximal value.

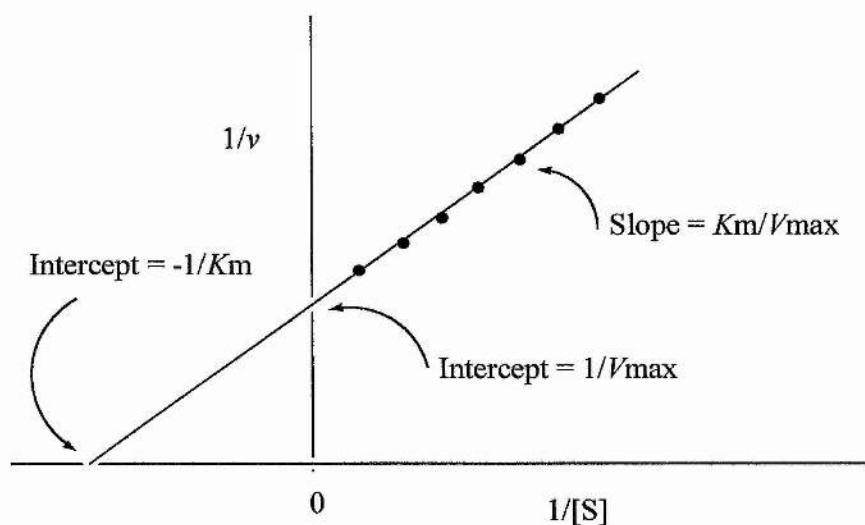
The Michaelis-Menten expression can be derived by measuring the rate of reaction with a variety of substrate concentrations, this can be transformed by a double reciprocal plot to give a straight line, i.e. a Lineweaver-Burk plot.

Lineweaver-Burk Equation :

$$\frac{1}{v} = \frac{1}{V_{\max}} + \frac{K_m}{V_{\max}} \cdot \frac{1}{S}$$

This is shown below diagrammatically in **Figure 75**

**Figure 75 Lineweaver – Burk Plot**



## A2.2 Significance of $K_m$ and $V_{max}$ values

The  $K_m$  of an enzyme usually lies between  $10^{-1}$  and  $10^{-7}$  M and can vary depending on conditions, substrates, ionic strength, pH and temperature. The  $K_m$  is an indication of the substrate concentration at which half of the active sites are filled.

But since

$$K_m = \frac{k_2 + k_3}{k_1}$$

This also gives an indication of the relative rates of reaction compared to each other.

## References

- Bamford, M. J. (1995) Neuraminidase inhibitors as potential anti-influenza drugs. *J. Enzyme Inhibition* **10**, 1-16.
- Byers, L. D., Dale, M. P., Ensley, H. E., Kern, K. and Sastry, K. A. R. (1985) Reversible inhibitors of  $\beta$ -glucosidase. *Biochemistry* **24**, 3530-3539.
- Byers, L. D., Dale, M. P., Kopfler, W. P. and Chait, I. (1986)  $\beta$ -Glycosidase: Substrate, solvent and viscosity variation as probes of the rate limiting steps. *Biochemistry* **25**, 2522-2529.
- Cassels, B. K., Morello, A., Lipchenca, I., Speisky, H., Aldunate, J. and Repetto, Y. (1994) Trypanocidal effect of boldine and related alkaloids upon several strains of *Trypanosoma cruzi*. *Com. Biochem. Phy. C-Tox. Endo.* **107**, 367-371.
- Colli, W. (1993) *trans*-Sialidase: a unique enzyme activity discovered in the protozoan *Trypanosoma cruzi*. *FASEB J.* **7**, 1257-1264.
- Frank, M., Hegenscheid, B., Janitschke, K. and Weinke, T. (1997) Prevalence and Epidemiological Significance of *Trypanosoma cruzi* Infection among Latin American Immigrants in Berlin, Germany. *Infect.* **25**, 31-34.
- Frasch, A. C. C., Cremona, M. L., Sanchez, D. O. and Campetella, O. (1995) A single tyrosine differentiates active and inactive *Trypanosoma cruzi trans*-sialidase. *Gene* **160**, 123-128.
- Frasch, A. C. C., Buschiazzo, A. and Campetella, O. (1996) Medium scale production and purification to homogeneity of recombinant *trans*-sialidase from *Trypanosoma cruzi*. *Cell. Mol. Biol.* **42**, 703-710.
- Frasch, A. C. C., Lederkremer, R. M. de, Agusti, R., Couto, A. S. and Campetella, O. (1997) The *trans*-sialidase of *Trypanosoma cruzi* is anchored by two lipids. *Glycobiology* **7**, 731-735.

Ferguson, M. A. J., Milne, K. G., Field, R. A. Masterson, W. J., Cottaz, S. and Brimacombe, J. S. (1994) *N*-Acetylglucosaminyl-phosphatidylinositol de-*N*-acetylase of glycosylphosphatidylinositol anchor biosynthesis in african trypanosomes. *J. Biol. Chem.* **269**, 16403-16408.

Gazzinelli, R. T. and Brener, Z. (1997) Immunological Control of *Trypanosoma cruzi* Infection and pathogenesis of Chagas' disease. *Int. Arch. Allergy. Immunol.* **114**, 103-110.

Haltiwanger, R. S., Kelly, W. G. K., Roquemore, E. P., Blomberg, M. A., Dong, L-Y. D., Kreppel, L., Chou, T-Y. and Hart, G. W. (1992) *Biochem. Soc. Trans.* **20**, 264-269.

Hindsgaul, O., Ding, Y., Labbe, J. and Kanie, O. (1996) Towards oligosaccharide libraries: A study of the random galactosylation of unprotected *N*-acetylglucosamine. *Bioorg. Med. Chem. Lett.* **4**, 683-692.

Hindsgaul, O. and McAuliffe, J. (1997) Carbohydrate drugs-an ongoing challenge. *Chem. and Ind.* **3**, 170-174.

Hindsgaul, O., Malet, C., Sujino, K. and Palcic, M. M. (1998) Acceptor hydroxyl group mapping of calf thymus  $\alpha$ -(1,3)-galactosyltransferase and enzymatic synthesis of  $\alpha$ -D-Galp-(1,3)- $\beta$ -D-Galp(1,4) $\beta$ -D-GlcNAc analogues. *Carbohydr. Res.* **305**, 483-489.

Hochuli, E., Dobeli, H. and Schacher, A. (1987) New metal chelate absorbent selective for proteins and peptides containing neighbouring histidine residues. *J. Chromatog.* **411**, 177-184.

Kirchhoff, L. V., Shulman, I. A., Appleman, M. D., Saxena, S. and Hiti, A. L. (1997) Specific antibodies to *Trypanosoma cruzi* among blood donors in Los Angeles, California. *Transfusion* **37**, 727-730.

Lowary, T. L. and Hindsgaul, O. (1993) Recognition of synthetic deoxy and deoxyfluoro analogues of the acceptor  $\alpha$ -L-Fucp-(1,2)- $\beta$ -D-Galp-OR by the blood-group A and B gene-specified glycosyltransferases. *Carbohydr. Res.* **249**, 163-195.

Lowary, T. L., Hindsgaul, O. and Swiedler, S. J. (1994) Recognition of synthetic analogues of the acceptor  $\beta$ -D-Galp-OR, by the blood-group H gene-specified glycosyltransferases. *Carbohydr. Res.* **256**, 257-273.

Lowary, T. L. and Hindsgaul, O. (1994) Recognition of synthetic *O*-methyl, epimeric and amino analogues of the acceptor  $\alpha$ -L-Fucp-(1,2)- $\beta$ -D-Galp-OR by the blood-group A and B gene-specified glycosyltransferases. *Carbohydr. Res.* **251**, 33-67.

Luo, M., Jedzejias, M. J., Singh, S., Brouillette, W. J., Laver, W. G. and Air, G. M. (1995) Structures of aromatic inhibitors of Influenza virus neuraminidase. *Biochemistry* **34**, 3144-3151.

Luo, M., Luo, Y., Li, S. C., Chou, M. Y. and Li, Y. T. (1998) The crystal structure of an intramolecular *trans*-sialidase with a NeuAc $\alpha$ 2 $\rightarrow$ 3Gal specificity. *Structure* **6**, 521-530.

Li, Y. T., Li, S. C., and Chou, M. Y. (1996) Cloning and expression of sialidase L, a NeuAc $\alpha$ 2 $\rightarrow$ 3Gal-specific sialidase from the leech, *Macrobdella decora*. *J. Biol. Chem.* **271**, 19219-19224.

Palcic, M. M., Hindsgaul, O., Nilsson, U. J., Heerze, L. D., Liu, Y-C. and Armstrong, G. D. (1997) Immobilisation of reducing sugars as toxin binding agents. *Bioconjug. J.* **8**, 466-471.

Paulson, J. C. and Ito, Y. (1993) Combined use of *trans*-sialidase and sialyltransferase for enzymatic synthesis of NeuAc- $\alpha$ -(2,3)- $\beta$ -Gal-OR. *J. Am. Chem. Soc.* **115**, 7862-7863.

Pereira, M. and Chuenkova, M. (1995) *Trypanosoma cruzi* trans-sialidase: enhancement of virulence in murine model of Chagas' disease. *J. Exp. Med.* **181**, 1693-1703.

Portner, A., Bousse, T. and Takimoto, T. (1995) A single amino acid change enhances the fusion promotion activity of human para-Influenza virus type 1 hemagglutinin- neuraminidase glucoprotein. *Virology* **20**, 654-657.

Previato, L. M., Previato, J. O., Jones, C., Goncalves, L. P. B., Wait, R. and Travassos, L. R. (1994) O-Glycosidically linked N-acetylglucosamine-bound oligosaccharides from glycoproteins of *Trypanosoma cruzi*. *Biochem. J.* **301**, 151-159.

Previato, L. M., Previato, J. O., Jones, C., Xavier, M. T., Parodi, A. J., Wait, R. and Travassos, L. R. (1995) Structural characterisation of the major glycosylphosphatidylinositol membrane anchored glycoprotein from the epimastigote forms of *Trypanosoma cruzi* Y-strain. *J. Biol. Chem.* **270**, 7241-7250.

Quash, G., Driguez, P. A., Barrere, B., Chantegrel, B., Deshayes, C. and Pouthau, A. (1992) Synthesis of sodium salt of ortho-9-difluoromethylphenyl- $\alpha$ -ketoside of N-acetyl neuraminic acid: a mechanism based inhibitor of *Clostridium perfringens* neuraminidase. *Bioorg. Med. Chem. Lett.* **2**, 1361-1366.

Randall, R. E. and Botting, C. H. (1995) Reporter enzyme-nitrilotriacetic acid-nickel conjugates for detecting histidine-tagged proteins. *BioTechniques* **19**, 362-363.

Schauer, R., Rothe, B., Rothe, B. and Roggentin, P. (1991) The sialidase gene from *Clostridium septicum*: cloning, sequencing and the expression in *E-coli*. Identification of conserved sequences in sialodases and other proteins. *Mol. Gen. Genet.* **226**, 190-197.

Schauer, R., Engstler, M., Talhouk, J. W. and Smith, R. E. (1997) Chemical synthesis of 4-trifluoromethylumbelliferyl- $\alpha$ -D-N-acetylneuraminic acid glycoside and its use for the fluometric detection of poorly expressed natural and recombinant sialidases. *Anal. Biochem.* **250**, 176-180.

Schenkman, S., Frevert, U. and Nussenzweig, V. (1992) Stage-specific expression and intracellular shredding of the cell surface *trans*-sialidase of *Trypanosoma cruzi*. *Infect. Imm.* **6**, 2349-2360.

Schenkman, S., Vandekerckhove, F., Pontes de Carvalho, L., Kiso, M., Yoshida, M., Hasegawa, A. and Nussenzweig, V. (1992) Substrate specificity of the *Trypanosoma cruzi trans*-sialidase. *Glycobiology* **2**, 541-548.

Schenkman, S. and Eichinger, D. (1993) *Trypanosoma cruzi trans*-sialidase and cell invasion. *Parasitology Today* **9**, 218-222.

Schenkman, S., Schenkman, R. P. F. and Vandekerckhove, F. (1993) Mammalian cell sialic acid enhances invasion by *Trypanosoma cruzi*. *Infect. Imm.* **61**, 898-902.

Schenkman, S., Brines, M. R. S., Egima, C. M., and Acosta, A. (1994) *trans*-Sialidase and sialic acid acceptors from insect to mammalian stages of *Trypanosoma-cruzi*. *Exp. Parasitol.* **79**, 211-214.

Schenkman, S., Chaves, L. B., Pontes de Carvalho, L. C. and Eichunger, D. (1994) A proteolytic fragment of *Trypanosoma cruzi trans*-sialidase lacking the carboxyl-terminal domain is active, monomeric and generates antibodies that inhibit enzyme activity. *J. Biol. Chem.* **269**, 7970-7975.

Schenkman, S., Eichinger, D., Pereira, M. and Nussenzweig, V. (1994) Structure and functional properties of *Trypanosoma cruzi trans*-sialidase. *Anal. Rev. Micro.* **48**, 499-523.



Schenkman, S., Ribeiro, M., Pereira-Chiocola, V. L., Eichinger, D. and Rodrigues M. M. (1997) Temperature differences for *trans*-glycosylation and hydrolysis reaction reveal an acceptor binding site in the catalytic mechanism of *Trypanosoma cruzi trans*-sialidase. *Glycobiology* **7**, 1237-1246.

Scudder, P., Doom, J. P., Chuenkova, M., Manger, I. D. and Pereira, M. E. A. (1993) Enzymatic characterisation of  $\beta$ -D-galactoside  $\alpha$ -(2,3) *trans*-sialidase from *Trypanosoma cruzi*. *J. Biol. Chem.* **268**, 9886-9891.

Sinnott, M. L., Guo, X., Li, S-C. and Li, Y-T. (1993) Leech sialidase cleaves the glycon, aglycon bond with the substrate in a normally disfavoured conformation. *J. Am. Chem. Soc. USA* **115**, 3334-3335.

Sinnott, M. L. and Guo, X. (1993) A kinetic isotope effect study of catalysis by *Vibrio cholera* neuraminidase. *Biochem. J.* **294**, 653-656.

Takle, G. B. and Cross, G. A. M. (1993) The surface *trans*-sialidase family of *Trypanosoma cruzi*. *Annu. Rev. Microbiol.* **47**, 385-411.

Taylor, G. L., Crennell, S. J., Garman, E. F., Laver, W. G. and Vimr, E. R. (1993) Crystal structure of the bacterial sialidase shows the same fold as Influenza virus neuraminidase. *Proc. Natl. Acad. Sci.* **90**, 9852-9856.

Taylor, G. L., Crennell, S. J., Garman, E. F., Laver, W. G. and Vimr, E. R. (1994) Crystal structure of *Vibrio cholera* neuraminidase reveals dual lectin-like domains in addition to the catalytic domain. *Structure* **2**, 535-544.

Taylor, G. L., Gaskell, A. and Crennell, S. J. (1995) The three domains of bacterial sialidase. A propeller, an immunoglobulin model and galactose-bonding jelly roll. *Structure* **3**, 197-1205.

Taylor, G. L., Crennell, S. J., Garman, E. F., Philippon, C., Vasella, A., Laver, W. G. and Vimr, E. R. (1996) The structures of *Salmonella typhimurium* LT2 neuraminidase and its complexes with three inhibitors at high resolution. *J. Mol. Biol.* **259**, 264-280.

Taylor, G. L. (1996) Sialidases: structures, biological significance and therapeutic potential. *Curr. Op. Struct. Biol.* **6**, 830-837.

Tolvanen, M. and Gahmberg, C. G. (1996) Why mammalian cell surface proteins are glycoproteins. *TIBS* **21**, 308-311.

Vetere, A. and Paoletti, S. (1996) Complete synthesis of 3'-sialyl-N-acetylactosamine by regioselective transglycosylation. *FEBS Letters* **399**, 203-206.

Von Itzstein, M., Holder, C. T., Jin, B., Pegg, M. S., Stewart, W. P. and Wu, W. Y. (1993) Inhibition of sialidases from viral, bacterial and mammalian sources by analogues of 2-deoxy-2,3-dihydro-N-acetylneuraminic acid modified at the C-4 position. *Glycoconjugate J.* **10**, 40-44.

Von Itzstein, M., Wu, W., Kok, G. B., Pegg, M. S., Dyason, J. C., Jin, B., Phan, T. V., Smythe, M. L., White, H. F., Oliver, S. W., Colman, P. M., Varghese, J. N., Ryan, D. M., Woods, J. M., Bethell, R. C., Hotham, V. J., Cameron, J. M. and Penn, C. R. (1993) Rational design of potent sialidase-based inhibitors of Influenza virus replication. *Nature* **363**, 418-423.

Von Itzstein, M., Wilson, J. C. and Angus, D. I. (1995) <sup>1</sup>H NMR evidence that *Salmonella typhimurium* sialidase hydrolyses sialosides with overall retention of configuration. *J. Am. Chem. Soc.* **117**, 4214-4217.

Von Itzstein, M., Tiralongo, J. and Pegg, M. S. (1995) Effect of substrate aglycon on the enzyme mechanism in the reaction of sialidase from Influenza virus. *FEBS. Lett.* **372**, 148-150.

Whittaker, M., Floyd, C. D. and Lewis, C. N. (1996) More leads in the haystack. *Chemistry in Britain* **3**, 31-35.

Withers, S. G. and Kempton, J. B. (1992) Mechanism of *agrobacterium*  $\beta$ -glucosidase: kinetic studies. *Biochemistry* **31**, 9961-9969.

### **Other references**

Müller, R. and Baker, J. R. (1990) *Medical Parasitology*. Gower Medical Publishings. 27-37.

Rosenberg, A. (Edited by) (1995) *Biology of sialic acids*. Plenum Press, New York.

Scopes, R. K. (1994) *Protein purification: Principles and practice*. Springer-Verlag. Third Ed. 296-297 and 303.

Smyth, J. D. (1994) *An introduction to animal parasitology*. Cambridge University Press. 63-71.

[http://vflylab.angis.org.au/edesktop/WWW\\_Projects/Animals\\_Plants/TrypanosomaCruzi\\_thuynh/Start.html](http://vflylab.angis.org.au/edesktop/WWW_Projects/Animals_Plants/TrypanosomaCruzi_thuynh/Start.html)